PB98-116585

TESTING OF ENHANCED AND REPAIRED PIER WALLS OF MODERN DESIGN

NOV 97

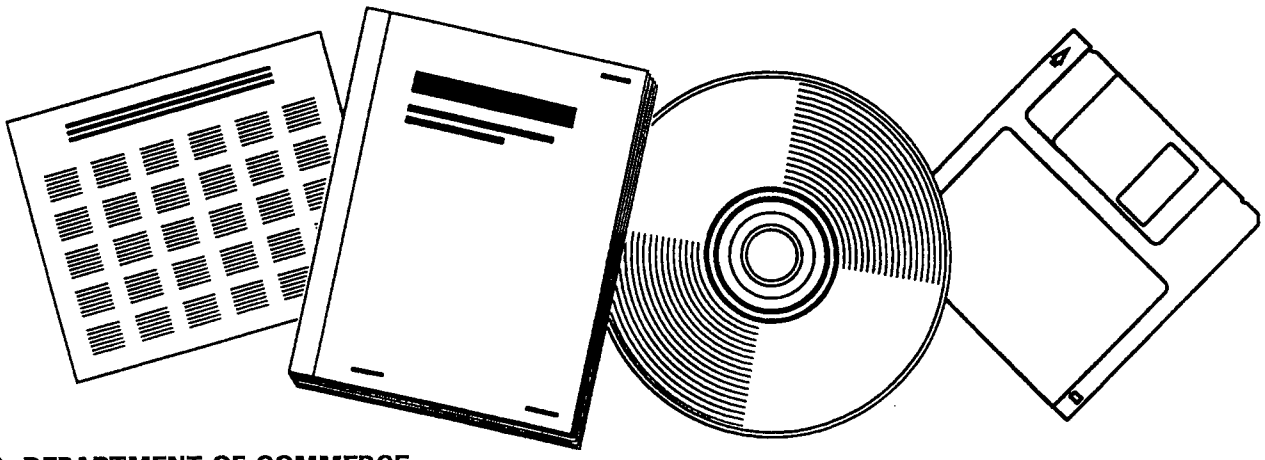

U.S. DEPARTMENT OF COMMERCE
National Technical Information Service

FINAL REPORT TO
THE CALIFORNIA DEPARTMENT OF
TRANSPORTATION

TESTING OF ENHANCED AND REPAIRED PIER WALLS OF MODERN DESIGN

RTA No. 59A200

by
Medhat A. Haroun, *Professor*
Gerard C. Pardoen, *Professor*
Hussain Bhatia, *Graduate Student Assistant*
Santosh Shahi, *Graduate Student Assistant*
and Robert P. Kazanjy, *Senior Development Engineer*

Department of Civil and Environmental Engineering
University of California, Irvine
November 1997

Technical Report Documentation Page

1. Report No.	2. Government Accession No.	3. Recipient's Catalog No.
FHWA/CA/UCI-97-01		

4. Title and Subtitle	5. Report Date
Testing of Enhanced and Repaired Pier Walls of Modern Design	November 1997
	6. Performing Organization Code: UC Irvine
7. Author's: Haroun, M.A., Pardoen, G.C., Bhatia, H., Shahi, S.B., Kazanjy, R.P.	8. Performing Organization Report No.
9. Performing Organization Name and Address: Civil and Environmental Engineering, 4130 Engineering Gateway, UC Irvine, Irvine, CA 92697-2175	10. Work Unit No. (TRAIS)
	11. Contract or Grant No.: RTA-59A200
12. Sponsoring Agency Name and Address: Caltrans- State Department of Transportation, 1801 30th Street, Sacramento, CA 95816	13. Type of Report and Period Covered: Final Report
	14. Sponsoring Agency Code: 20.10.010-59-304-910173

15. Supplementary Notes

This project was performed in cooperation with the United States Department of Transportation, Federal Highway Administration.

16. Abstract:

Large acceleration in a severe earthquake may force a pier wall to experience force levels beyond the elastic range, causing substantial localized damage. Instead of demolishing a damaged pier wall and building a new one, in some cases it may be beneficial to repair the damaged wall resulting in substantial savings in material and labor along with a quick restoration time to its intended use. The main objective of this research was to repair six damaged pier walls from a previous Caltrans testing program and to compare the strength, ductility and cross-tie performance of the repaired pier walls with the original undamaged pier walls. Two different repair techniques were utilized. The experiments results achieved by repairing the damaged pier walls were comparable with the original undamaged pier walls.

To assess the structural performance of reduced scale models with that of full-scale models, two full scale pier walls were also built and tested. A good correlation between half-scale and full-scale walls was achieved for displacement ductility factors and curvatures. Accordingly experimental results obtained from half scale samples can be applied to pier walls in the field.

17. Key Words	18. Distribution Statement
Pier walls, Repaired Pier walls, Full Scale Pier Walls, T-headed bars, Seismic Design, Ductility, Cyclic Load Testing, Cross-ties.	

19. Security Classif. (of this report)	20. Security Classif. (of this page)	21. No. of Pages	22. Price
Unclassified	Unclassified	122	

FINAL REPORT TO
THE CALIFORNIA DEPARTMENT OF
TRANSPORTATION

TESTING OF ENHANCED AND REPAIRED PIER WALLS OF MODERN DESIGN

RTA No. 59A200

by
Medhat A. Haroun, *Professor*
Gerard C. Pardoen, *Professor*
Hussain Bhatia, *Graduate Student Assistant*
Santosh Shahi, *Graduate Student Assistant*
and Robert P. Kazanjy, *Senior Development Engineer*

Department of Civil and Environmental Engineering
University of California, Irvine
November 1997

ACKNOWLEDGEMENTS

The financial support of the Division of Structures, the California Department of Transportation under Research Technical Agreement (RTA) no. 59A200 is appreciated. The technical advice from Caltrans senior bridge engineers Thomas Sardo and Fadel Alameddine is acknowledged with gratitude. The authors wish to express their appreciation to the many students who contributed to the success of the project, especially, Brook Sutherland, Daniel Del Carlo, Dave Larsen, John Whiteman and Trisha Park.

Contents

List of Figures

List of Tables

Chapter 1

Introduction

1.1 Project Scope

Large accelerations in a severe earthquake may force a pier wall supporting a bridge deck to experience force levels beyond the elastic range causing substantial localized damage. In the aftermath of such earthquakes, the damaged pier wall may need to be restored to its original use. Instead of demolishing the damaged pier wall and constructing a new one, in some cases it may be beneficial to repair the damaged wall resulting in tangible savings in material and labor along with a quick restoration time to its intended use.

The primary focus of the current research project has been to repair damaged pier walls from a previous experimental program and to compare the strength, stiffness, ductility and cross-tie performance of the repaired pier walls with the original, undamaged pier walls. Various repair schemes were developed to see if similar procedures could be implemented in the field should a pier wall be damaged due to an earthquake. An additional focus of the project has been to compare the experimental results from two full-scale pier walls with the previously determined results from the half-scale pier walls.

1.2 Previous UCI Pier Wall Research Programs

1.2.1 Samples Built to Pre-1971 Design Specifications

An experimental and theoretical study was conducted on pier wall samples representing pre-1971 design specifications to better understand the performance and failure mechanism of bridge pier walls[1]. The performance of the pier wall samples was assessed primarily by their strength and ductility. Different retrofit schemes were also investigated to improve the strength and ductility capacity of existing pier walls. Two different splice lengths — class 'A' ($16d_b$) and class 'C' ($28d_b$)— were utilized to model the existing splices in the pier walls. All pier wall samples were subjected to a series of cyclic horizontal loads under the influence of a constant axial load.

The two main objectives of the study were to understand the performance and failure mechanism of the pier walls as well as to evaluate different retrofit techniques to improve their ductility and strength. The experimental investigation was conducted in three phases.

In the first phase, two one-third scale models of existing pier walls were tested in the strong-axis direction. One sample had a class 'A' splice whereas the other sample had a class 'C' lap splice. The pier wall samples performed well when loaded in the their strong-axis direction. Shear failure was the dominant mode of failure and relatively large load capacity was observed.

In the second phase, seven half-scale models with either the 'A' or 'C' lap splice were tested in their weak-axis direction. Two samples from this group were additionally tested for the shear strength in their strong-axis direction after a flexural failure in the weak-axis direction.

In the third phase, similar but wider specimens, retrofitted to increase their strength and ductility, were tested to evaluate the effectiveness of the corrective measures.

This phase involved the testing of five specimens, four of which had different retrofit schemes. Throughout the study, the two different types of lap splices were evaluated.

In most circumstances good correlation was found between the analytically-computed and experimentally-measured parameters such as the ultimate loads and the displacement ductility factors. The behavior of the pier wall samples tested in the strong-axis direction showed acceptable performance, and therefore, no retrofit was recommended to strengthen full-scale, in-situ pier walls in the strong-axis direction. The pier wall samples' behavior in the weak-axis direction was generally much better than originally anticipated before this research project was conducted. All pier walls samples tested achieved a minimum measured displacement ductility factor of six. In the case of deficient walls, an effective retrofit scheme for each of the two tested classes of lap splices was recommended. A theoretical seismic analysis of two bridges, built prior to 1971, was conducted to estimate the demand. A ductility analysis was also performed on all wall samples.

1.2.2 Samples Built to Current Design Standards

Another extensive test program was conducted to evaluate the ductility and strength of bridge pier walls built to modern seismic design standards [2]. These new standards have avoided the perceived problems of the older designed pier walls such as slip of the lap splices, buckling of the vertical reinforcement bars and lack of confinement at the plastic zone. This most recent study of six pier wall samples examined a range of cross-tie provisions with the objective of establishing whether existing standards are unnecessarily severe and if so, what level of confinement would be acceptable.

These six pier walls samples, comprised of two different vertical reinforcement ratios with three different cross-tie distributions, were subjected to cyclic horizontal loads about the weak-axis. The research noted that less ductility was achieved for the

three pier wall samples with the higher vertical reinforcement ratio. Furthermore, it was observed that pier wall samples having uniformly distributed cross-ties over the wall height behaved similarly to those which had cross-ties only in the plastic zone. Based on the pier walls samples' observed behavior, recommendations were made for further improving current design standards while implementing cost-reduction measures.

1.3 Current Pier Wall Research Program

The current research program has investigated the performance of six repaired, half-scale pier walls subjected to cyclic lateral loading. The six pier walls were the remnants of the previous experimental program which had studied the performance of cantilevered pier walls loaded in the weak-axis direction under cyclic loading. Although the six pier walls had significant damage as a result of the first round of tests, these damaged pier walls were repaired with various schemes and re-tested using the same cyclic loading as with the original pier walls. In consultation with various Caltrans designers and field maintenance engineers, several repair schemes were developed so that similar repair procedures could be implemented in the field should an earthquake-damaged pier wall justify repair rather than reconstruction.

1.4 Research Objectives

The principal thrust of the current research has been to repair previously damaged pier wall models and re-test these samples to the same load conditions as the original samples. A comparison of performance results between the original and repaired samples has been used to evaluate the suitability of recommending one or more repair schemes for damaged pier walls. The specific project objectives have been:

- Design a practical field-based repair procedure.
- Compare the strength of the repaired samples with the original samples.
- Compare the ductility of the repaired samples with the original samples.
- Compare the performance of standard cross-ties with -
  - enhanced cross-ties
  - T-headed reinforcement
- Assess the structural performance of reduced scale models with that of the full-scale models.

To meet the penultimate objective, two different repair schemes were used to repair the samples. Five of the samples were repaired with a pair of enhanced cross-ties by alternating the 90° and the 135° leg at each location. The cross-ties were enhanced by increasing the 135° leg length from previous tests. The sixth sample was repaired with T-headed reinforcement bars as the cross-ties. A T-headed cross-tie consists of two metal plates attached to a reinforcing bar in a 'dumbbell' arrangement.

1.5 Report Format

This report consists of seven chapters. The first five chapters deal with the repairing of damaged pier walls. The first chapter provides the scope, background and objectives of repairing pier walls. The second chapter describes the repair of the damaged pier walls. The third chapter presents the experimental program whereas the test results are presented in the fourth chapter. The fifth chapter describes the experimental modal analyses that were performed on the repaired pier walls before and after their

re-test. Chapter six covers the full-scale pier walls. Lastly, in the seventh chapter, the conclusions of the study are summarized.

Chapter 2

Repair of Damaged Pier Walls

Six pier wall samples from a previous Caltrans project were constructed and then subjected to reversed cyclic horizontal loads. Without exception each pier wall sample experienced major structural damage due to the imposed loads. Typically the significant damage in each wall was confined to concrete spalling, vertical reinforcement bar buckling and opening of the cross-tie hooks in the lower 20% of the wall. A description of the original pier wall specimens and the repairs undertaken to prepare the walls for further cyclic loading follows.

2.1 Original Pier Wall Samples

Each of six pier walls with a height of 127 inches, a width of 96 inches and a thickness of 10 inches were built to present Caltrans specifications [3]. These test specimens were approximately one-half scale models of existing pier walls in California. Previous research [1]had noted that pier wall length had little influence on the weak-axis bending results. A ready-mix pea gravel concrete, of nominal strength, $f_c' = 4000$ psi, was used to construct both the pier walls and the footings. The pier wall footings were 18 inches thick, 116 inches long, 56 inches wide. The footings were anchored to the UC Irvine Structural Engineering Test Hall's strong floor with pre-tensioned

rods.

The six pier walls were divided into two groups. One group had a vertical reinforcement ratio of 1.3%, while the other group had vertical reinforcement ratio of 2.3%. The letter 'L' was used to denote the low vertical reinforcement ratio (1.3%) whereas the letter 'H' was used to denote the high reinforcement ratio (2.3%). These ratios were chosen to represent typical minimum and maximum vertical reinforcement ratios of Caltrans' recommendations [3]. The seven inches spacing of the vertical reinforcing bars was the same for both groups. In walls with the high reinforcement ratio, #8 bars were used whereas #6 bars were used in walls with the low reinforcement ratio. The vertical bars had a nominal yield strength of $f_y = 60$ ksi and were terminated in the footings with standard hooks. For each of the two groups, three different cross-tie distributions were used: no cross-ties whatsoever, uniform distribution of cross-ties over the wall heights and partial distribution of cross-ties over the wall heights. The pier walls were further designated with letter 'N', 'U' or 'P' to denote *no, uniform* or *partial* cross-tie distributions as shown in Figure 2.1. Deformed wire (D5) was used for the standard shape cross-tie with 90° and 135° legs. The D5 wire had a nominal yield strength of $f_y = 90$ ksi.

The horizontal reinforcement was provided by placing #3 bars on the outside of the vertical bars with a vertical spacing of 9.0 inches to achieve a Caltrans recommended reinforcement ratio of 0.25 %. The horizontal reinforcement spacing of the LP and HP walls was reduced to 4.5 inches from the base of the wall up to a height of 20.25 inches. This height, which represents, approximately, the expected plastic hinge length L_p, was based on the empirical formula [4]

$$L_p = 0.08L + 0.15 f_y d_b \tag{2.1}$$

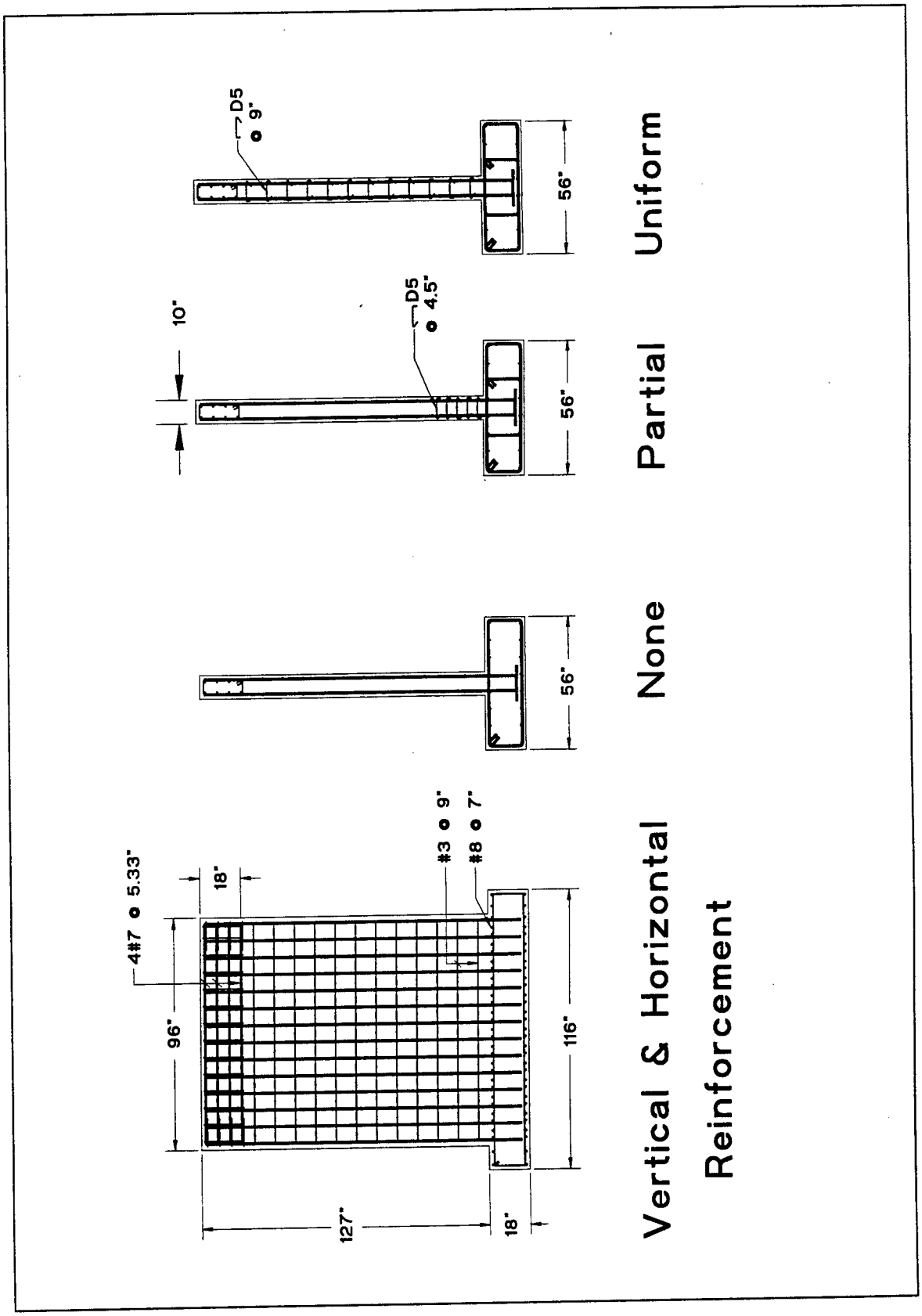

Figure 2.1: Arrangement of Cross-ties in Original and Repaired Walls

where L is the wall height, f_y is the yield stress of the reinforcement in ksi and d_b is the diameter of a vertical reinforcing bar. The first horizontal reinforcement bars were placed at a distance of 4.5 inches from the upper edge of the footing for samples LN, HN, LU, HU. In samples LP and HP this spacing was reduced to 2.25 inches. Furthermore, in samples LP, HP, LN, HN, 'U' shaped #3 bars were placed at each end of the walls. Figures 2.2 to 2.7 show the detailed drawings of the original half-scale pier wall samples.

2.2 Repair of Damaged Pier Walls

2.2.1 Pier Wall Damage and Repair

The six original pier walls, previously tested under displacement controlled cyclic lateral loading about the weak-axis, had varying degrees of damage at the conclusion of the tests. As a result of this cyclic loading the concrete cover in the bottom portion of the pier wall, approximately 18 to 20 inches from the top of the footing, spalled off exposing the buckled vertical reinforcement bars. However, the concrete above the spalled zone was intact except for some horizontal cracks present on the white-painted surface of the pier walls.

Most of the 135° legs of the D5 cross-ties, in those walls with cross-ties, had opened. The horizontal bars, for the most part, remained relatively straight. The damage in the vertical reinforcement bars was about the same for five of the pier walls in that the bars were severely buckled in the plastic hinge zone. The vertical reinforcement bars of the sixth pier wall, HN, had the most buckling distortion of the group. This damage was the result of having pushed the HN wall to a displacement of 18 inches at the conclusion of the test.

The bonding of all the vertical reinforcement bars to the footing remained intact

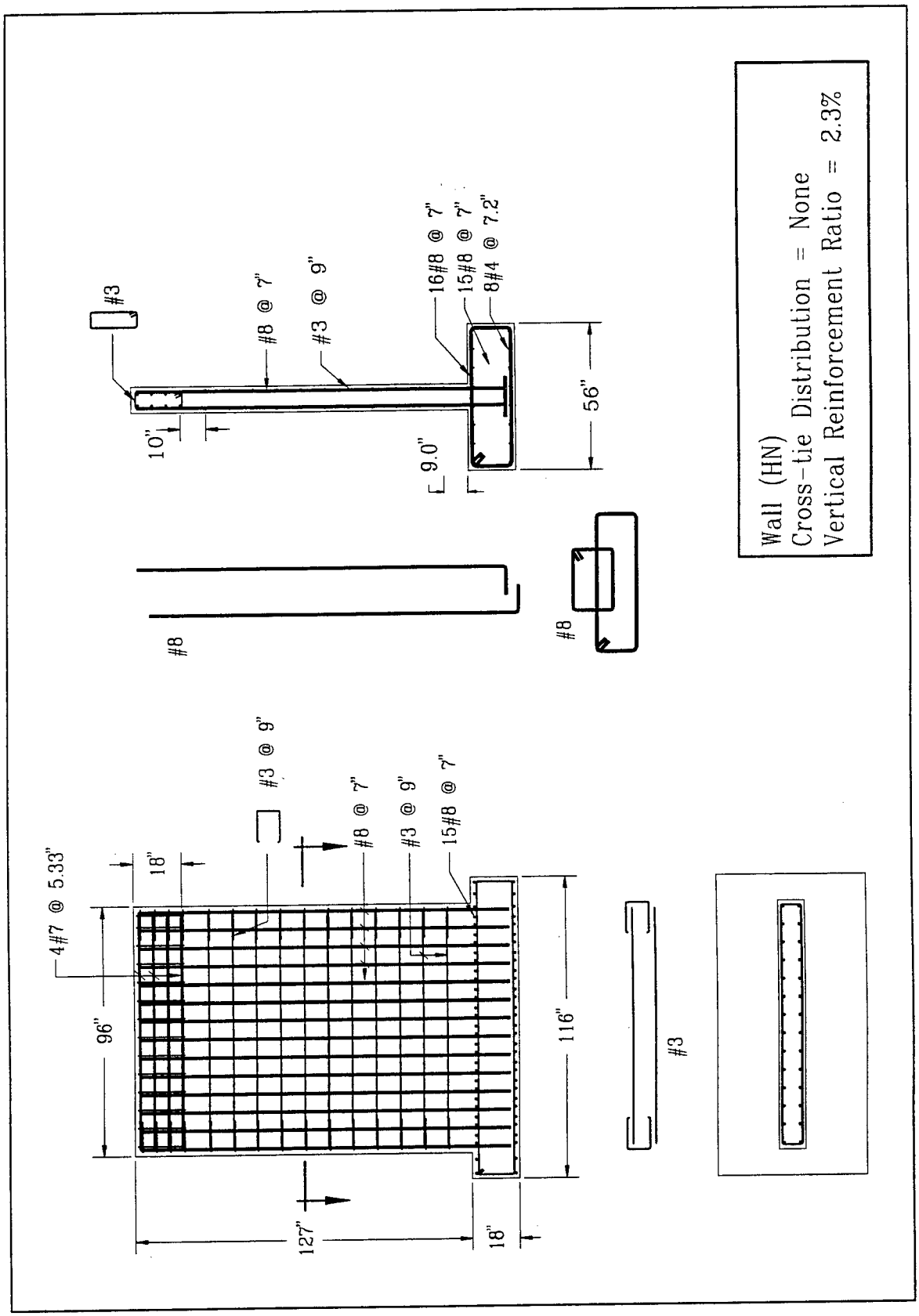

Figure 2.2: Reinforcement Details of the Original HN Wall

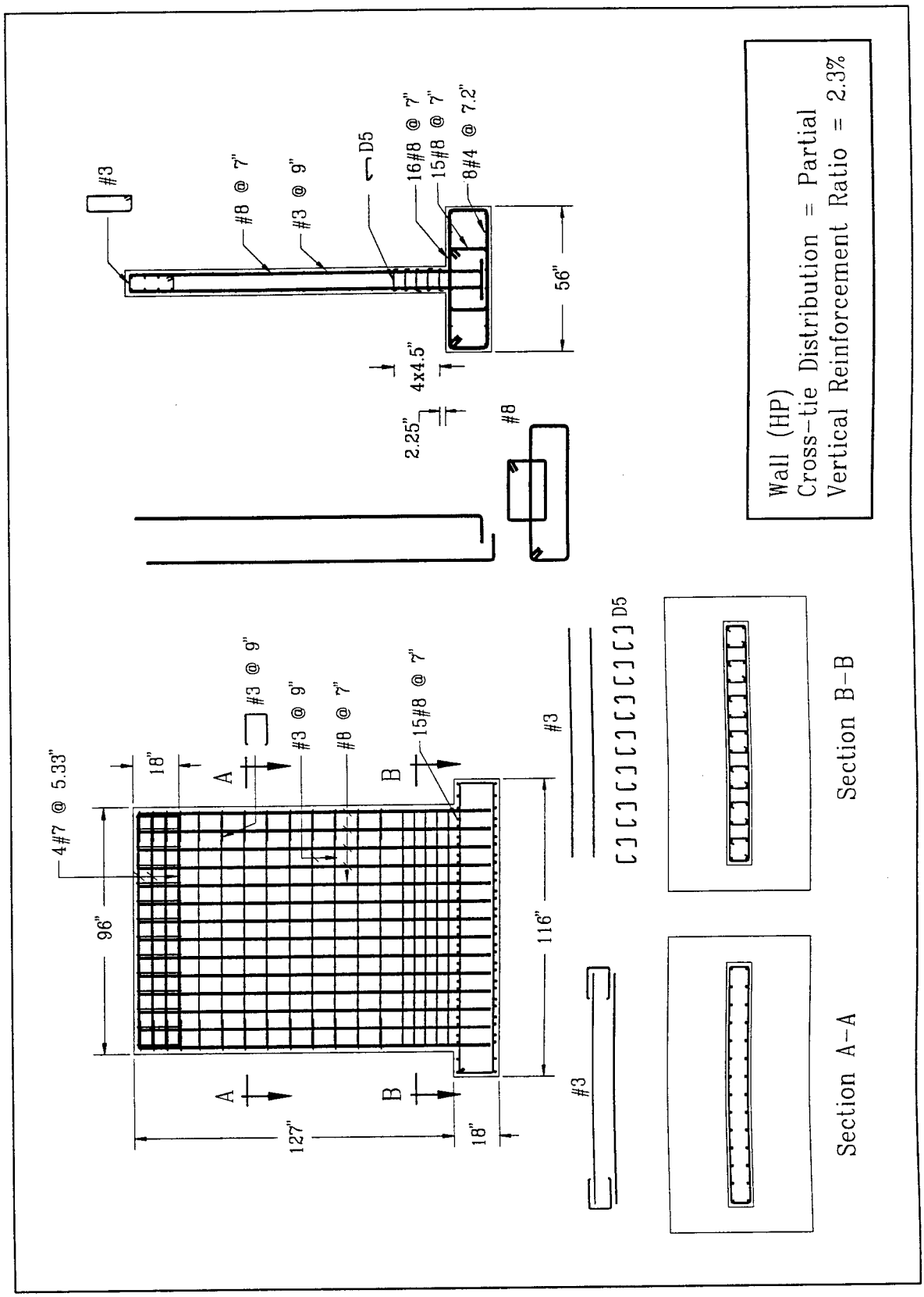

Figure 2.3: Reinforcement Details of the Original HP Wall

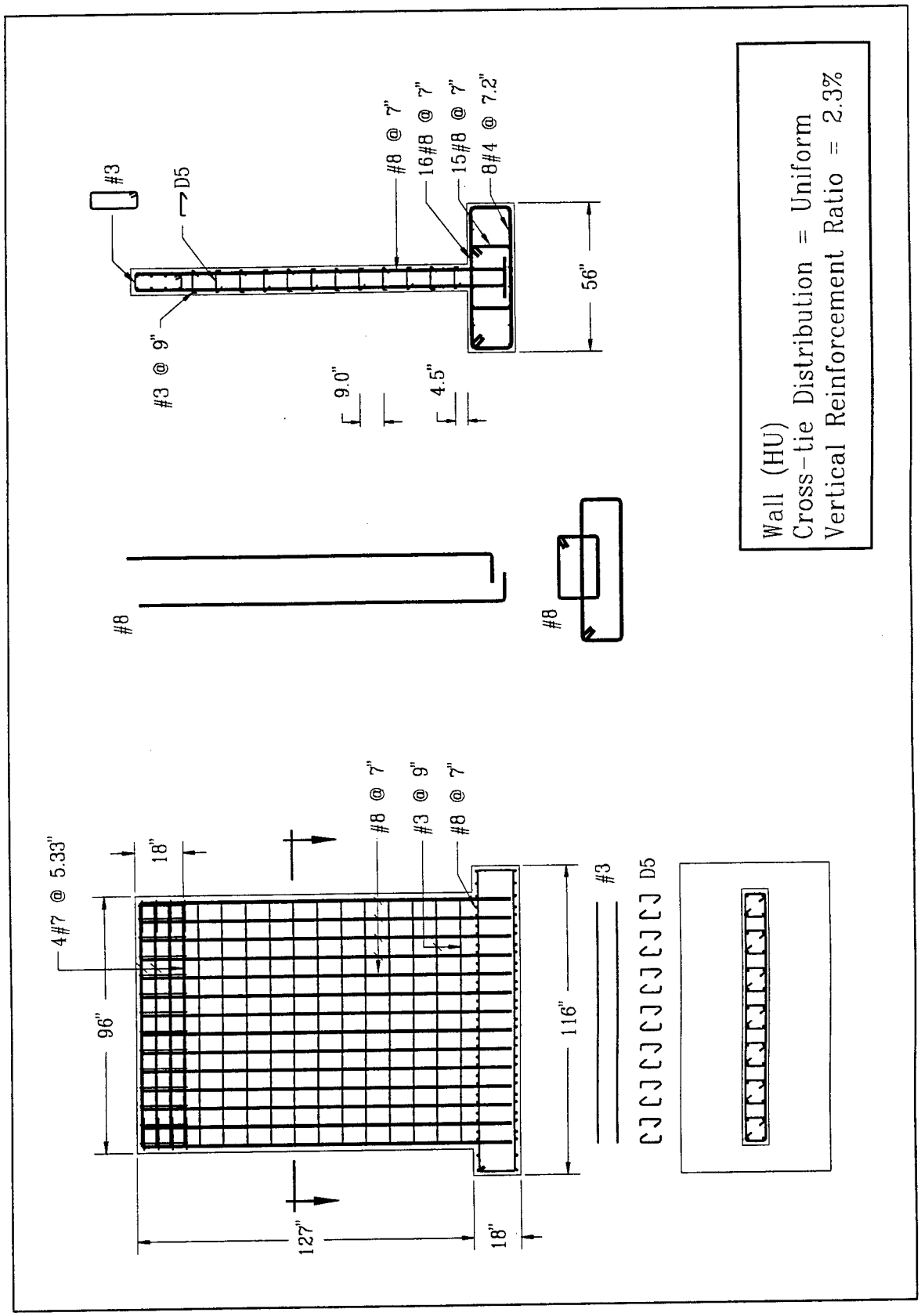

Figure 2.4: Reinforcement Details of the Original HU Wall

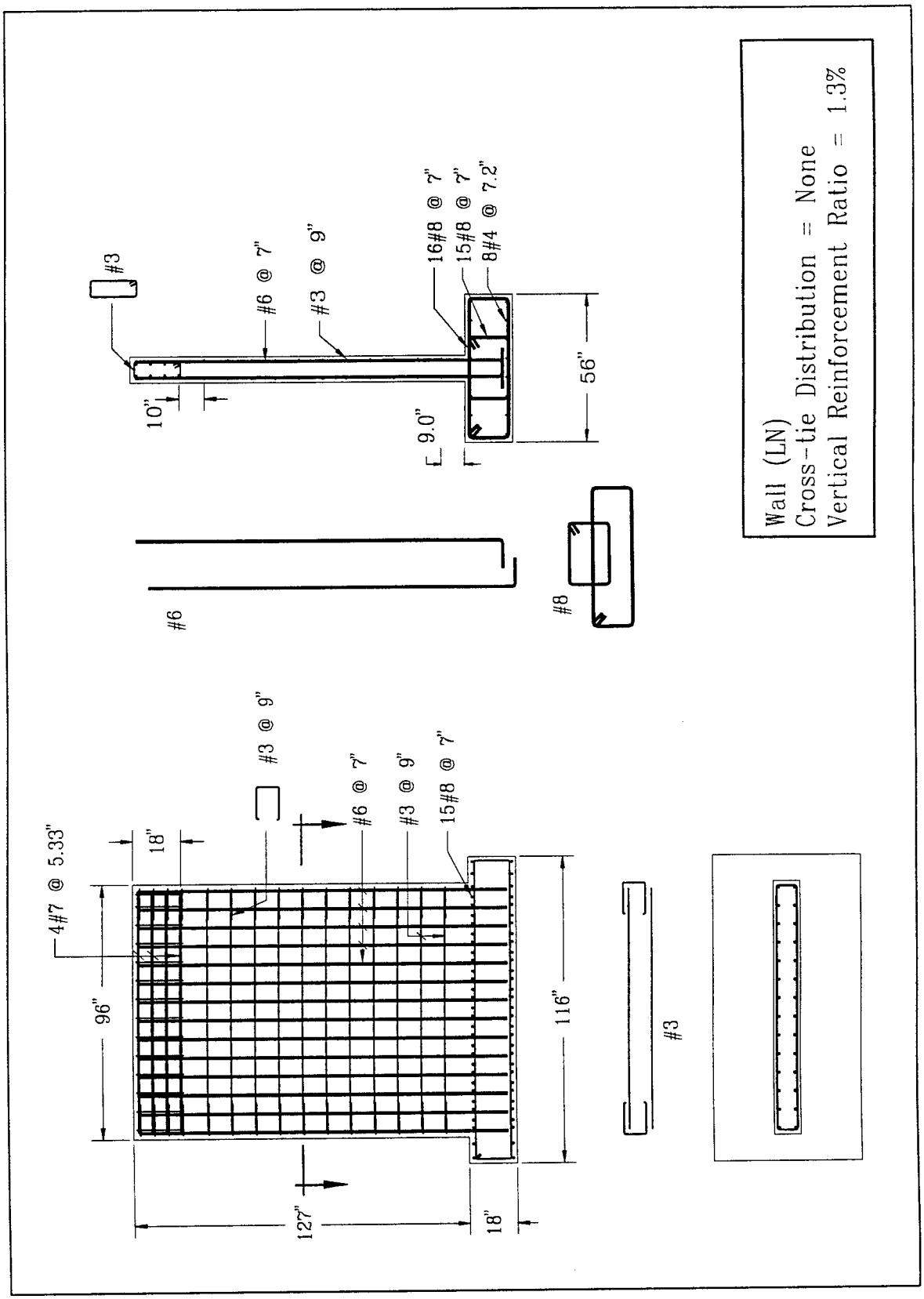

Figure 2.5: Reinforcement Details of the Original LN Walls

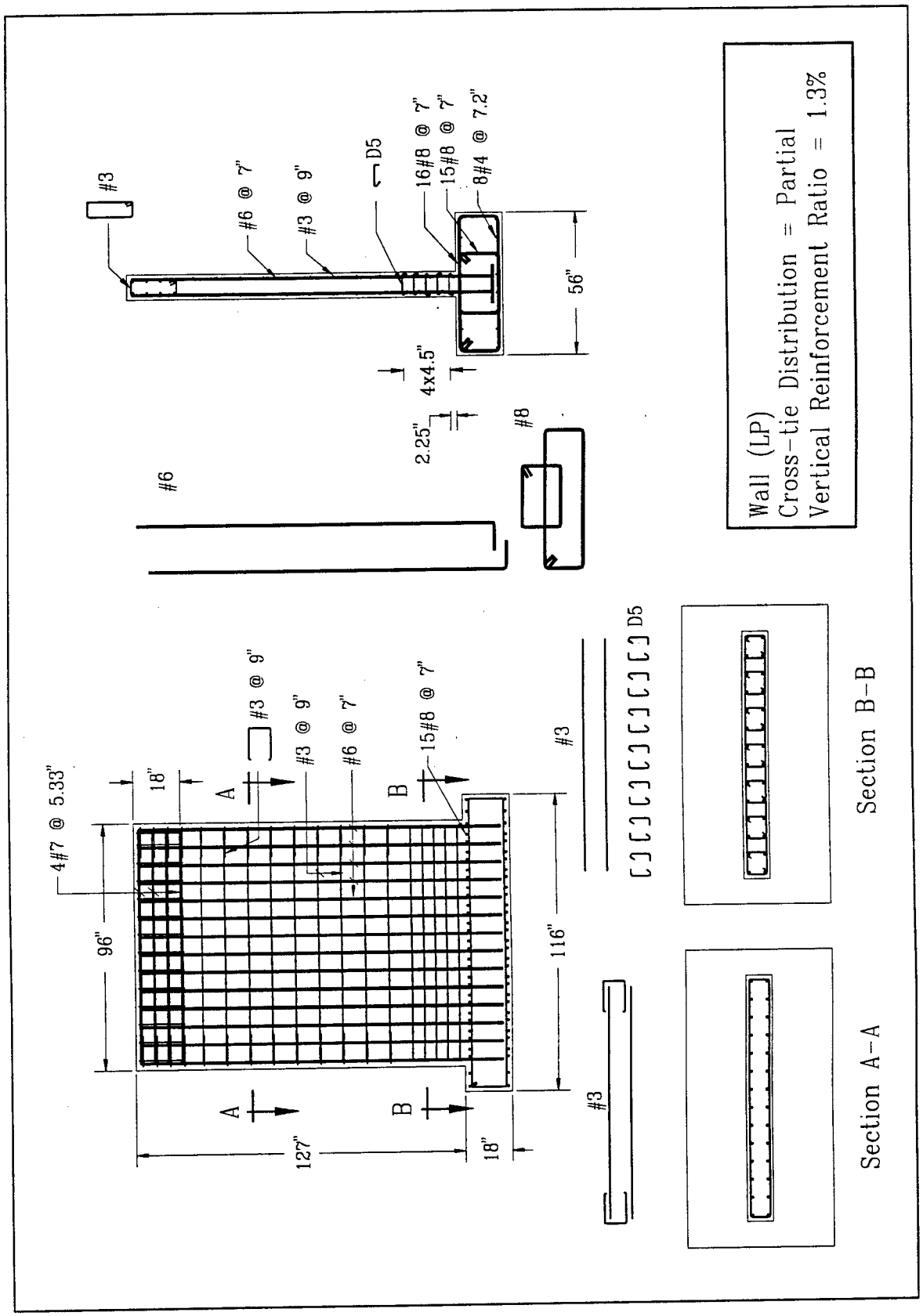

Figure 2.6: Reinforcement Details of the Original LP Wall

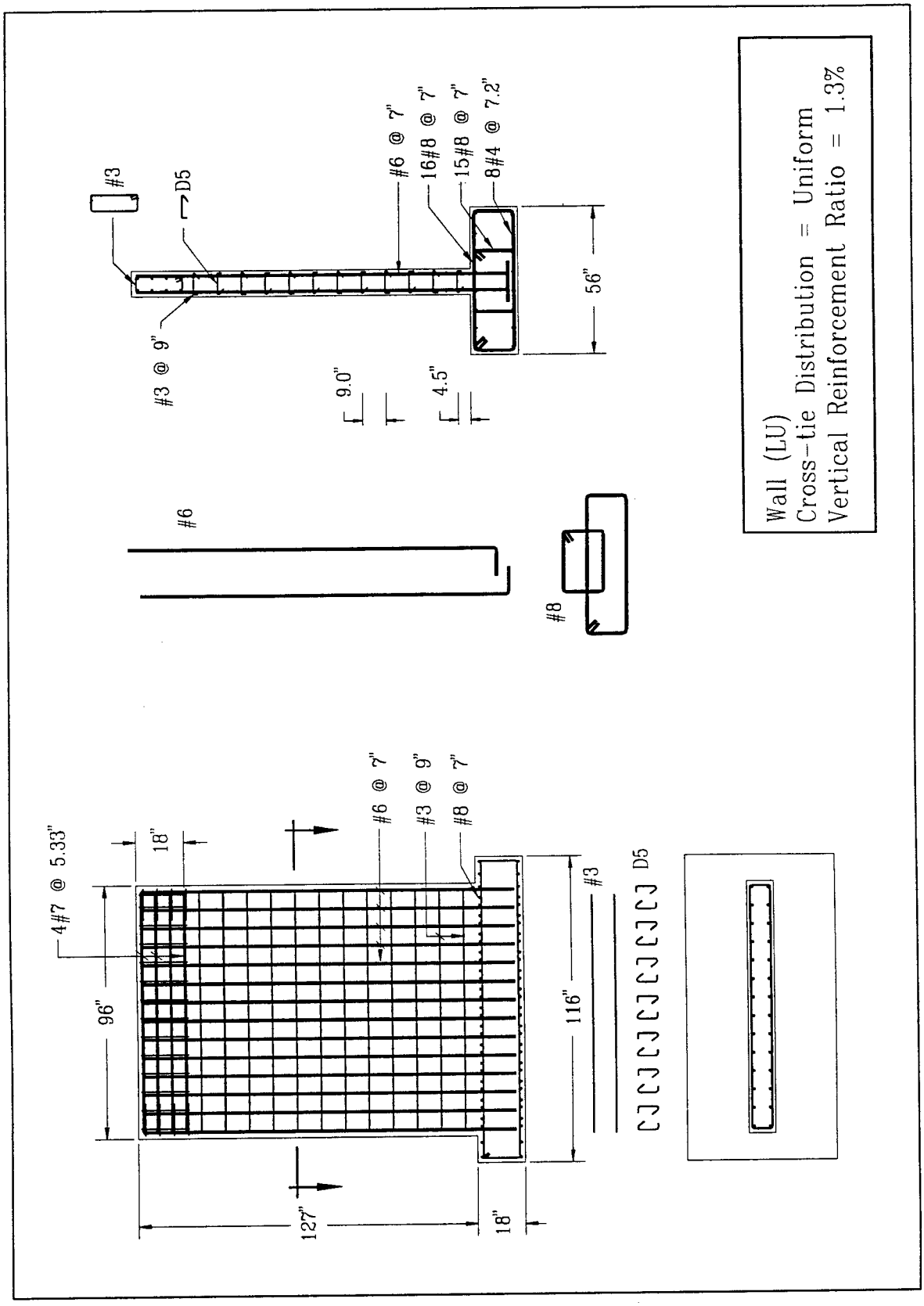

Figure 2.7: Reinforcement Details of the Original LU Wall

as no splitting of the concrete could be observed. In the HP pier wall, a vertical reinforcing bar was broken at the base of the wall.

The underlying theme behind the repair schemes was to remove the damage concrete in the plastic hinge zone, provide new horizontal reinforcement bars, provide more confinement in the damaged section of the walls and place new concrete in the damaged section. Two different cross-tie repair schemes were implemented in repairing the damaged pier walls. Five of the samples were repaired using a 90°/135° cross-tie configuration whereas the HN sample was repaired using a T-headed reinforcement bar as the cross-tie.

2.2.2 Vertical Reinforcement Damage and Repair

Nothing was done to repair or straighten the vertical reinforcement bars damaged in the original pier wall samples' tests. The buckled vertical reinforcement bars were left intact and were not straightened since it was assumed that it would be very difficult to straighten the buckled bars under field conditions. Since the buckled vertical reinforcement bars were not straightened, the width of the repaired pier wall samples had to be increased from that of the original width to accommodate the increased width due to the buckled vertical reinforcement. It should be noted that no appreciable vertical displacement was noted in the damaged walls due to the buckled vertical reinforcement. This increased pier wall width at the base is shown in Figure 2.8. The broken vertical reinforcement bar in sample HP was repaired by welding a segment of reinforcing steel in the fracture region in order to provide a contiguous vertical reinforcing bar.

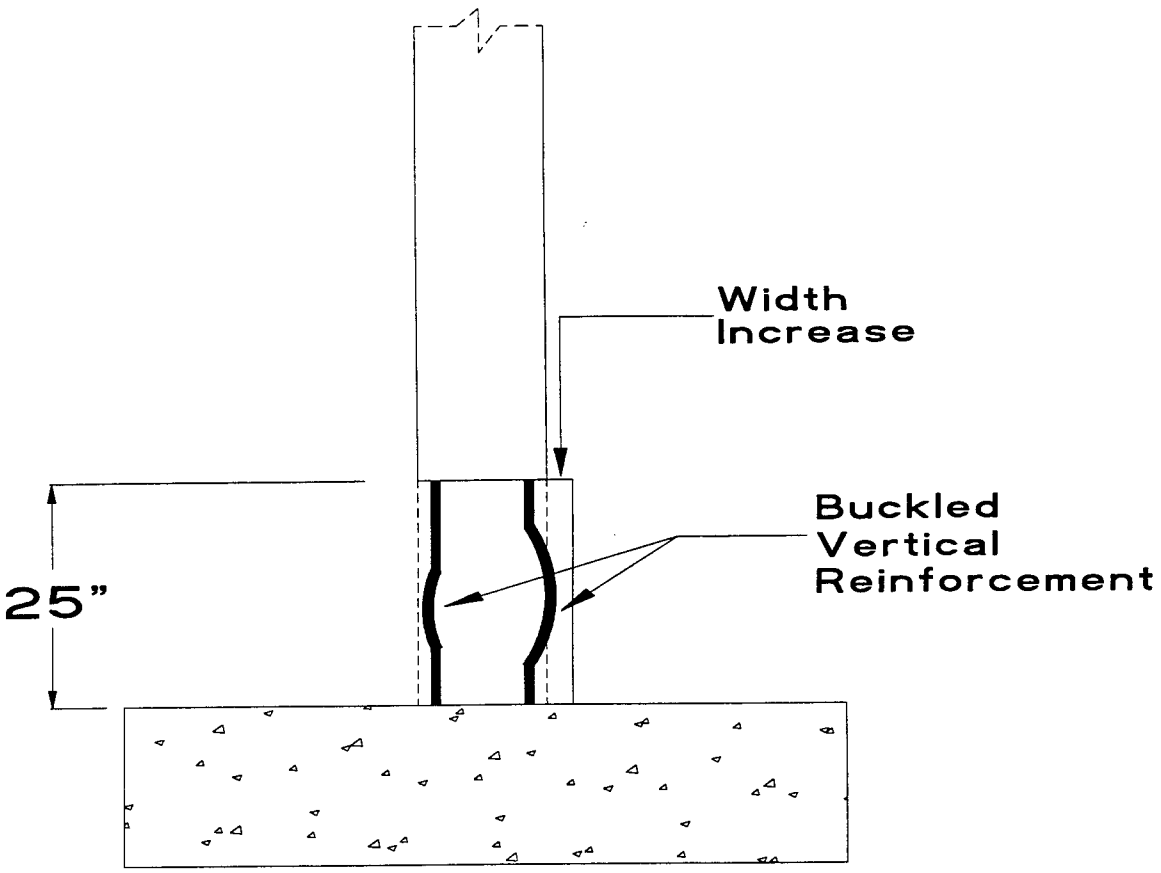

Figure 2.8: Vertical Reinforcement Bars

2.2.3 Horizontal Reinforcement Damage and Repair

In general the horizontal reinforcement remained intact as a result of the reversed cyclic loads. In the course of removing the damaged concrete in the plastic hinge zone, the horizontal reinforcement was also removed. Accordingly, a new cage consisting of horizontal reinforcement bars and cross-ties was constructed in the plastic hinge zone.

Analytical studies done by Mau [5] as well as Mau and El-Mabsout [6] concluded that the critical vertical spacing-to-diameter ratio should be between 5 to 7 for Grade 60 reinforcing steel. In their study, an inelastic finite element buckling analysis of reinforcing bars was performed to obtain the analytical results in concrete columns.

Taking the average of these two values, the critical vertical spacing-to-diameter spacing was chosen to be 6 in the re-built section. Based on this study and the horizontal spacing used with the original 'P' pier walls, the horizontal reinforcement in the repaired walls was spaced at an interval of 4.5 inches. However, the first horizontal reinforcement bar was placed at a nominal distance of 2.25 inches from the upper edge of the footing since the first layer of reinforcement is usually placed at a distance that is approximately half way between the regular spacing.

2.3 Cross-tie Repair Schemes

2.3.1 Repair Scheme 1: Enhanced Cross-tie

Based upon the less-than-satisfactory performance of the cross-ties from the previous pier wall tests, it was determined that the anchorage of the cross-tie legs was insufficient. In order to improve the anchorage performance of the 135° leg, the leg length of the original samples was increased to provide better anchorage in the pier wall's concrete core. The leg length of the 135° legs was doubled from the original length of 1.75 inches to 3.5 inches. The 90° leg was not changed. Since the concrete cover spalled after a couple of cycles, increasing the 90° leg length would not have been effective.

Additionally, two cross-ties with alternating 90° and 135° legs were provided at each horizontal/vertical bar intersection. This resulted in horizontal steel reinforcement ratio to be 0.32%. Figure 2.9 shows the difference in the arrangement of cross-ties between the enhanced cross-ties with alternating 90° and 135° legs and the original cross-ties. The dimensions of the original and the enhanced cross-ties are shown in Figure 2.10. A photograph of the cross-ties with alternating 90° and 135° legs is shown in Figure 2.11. The detailed drawings of Repair Scheme 1 are shown in Figure

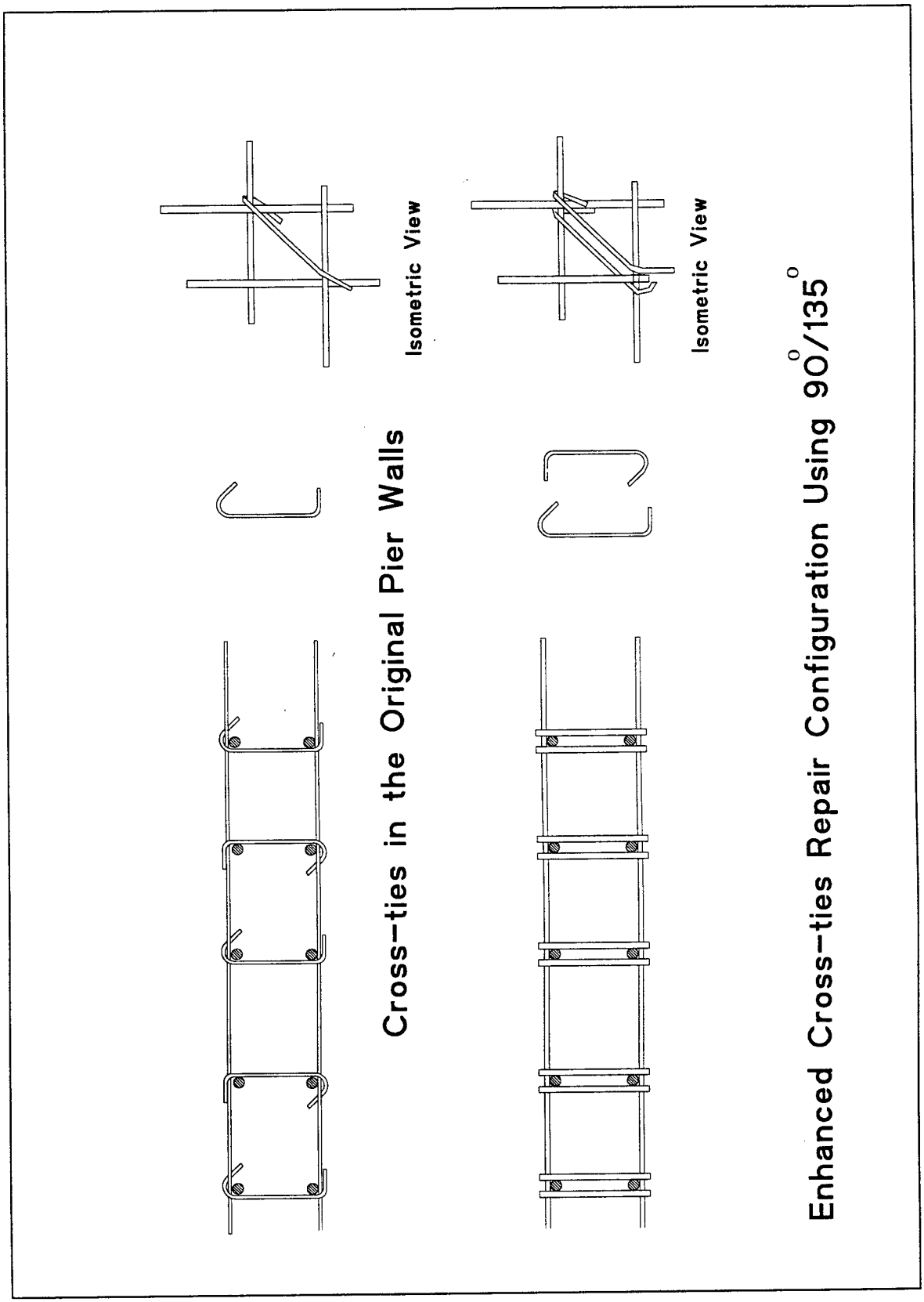

Figure 2.9: Different Cross-tie Configuration

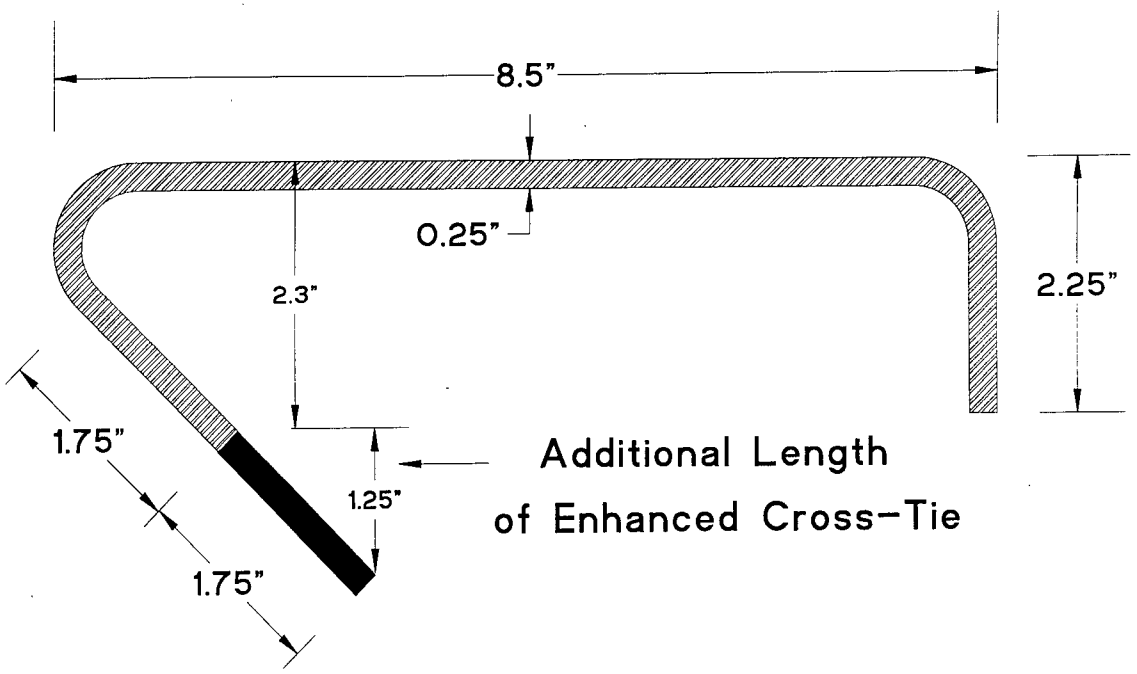

Figure 2.10: Dimensions of As-Built and Enhanced Cross-Tie

2.12.

2.3.2 Repair Scheme 2: T-Headed Cross-Ties

At Caltrans' suggestion, pier wall HN was repaired somewhat differently from the other five pier walls. This repair scheme was exactly the same as the previous repair scheme except that a different type of cross-tie was used in place of D5 with alternating 90°/135° cross-ties. A T-headed reinforcement scheme was used as the cross-tie in repairing the HN pier wall.

The T-headed reinforcement consisted of two square metal plates friction welded to either end of a section of standard reinforcing steel. The head of the T-headed reinforcement was a 2 inch × 2 inch square metal plate with a thickness of 0.5 inch. A standard #5 reinforcement bar was used as the stem. All T-headed cross-ties were of one standard length as shown in Figure 2.13. The length of the T-headed cross-

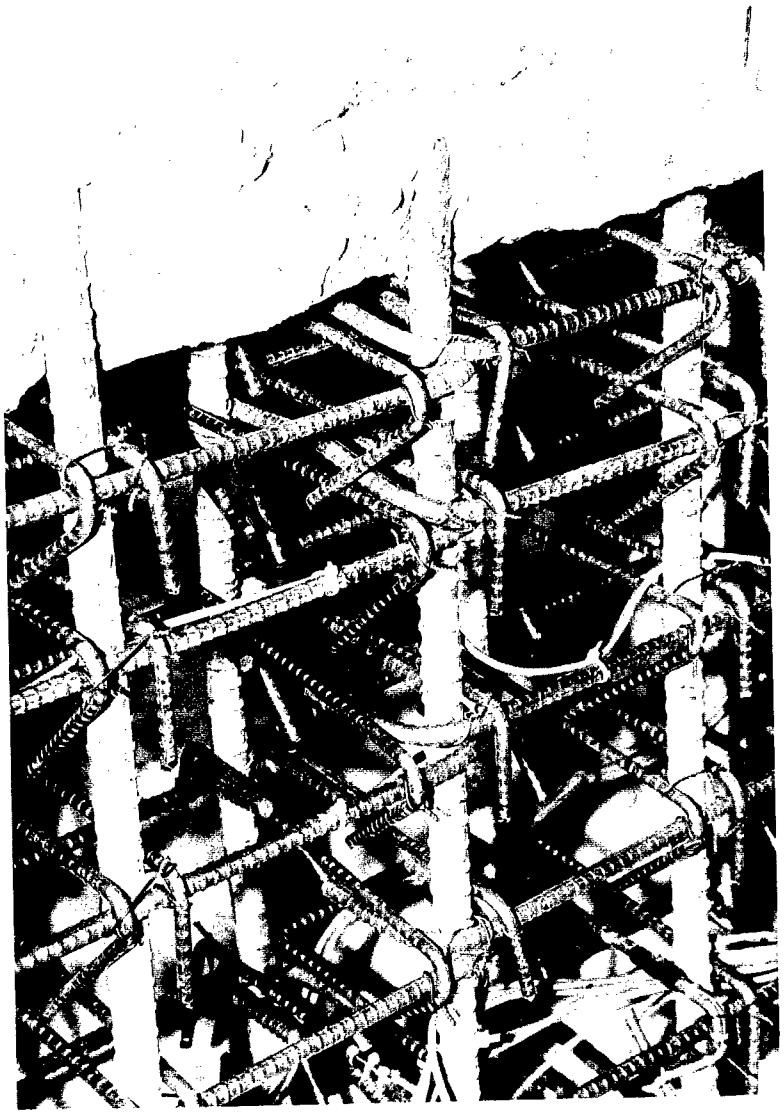

Figure 2.11: Cross-ties with Alternating 90° and 135° Legs

ties was chosen to fit the vertical reinforcement bar at the point of widest buckled shape. As a consequence some of the T-headed bars were longer than necessary. It was decided for ease of manufacturing, field inventory and installation that a single length T-headed cross-tie should be made.

The confinement provided by a T-headed reinforcement bar depends on the area

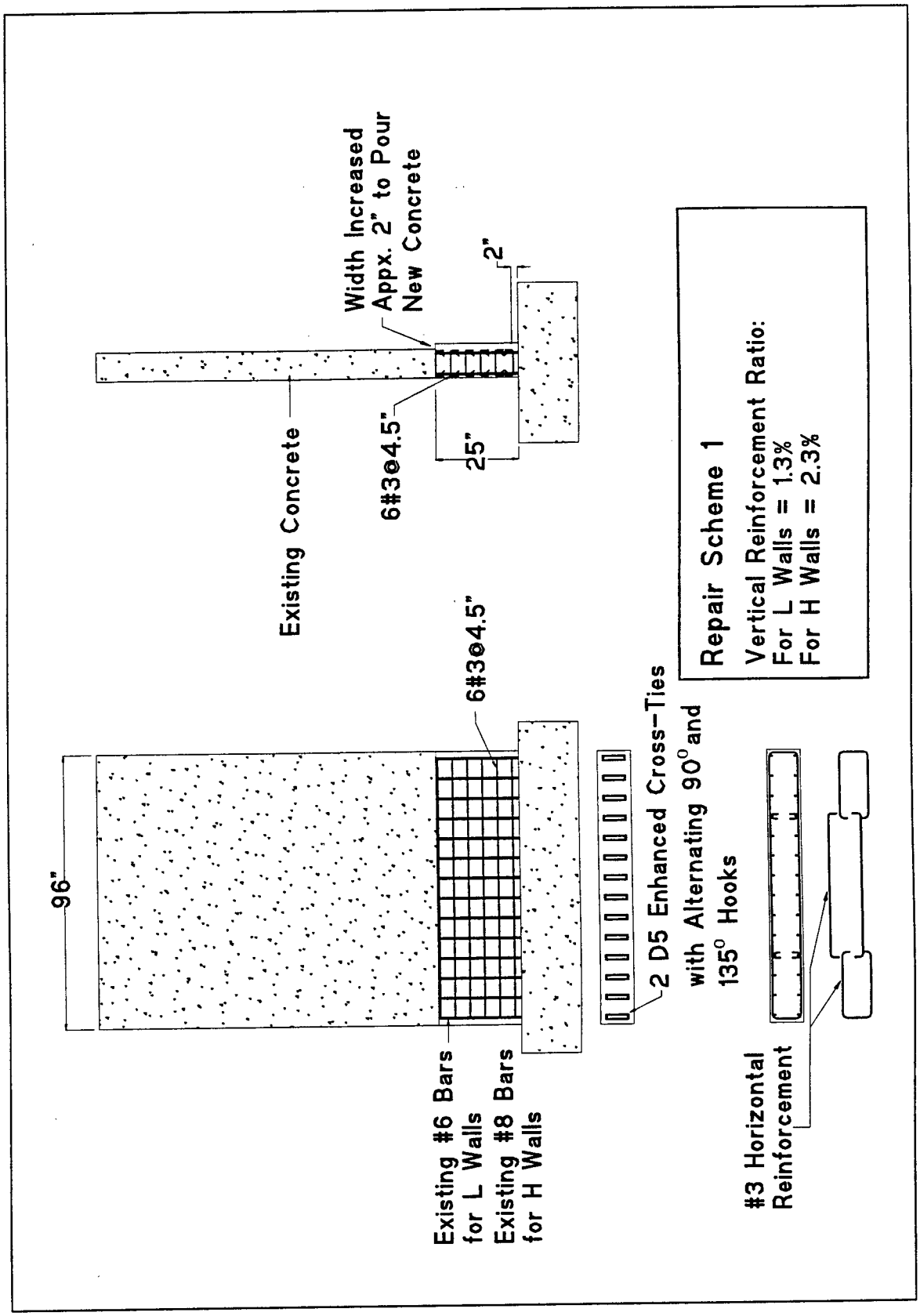

Figure 2.12: Repair Scheme 1

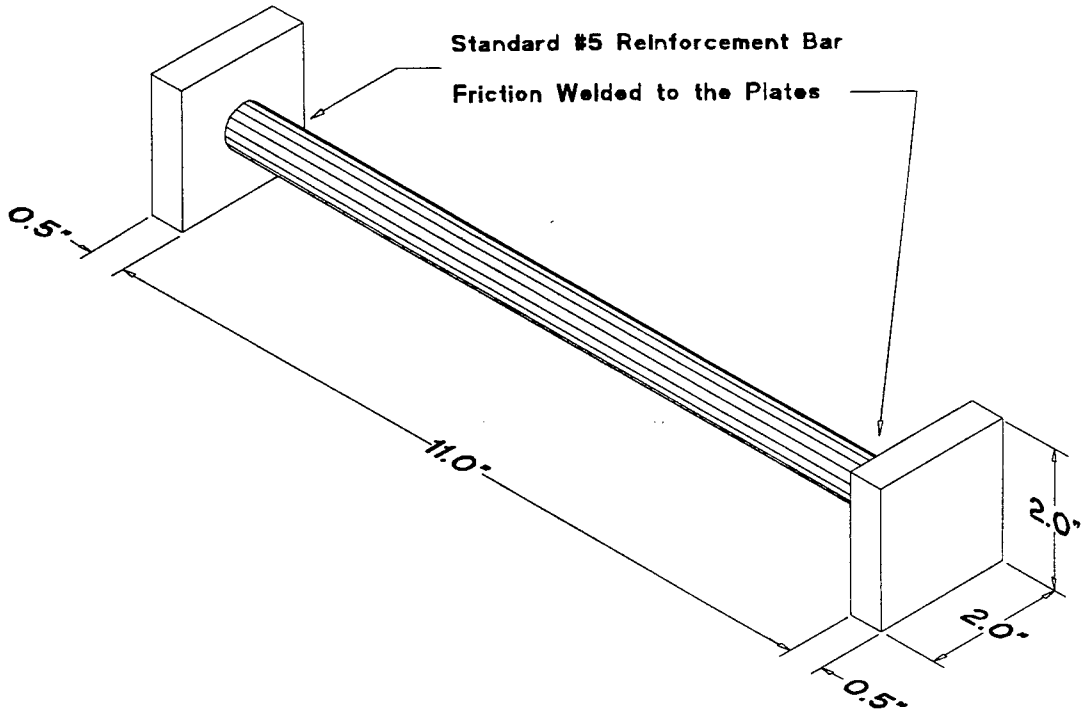

Figure 2.13: Dimensions of T-Headed Cross-Tie

of the head, the diameter of the bar as well as the horizontal and vertical spacing. Figure 2.14 shows two configurations of T-headed reinforcement and their respective confined regions. One configuration shows a dense distribution of the T-headed cross-ties while the other configuration shows a sparse distribution [7]. The repaired pier wall sample HN more closely resembled the configuration with a sparse T-headed reinforcement. The ratio of $A_h/A_b = 13$ used in the repaired pier wall is based upon a plate area (A_h) of 4.0 square inches and a bar area (A_b) of 0.31 square inches. The vertical and horizontal spacing of the T-headed cross-ties was 4.5 inches and 7.0 inches, resulting in a confinement steel ratio of 1.0%. Repair Scheme 2 is shown in Figure 2.15.

The damaged sample pier walls were repaired using either Repair Scheme 1 or Repair Scheme 2. These repair schemes were chosen as the most practical when implemented under field conditions. Several other repair schemes were considered

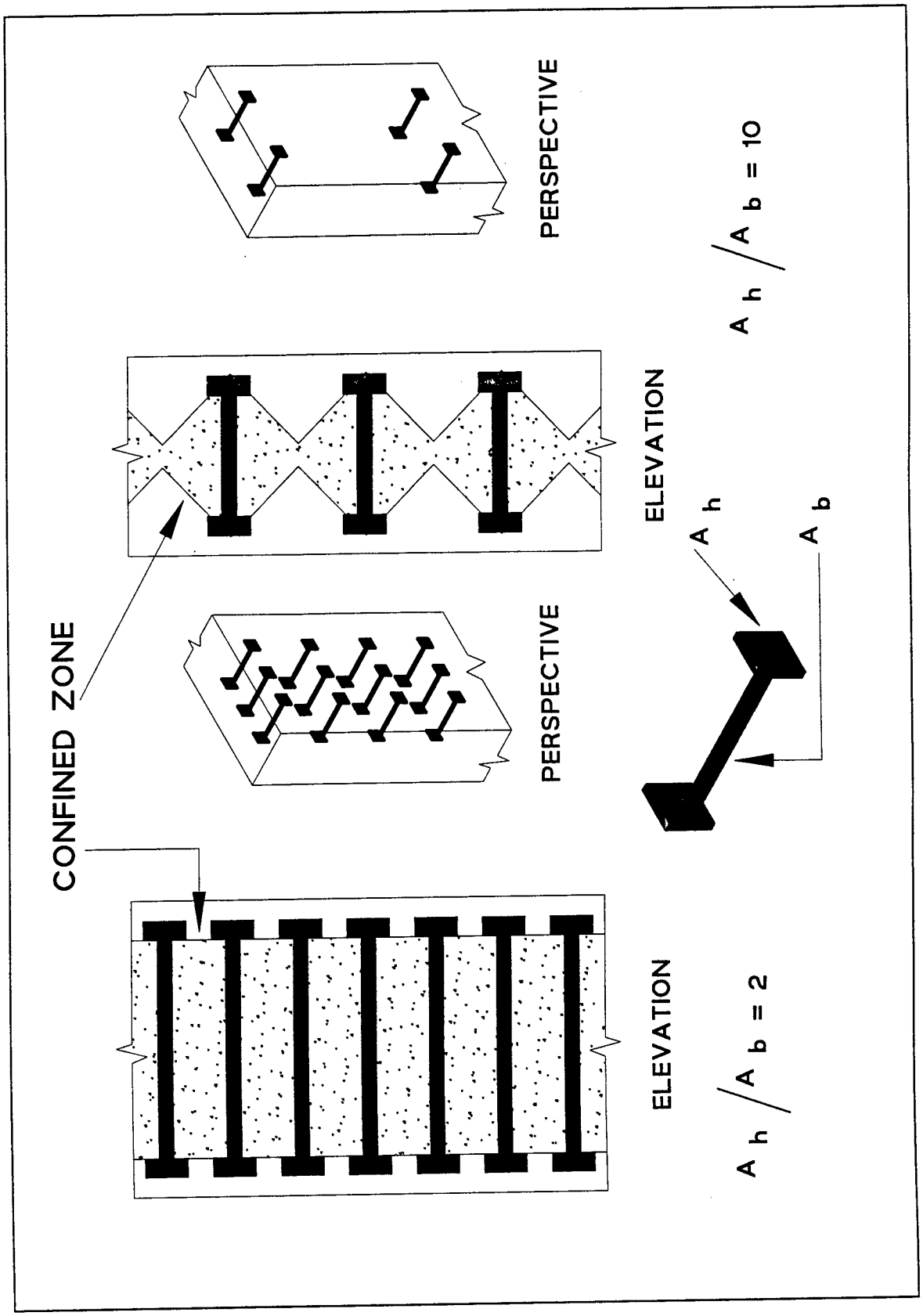

Figure 2.14: Different T-Headed Confinement Reinforcement Configurations

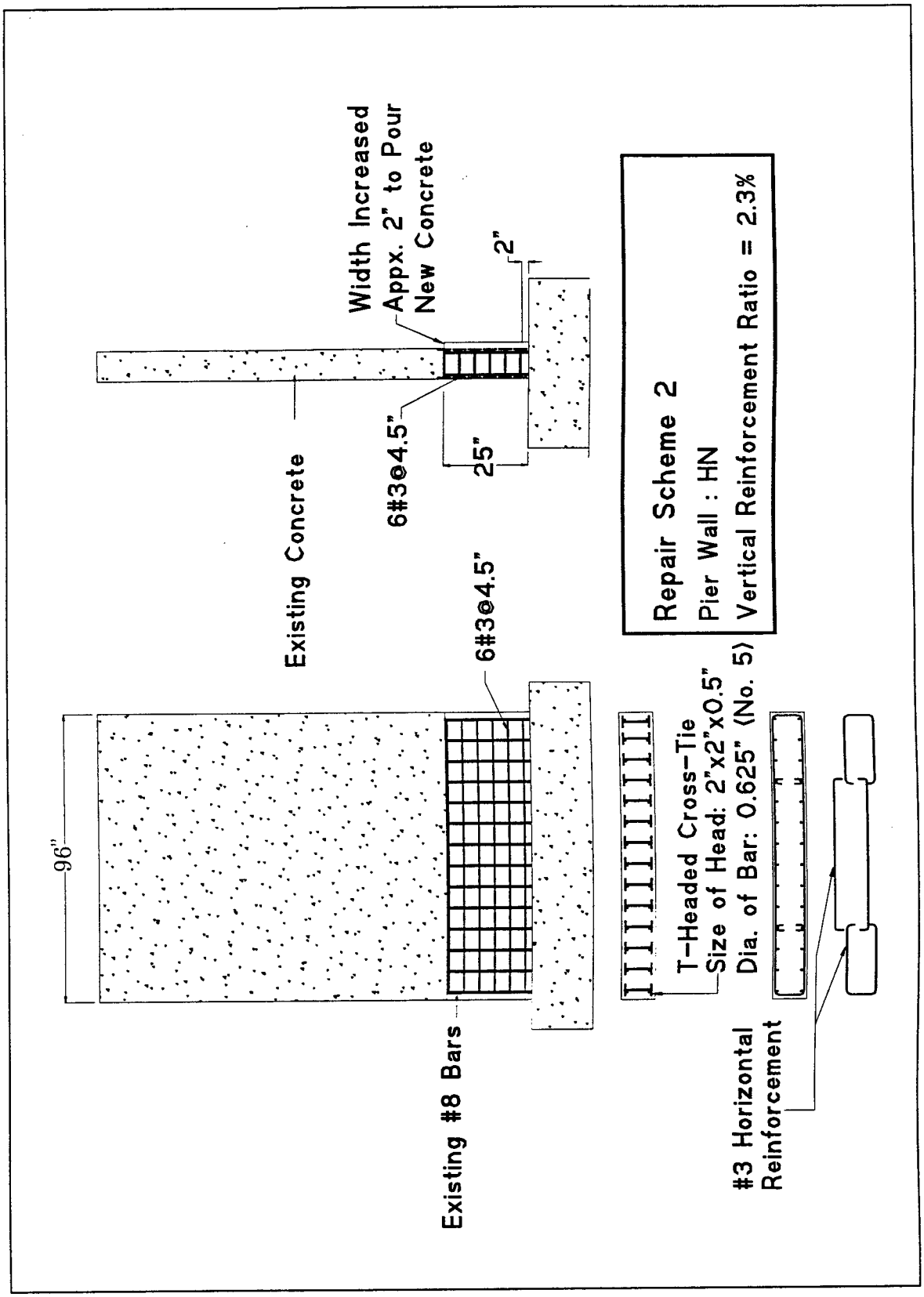

Figure 2.15: Repair Scheme 2

but these were rejected as being either too difficult to install in the field or adversely increasing the pier wall thickness in the plastic hinge zone.

Chapter 3

Pre-Test Pier Wall Preparation

This chapter describes the pier wall repair process, the properties of the materials used in the repair, the test setup, the instrumentation used in the pier wall tests as well as the test procedure itself.

3.1 Repair of Each Pier Wall's Damaged Region

Each pier was repaired by removing the concrete in the lower 20% of the wall, providing new horizontal and cross-tie reinforcement as well as placing new concrete in the formerly damaged region. With little exception the repair process was similar for all six damaged pier wall samples.

The damaged bottom portion of each pier wall sample was entirely removed by chipping away the cracked concrete to a height of 25 inches from the top of the footing. Although the removal of the damaged concrete was a significant step in each pier wall's repair, the task was an extremely labor intensive, dirty and tiresome process. This task could be a factor in deciding whether an earthquake damaged pier wall should be repaired or completely rebuilt.

Each pier wall sample was shored prior to the debris removal process. Shoring was provided to (a) simulate a field repair condition, (b) prevent further buckling of the

vertical reinforcement bars, and (c) establish a safe and secure environment for the laboratory workers who repaired the damaged pier wall.

Once the damaged concrete was removed from the lower portion of the pier wall sample, the horizontal reinforcement and cross-ties were placed. The 25 inch repair height zone — a few inches more than the predicted plastic hinge length of 21.25 inches — enabled six layers of horizontal reinforcement to be placed. Strain gages were mounted at strategic locations on the horizontal and vertical bars as well as the cross-ties. The strain gage cables were bundled together and threaded through a PVC pipe to the exterior of the wall.

Plywood forms were built around the entire bottom of the pier wall to provide an enclosure for the new concrete. The three sides of the pier wall were made flush with the previous dimensions while one of the sides was slightly increased by approximately 2 inches to provide sufficient cover for the buckled vertical bars. This procedure resulted in the rebuilt lower section having the same dimensions as the original wall except for the one side which was slightly wider. Two 'trap door' chutes were provided to enable placement of the new concrete. The 'trap doors' were of sufficient size to (a) accommodate the hose used to pour concrete into the enclosed section and (b) permit a vibrator to be inserted in order to compact the pumped concrete. This repair detail is shown in Figure 3.1.

3.2 Concrete and Steel Material Properties

The cross-ties in the repaired samples were made from Grade 90 D5 wire whereas Grade 60 steel was used as the horizontal reinforcement. The yield stress and the ultimate tensile strength values for both the cross-ties and the horizontal reinforcement, shown in Table 3.1, were obtained from the supplier, Rebar Engineering.

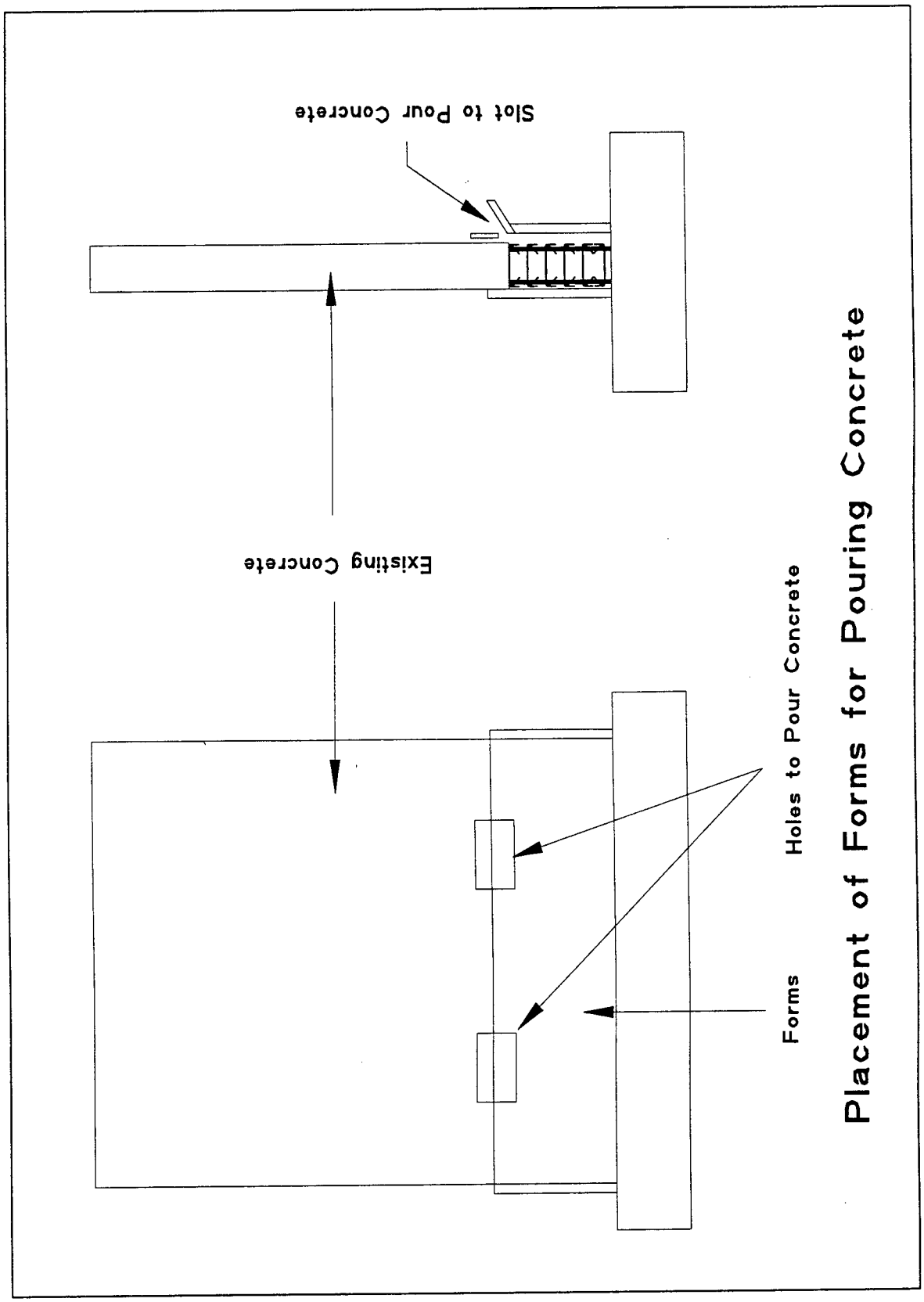

Figure 3.1: Formwork to Pour Concrete

Reinforcement Type	Grade	Yield Stress (ksi)	Ultimate Tensile Strength (ksi)
D5 Wire	90	96	101.5
#3 Bar	60	68	106

Table 3.1: Yield and Ultimate Tensile Stress of the Steel Reinforcement

A pea gravel concrete mix with the nominal strength $f_c^{'} = 4000$ psi was used to repair all six samples. Four different batches of concrete mix were used in repairing the samples. The slump and compressive strength for each different batch and the corresponding repaired pier wall sample are shown in Table 3.2. A 7.5 sack mix was utilized to obtain the nominal concrete strength of 4000 psi. The mix proportions are as follows:

Cement	705 pounds/yard^3
Water	48 gallons/yard^3
Sand	1835 pounds/yard^3
3/8 inch Pea Gravel	975 pounds/yard^3
Water Reducing Admixture (WRDA79)	35.25 fluid ounces/yard^3
w/c	0.57
Expected Slump	5 inches

Slump tests were performed on three different batches of the pumped concrete. These results are also tabulated in Table 3.2. Standard cylinder samples, (6.0 inches in diameter, 12.0 inches in height) were made from the different batches and tested in compression. Three cylinders from each batch were tested on the seventh and twenty-eighth day after the pour as well as on the day of the pier wall test itself. There are no results for Batch No. 1 and Batch No. 2 for the test day since the LU pier wall sample was tested on the twenty-ninth day following the pour whereas the HU pier wall sample was tested on the twenty-eighth day following the pour. The results from the compressive cylinder tests are also presented in Table 3.2.

Batch No.	Slump (inches)	Pier Wall Samples	Tested on (Day)	f_c'(psi) for Sample No.			Mean (psi)
				1	2	3	
1	NA	LU	7^{th}	3460	1768	2865	2700
			28^{th}	4490	3785	4740	4340
2	5	HU	7^{th}	3430	3610	3360	3470
			28^{th}	4420	4770	5130	4770
3	7	LN,LP,HP	7^{th}	2900	3000	3000	2970
			28^{th}	3900	4350	4070	4110
		LN	33^{th}	4280	4320	4350	4320
		LP	39^{th}	4350	4070	3890	4100
		HP	41^{th}	4030	3890	4070	4000
4	6	HN	7^{th}	2970	3250	3530	3250
			28^{th}	4390	5130	4950	4820
			29^{th}	4700	4775	5164	4880

Table 3.2: Slump and Compressive Strength for Different Concrete Batches

3.3 Test Setup

All six pier wall samples were fixed to the strong floor of the UCI Structural Test Hall by anchoring the footing with twelve 1.25 inch diameter high strength bars. Thick plates were used as washers with the bars to prevent any local crushing of the concrete footing due to the high bearing stress caused by the tensioning forces.

A simulated dead load on five of the six pier wall samples was provided by pre-stressing the samples with high strength bars. In order to assess the effect of dead load on the pier wall's flexural behavior, the sixth pier wall was subjected to horizontal cyclic loading without the simulated dead load.

A steel section fabricated from channels and plate sections was used as a load cap to uniformly distribute the compressive axial load to the five pre-stressed pier wall samples. Two 1.5 inch diameter steel bars were used to apply axial loads. These bars were attached to a hinge mechanism placed on top of the footing at one end and passed through a hollow hydraulic actuator placed on top of the load cap at the

other end. The hinge mechanism was provided to reduce the bending effects on the two bars due to large displacement at the top of the wall.

The axial compressive stresses were transmitted to the pier wall by tensioning two 1.5 inch diameter high strength bars with the hydraulic actuator placed on top of the load cap. The bars were tensioned to produce axial loads approximately equal to 5% of the calculated axial load capacity of the wall. A 155-kip Ortman hydraulic actuator with a long stroke ($\approx \pm 16$ inches) was attached to the top of the pier wall sample at a height of 118 inches from the top of the base of the wall to apply the horizontally cycled load. One end of the actuator was mounted to the strong wall while the other end was attached to the surface of the pier wall. Both ends of the actuator had pinned connections and were free to rotate. The pier wall sample under this test setup behaved as a cantilever driven by a reversed horizontal load under a constant compressive axial load.

The test setup for repaired pier wall LN was slightly different from the other five in that no axial load was imposed on the sample. Accordingly, the mechanisms used to apply the axial load — the load cap, the two 1.5 inch diameter bars, the actuators on top of the load cap, the hinge on top of the footing — were not utilized. However the rest of the test setup for pier wall LN was exactly the same as that of the other five samples. Figure 3.2 shows the test setups corresponding to the presence or absence of the axial load.

3.4 Instrumentation

In order to acquire data generated during the testing of each repaired pier wall sample, various components of the sample were electronically monitored. A load cell was mounted on the hydraulic actuator to measure the applied lateral loads. Seven

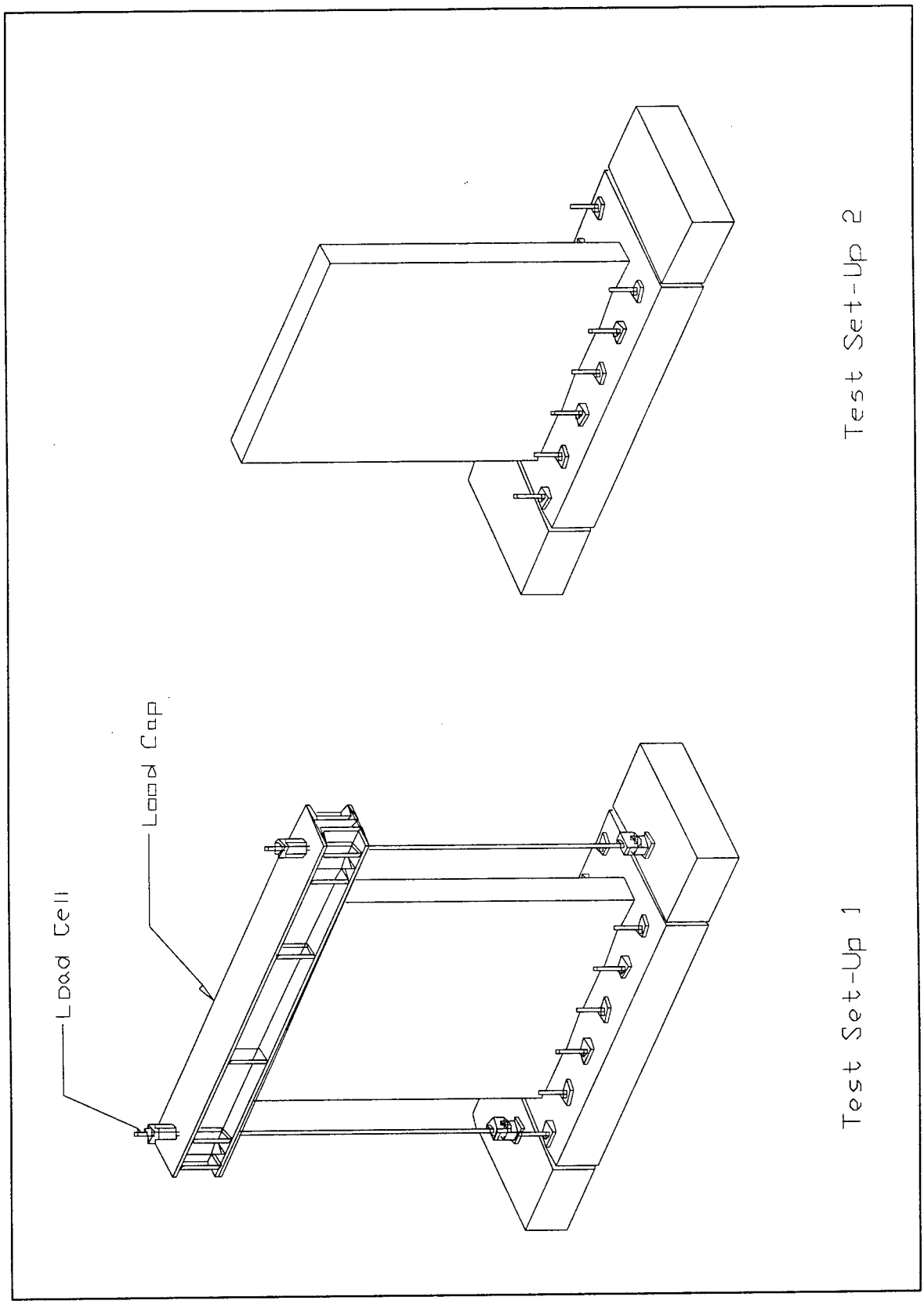

Figure 3.2: Test Setup 1 and 2

string potentiometers were installed to measure the horizontal displacements along the height of the wall. This instrumentation setup is shown in Figure 3.3.

Strain gages were used to measure the strains in various steel reinforcement bars. Strain gages were also attached to the cross-ties. The number and location, along with the designation of the strain gages for vertical, horizontal and cross-ties are shown in Figures 3.4 to 3.10. No strain gages were utilized in repaired sample LN because the objective was testing the sample without applying any axial load and comparing the results with the original sample to observe the effect of axial load. Additionally strain gages were placed only on the cross-ties in repaired sample HN. In general all signals from the gages were first amplified and conditioned and then connected to the data logging system.

A Strawberry Tree T51 data logging system, with an 8-channel terminal board, was used to collect the analog input signals. The terminal board, in turn, was connected to the Strawberry Tree analog-to-digital card within a Macintosh computer. Typically Strawberry Tree's Workbench data acquisition software was used to gather and log the data for the duration of each test. The Workbench program was setup to continuously log the applied load of the hydraulic actuator and the displacements of the string potentiometers as well as the signals from the strain gages.

3.5 Test Protocol / Test Procedure

A primary objective of the test program was to compare the performance between the original and the repaired pier wall samples. In order to properly compare the original and the repaired samples, the same displacement test protocol used in the original samples was applied to the repaired pier walls. With the exception of the LN wall which had no axial load applied, the test procedure for the other five pier wall

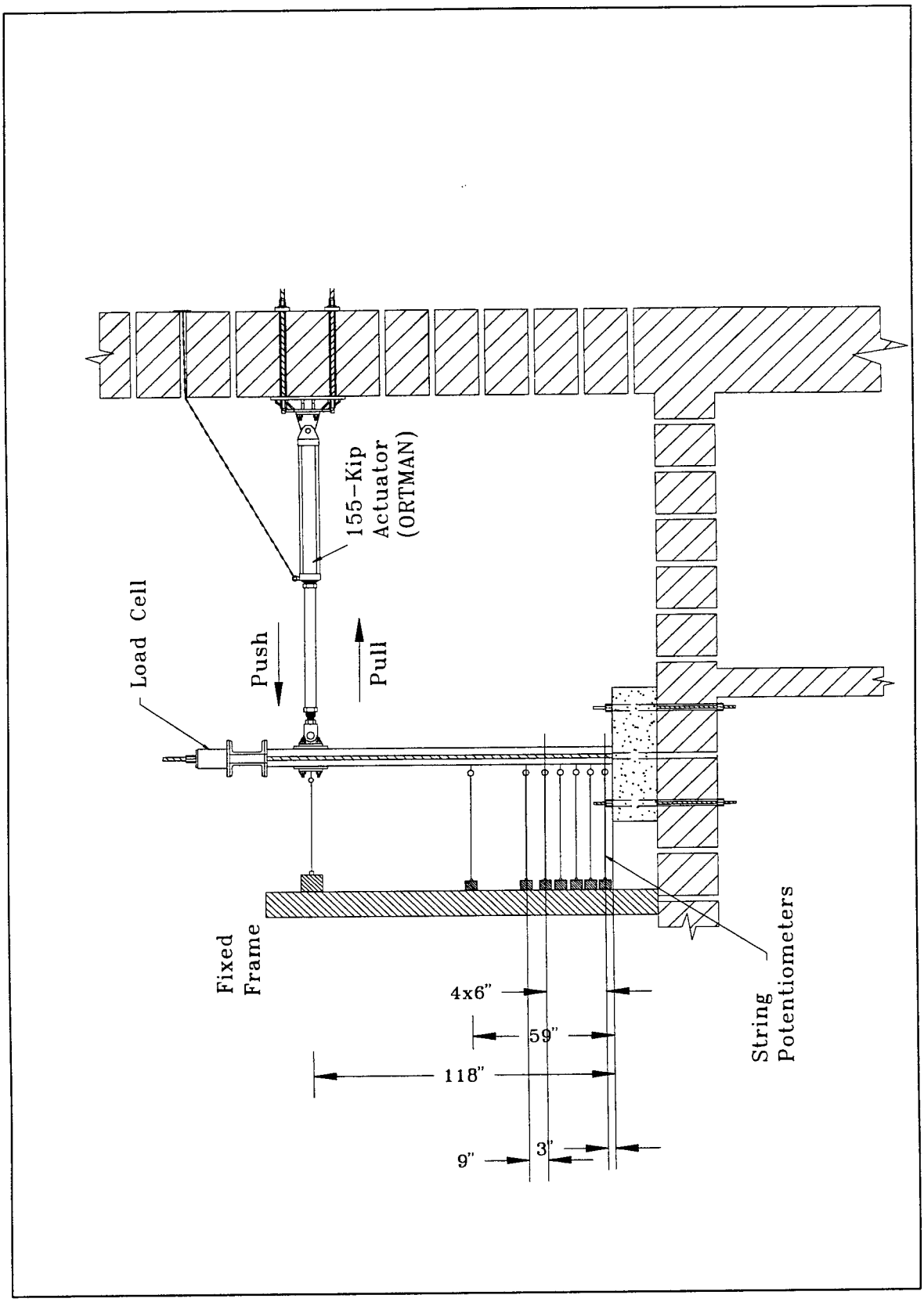

Figure 3.3: Instrumentation

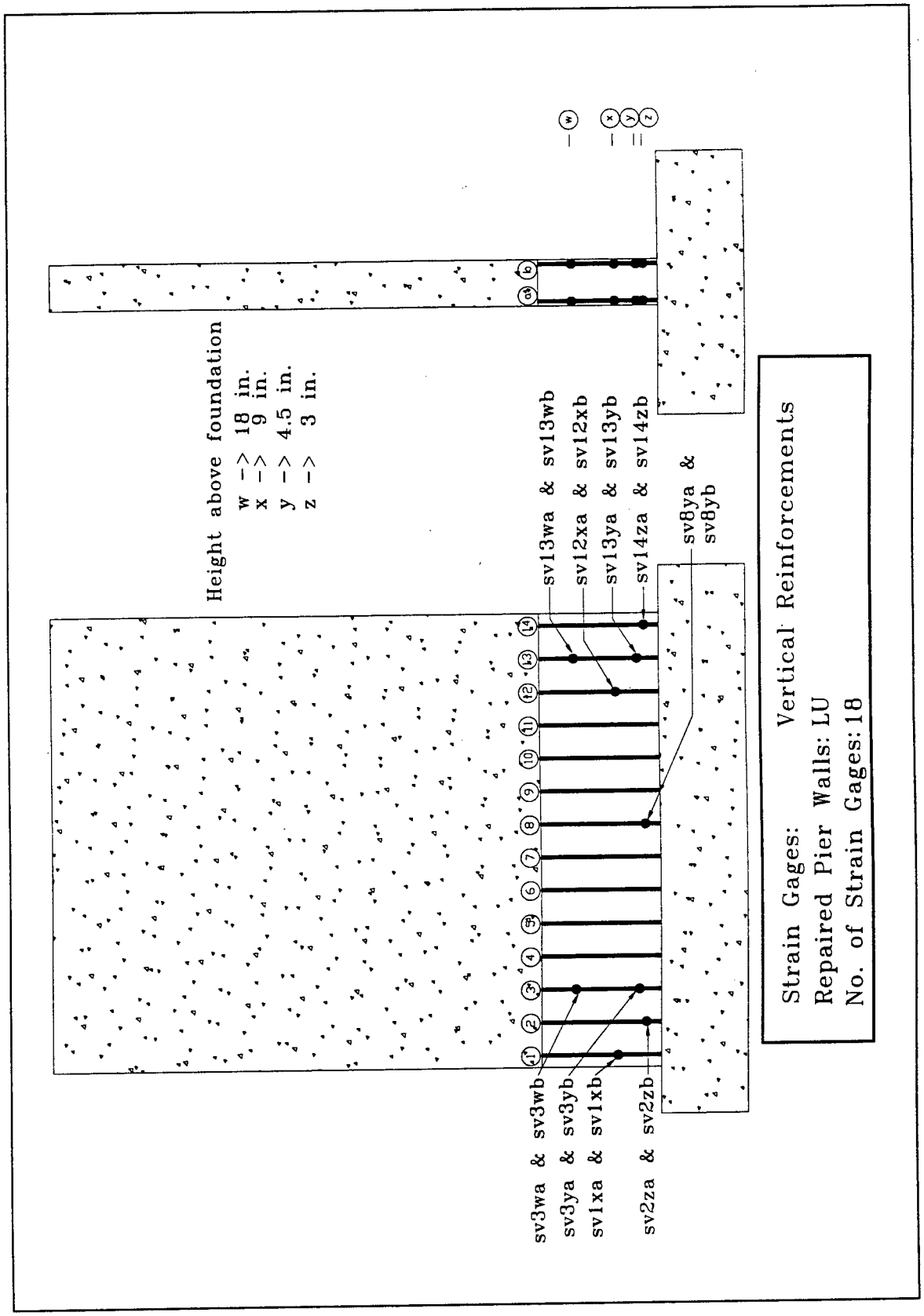

Figure 3.4: Strain Gages on the Vertical Reinforcements for LU Wall

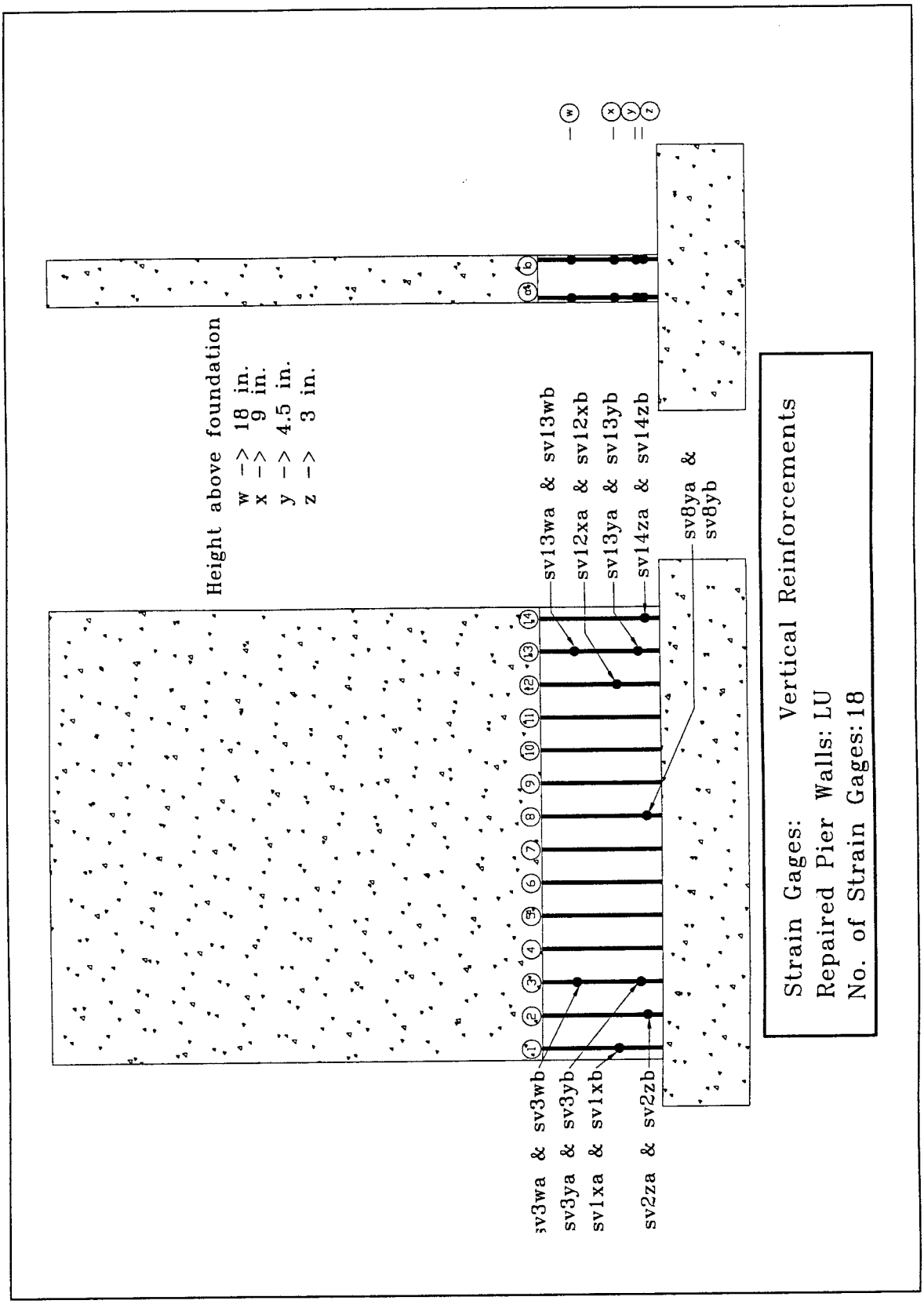

Figure 3.5: Strain Gages on the Vertical Reinforcements for LU, HU and HP Walls

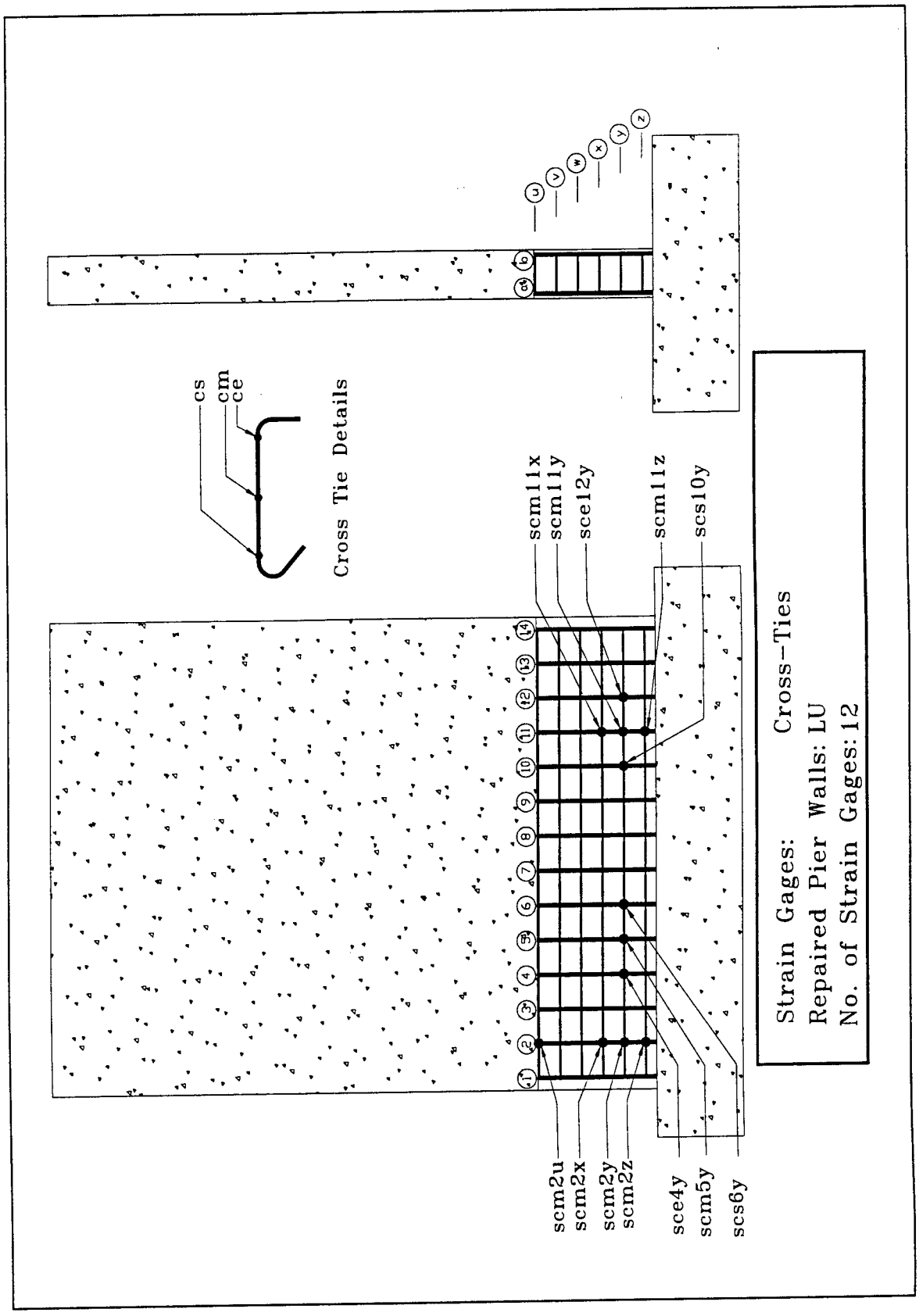

Figure 3.6: Strain Gages on the Cross-ties for LU Wall

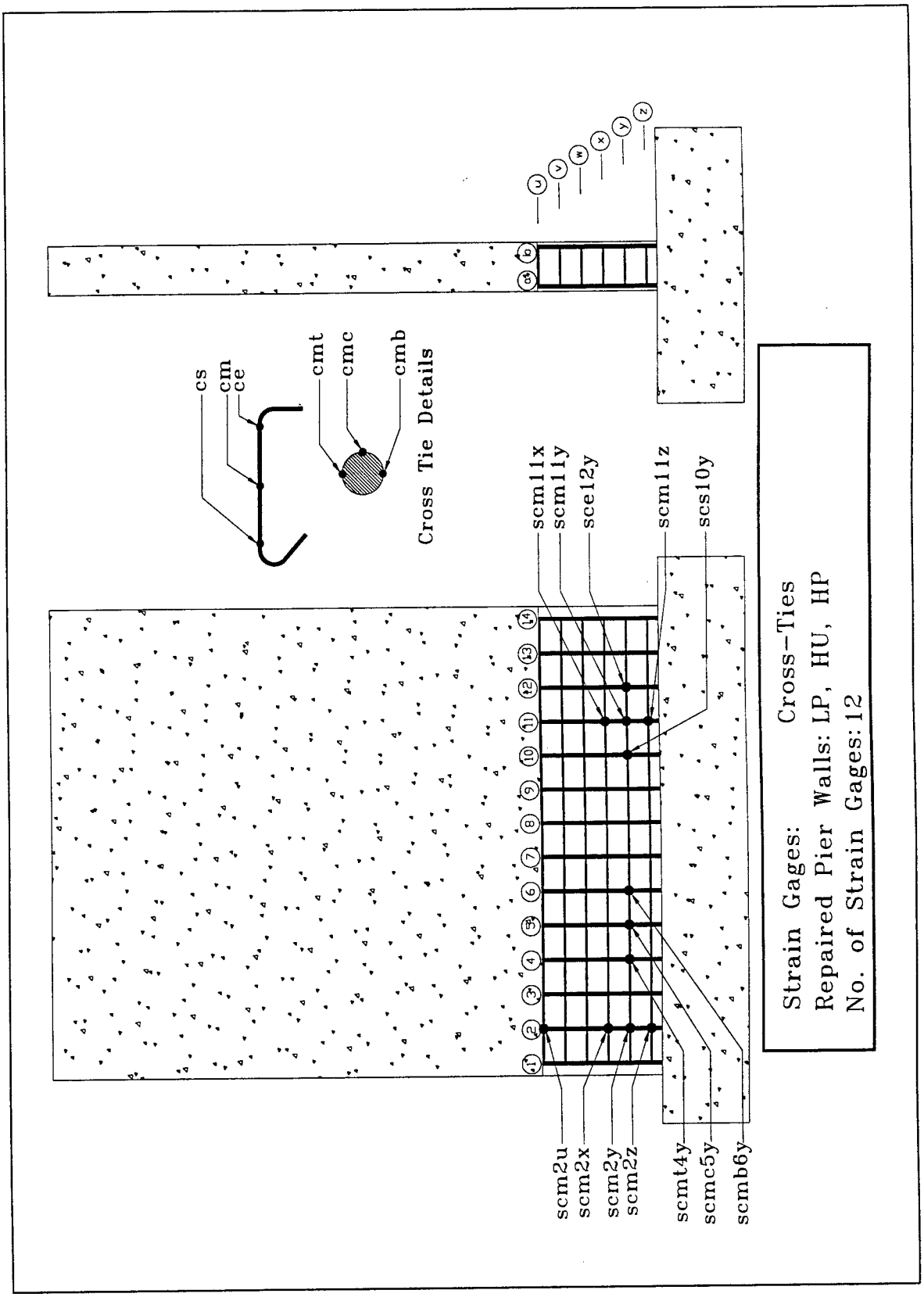

Figure 3.7: Strain Gages on the Cross-ties for LP, HU and HP Walls

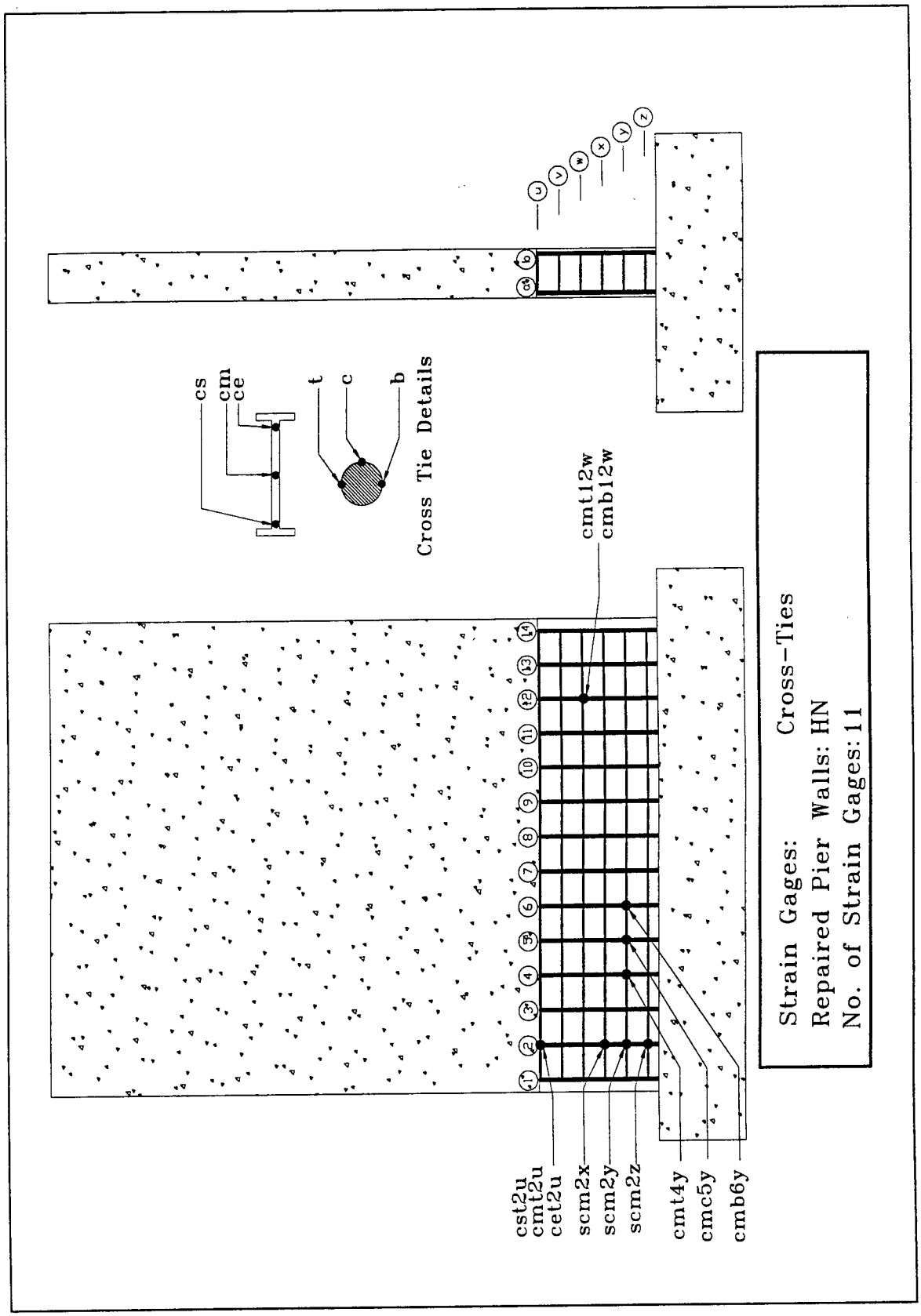

Figure 3.8: Strain Gages on the Cross-ties for HN Wall

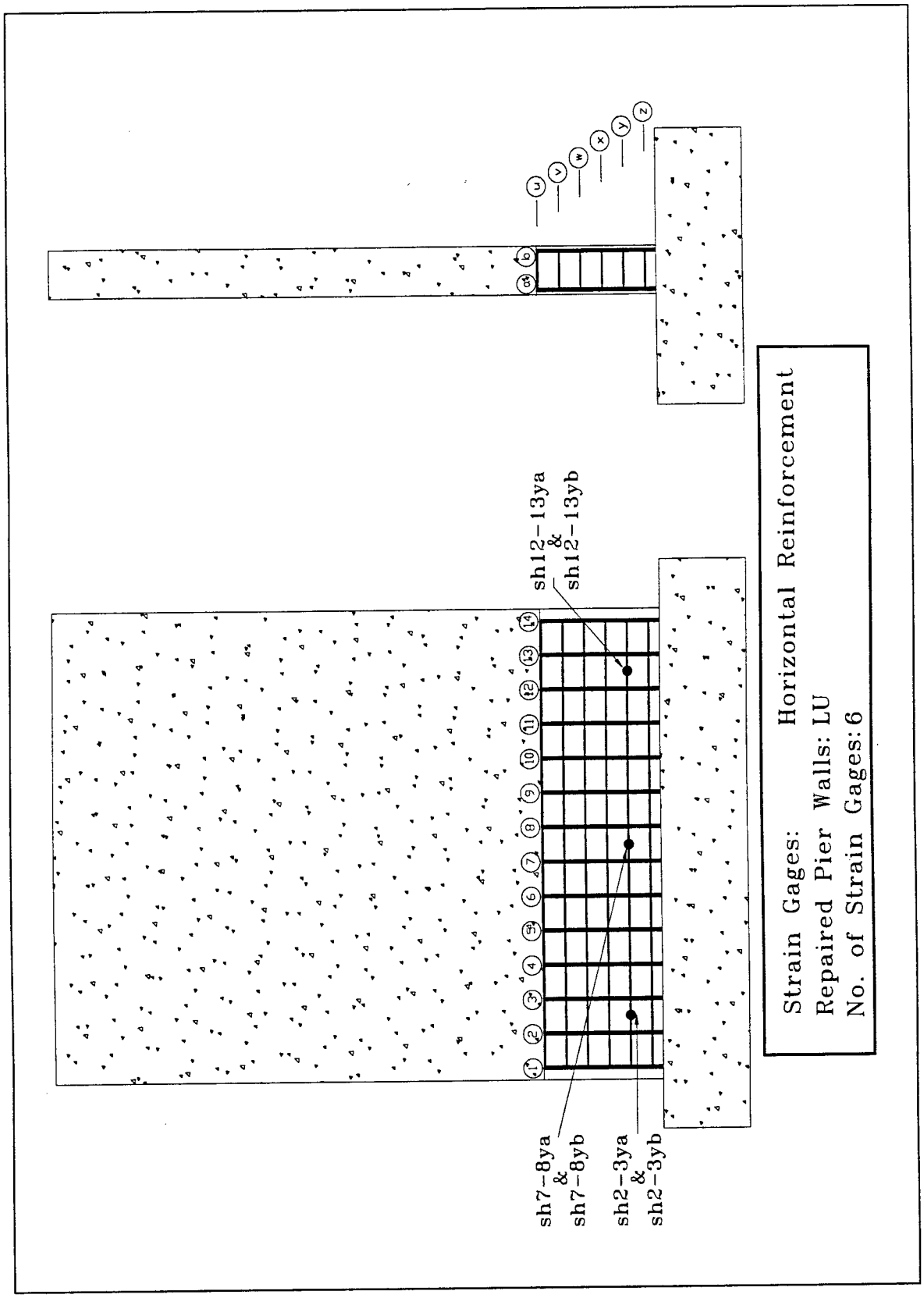

Figure 3.9: Strain Gages on the Horizontal Reinforcement for LU Wall

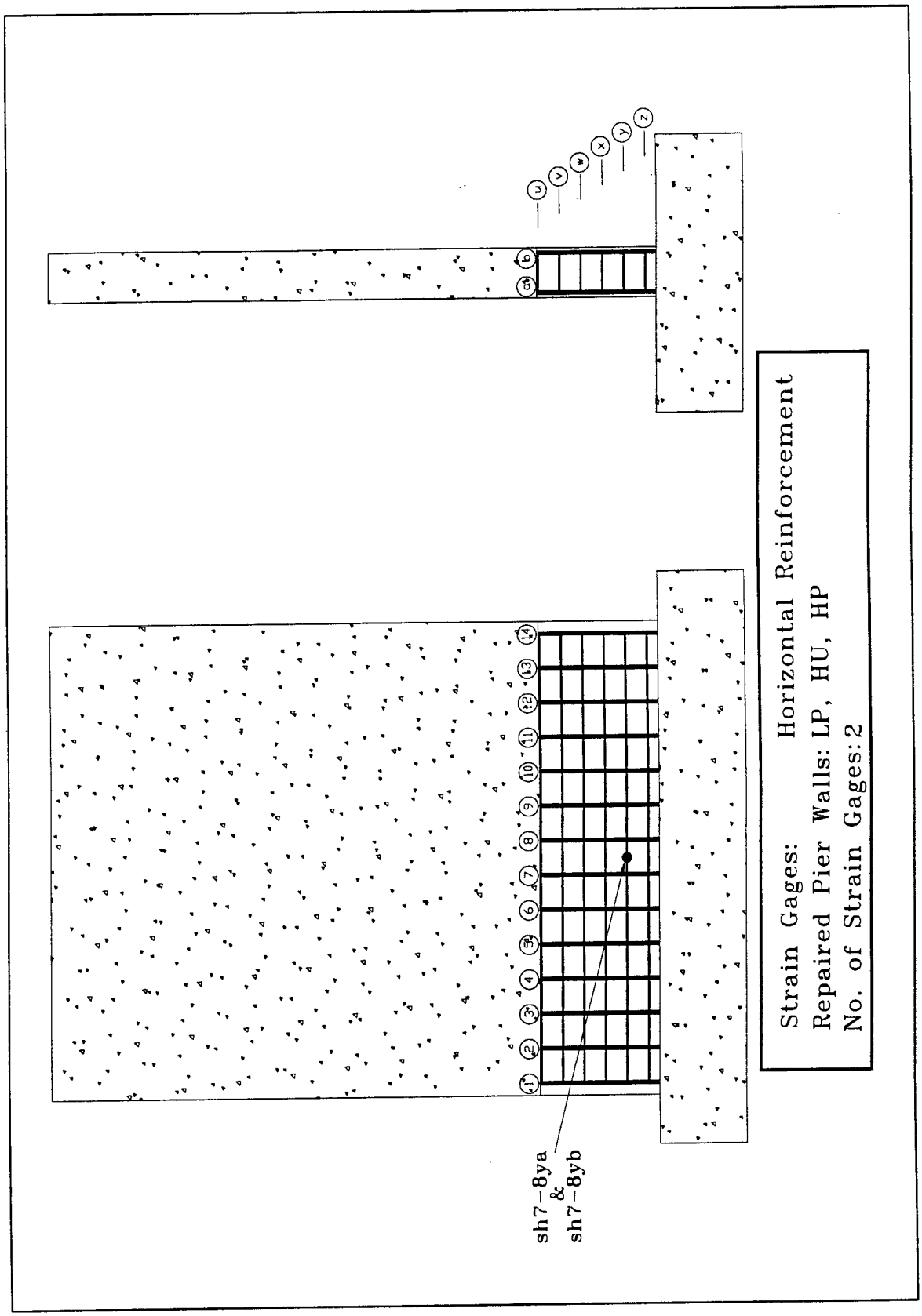

Figure 3.10: Strain Gages on the Horizontal Reinforcement for LP, HU and HP Walls

samples was similar to the original test procedure and is described as follows:

1. The two 1.5 inch diameter steel bars were tensioned to produce axial loads approximately equal to 5% of the calculated axial load capacity of the wall. Thus axial loads of 225 kips and 198 kips for the "H" and "L" walls, respectively, were calculated from

$$P = 0.05(0.85f_c^{'}(A_g - A_{st}) + f_y A_{st}) \tag{3.1}$$

2. The hydraulic actuator jack was driven to the first displacement level ($\approx$ 0.3 inches) as defined by the original pier wall test series.

3. Each pier wall was cycled three times at that initial lateral displacement level.

4. The actuator load was increased to produce the next displacement level defined in the original test series. Each wall was cycled three times at that new displacement level.

5. Each test was briefly stopped at the end of a displacement level to observe the crack development and to save the logged data.

6. Steps 4 and 5 were repeated. Table 3.3 shows the displacement level and the number of cycles at each displacement step.

7. A given test was stopped when the pier wall lost more than 20% of its lateral load strength.

The repaired sample LN was tested using a different set of displacement values since the axial load was not applied to this sample.

Level No.	HN Wall		HP Wall		HU Wall	
	Δ (in.)	Cycles	Δ (in.)	Cycles	Δ (in.)	Cycles
1	0.30	3	0.30	3	0.30	3
2	1.00	3	1.00	3	1.00	3
3	1.50	3	1.50	3	1.22	3
4	2.25	3	2.23	3	1.83	3
5	3.00	3	2.98	3	2.44	3
6	3.75	3	3.72	3	3.05	3
7	4.50	3	4.47	3	3.66	3
8	5.25	3	5.21	3	4.27	3
9	6.00	3	5.96	3	4.88	3
10	6.75	3	6.70	3	5.49	3
11	7.50	3			6.10	3
12	8.25	3			6.71	3
13	9.00	3			7.32	3
14					7.93	3
15					8.54	3
16					9.15	3
17					9.76	3

Level No.	LP Wall		LU Wall		LN Wall		
	Δ (in.)	Cycles	Δ (in.)	Cycles	Load(kips)	Δ (in.)	Cycles
1	0.30	3	0.30	3	11		3
2	0.86	3	0.87	3	22		3
3	1.29	3	1.30	3		2.64	3
4	1.72	3	1.70	3		3.52	3
5	2.58	3	2.10	3		4.40	3
6	3.44	3	2.53	3		5.28	3
7	4.30	3	3.37	3		6.16	3
8	4.73	3	4.22	3		7.04	3
9	5.16	3	5.06	3		7.92	3
10	5.59	3	5.90	8		8.80	3
11	6.02	8	6.75	8		9.68	8
12	6.45	8	7.59	8		10.56	8
13	6.88	8	8.43	8			
14	7.31	6	9.28	8			
15	7.74	8	10.12	4			
16	8.17	4					
17	9.00	4					
18	10.00	4					

Table 3.3: Applied Maximum Displacements at Each Level

Chapter 4

Post-Test Investigation

4.1 Repaired Pier Wall Performance

4.1.1 Pier Wall Performance

As with the original pier wall samples, cracks started to form at the bottom corners of the walls and spread to the middle as the load level increased. Eventually, the cracks from each end of the walls merged. Thereafter, no new crack formation was observed. As the load level increased, the wider crack developed. The increased widening of the cracks led to the spalling of the concrete cover. All the cracks were almost horizontal, parallel to the load cap.

4.1.2 Enhanced Cross-Tie Performance

The enhanced cross-ties used in repairing the five samples worked well. None of the 135° ends opened in walls with the vertical reinforcement ratio equal to 1.3%, the 'L' walls. However, in walls with the vertical reinforcement ratio equal to 2.3%—the 'H' walls — some of the enhanced cross-ties opened during the latter stages of the test.

4.1.3 T-Headed Cross-Tie Performance

The T-headed cross-tie used in repairing the 'HN' pier wall worked better than anticipated. Despite pre-test skepticism the T-headed cross-tie performed as well as or

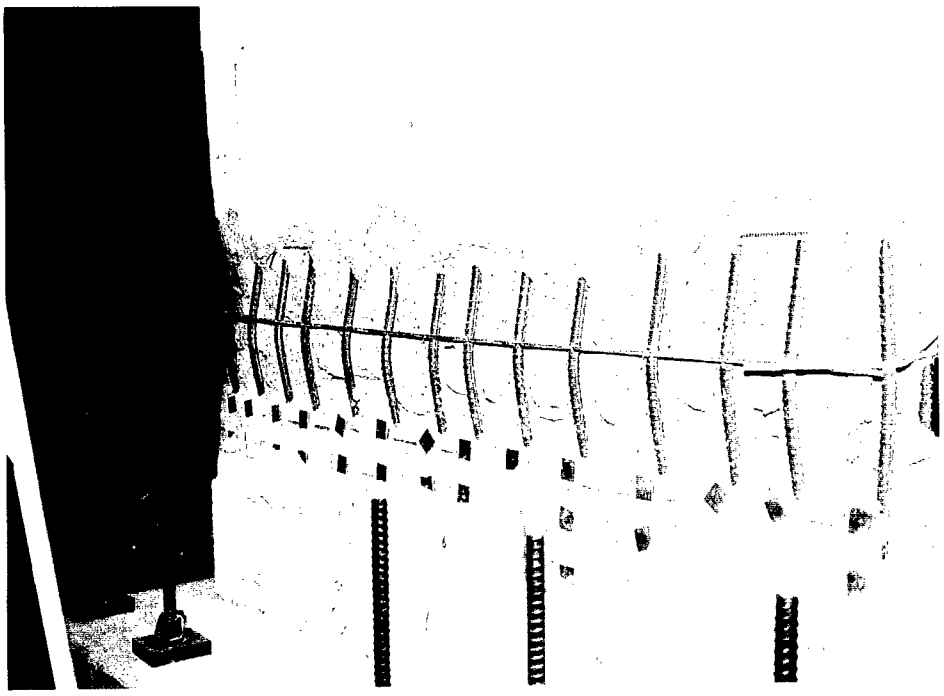

Figure 4.1: T-Headed Bars in the Pier Wall

better than the regular cross-ties. The T-headed reinforcement added confinement to the concrete core of the pier wall to the point of shifting the buckling of the longitudinal reinforcement to the higher, non-confined region of the pier wall. Unlike the 90°/135° cross-ties, where confinement of the core is based on the cross-tie restraining the longitudinal steel against the core, confinement by the T-headed reinforcement is provided by the head bearing directly against the core concrete. See Figure 4.1. Post-test examination of the concrete core confirmed the presence of a rigid conical core directly behind each head.

4.1.4 Vertical Reinforcement Performance

The vertical reinforcement bars in the 'L' samples worked well with no vertical reinforcement bar failure. During the testing of the repaired sample 'HP', loud popping

sounds were heard. The popping sounds were caused by the vertical reinforcement bars being broken in tension. Four vertical reinforcement bars were seen to be broken at about the base of the pier wall. The test was stopped when a fifth popping sound was heard fearing the collapse of the pier wall. Post-test examination revealed that five vertical reinforcement bars were indeed broken. All broken bars were confined to one particular side of the pier wall.

One of the vertical reinforcement bars that had been broken during the original test series was repaired by welding a new bar segment in the fracture area prior to re-testing. It was found that this repaired vertical reinforcing bar was one of the bars broken during the test and it broke at the welded spot.

4.1.5 Horizontal Reinforcement Performance

The horizontal reinforcements were still intact at the conclusion of the tests. Visual inspection of the horizontal reinforcement reveled hardly any damage. No noticeable large deformations could be observed. The horizontal reinforcements along with the enhanced cross-ties prevented excessive buckling of the vertical reinforcements. The analysis of the strain gages, mounted on some of the horizontal reinforcement, reveal very little strains.

4.2 Definition of Ductility

The ductility of a structural element is generally defined as the member's ability to undergo deformation without a substantial reduction in its load resisting capacity. The ductility can be defined either by the curvature ductility factor which is the ratio of the section curvature at ultimate strength to the curvature when the tension reinforcement reaches the yield state, or the displacement ductility factor which is the ratio between the maximum horizontal displacement of the wall at ultimate

and at first yield. Since it is difficult to pinpoint the yield state experimentally, an elasto-plastic model was proposed [8] to approximate the moment-curvature or the load-displacement relations. The theoretical value for the yield displacement, $\Delta_y^{'}$, is calculated from the following relation

$$\Delta_y^{'} = \Delta_y \frac{Q_i}{Q_y} \tag{4.1}$$

where Δ_y and Q_y are the displacement and the applied load at first yield of the vertical reinforcement and Q_i is the ideal load calculated from the moment capacity of the wall section using the ACI-318-89 code approach [9]. The ideal load, Q_i, is calculated assuming the ϵ_{cu}, the ultimate concrete strain, to be 0.003. The load at first yield, Q_y, is calculated as 75% of Q_i. Figure 4.2 shows the parameters used for idealized yield displacement calculation.

4.3 Ductility of Repaired Samples

The displacement ductility factors for the repaired walls were obtained using the procedure described below. The cross-sectional area of the repaired walls was slightly larger then the original walls. However, in the calculation of the moment capacity, the increased cross-sectional area was disregarded. This made the moment capacity of the repaired samples to be the same as the original samples. Similarly, the increase in the yield stress of the vertical reinforcement bars due to strain hardening was also not taken into account.

The steps used in obtaining the displacement ductility factor for the repaired walls were as follows:

1. The envelope of the hysteresis loop of the repaired wall obtained using the same displacement test protocol as the original sample was plotted.

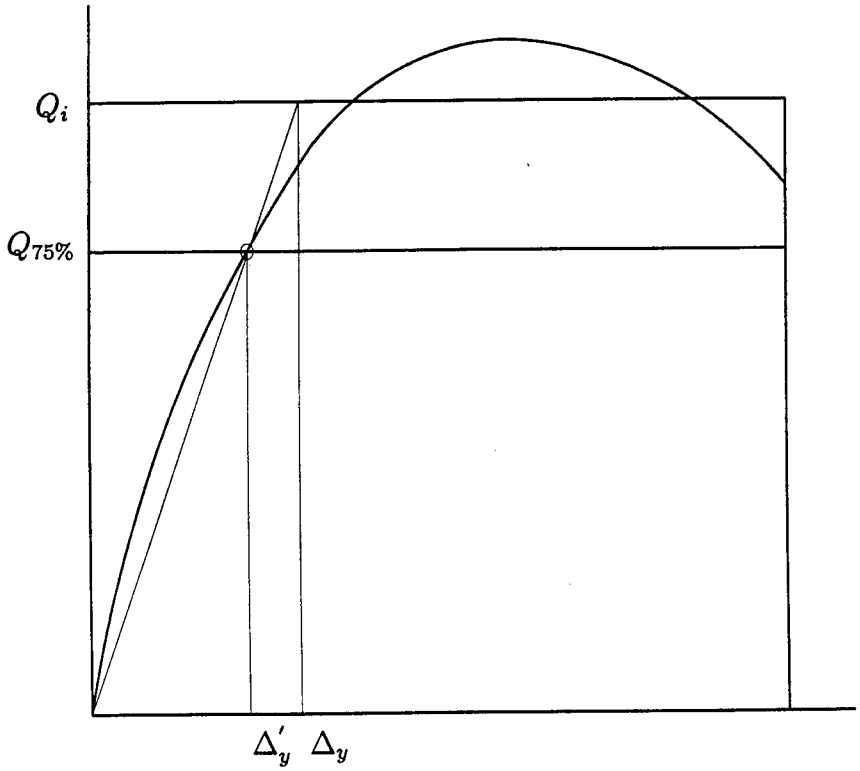

Figure 4.2: Idealized Yield Displacement

2. The moment capacity of the pier wall about the weak-axis was calculated assuming the ultimate strain in the concrete, ϵ_{cu} to be 0.003. The ultimate moment was calculated assuming the strength of the concrete ,$f_c' = 4000$ psi and the yield strength of the vertical reinforcement steel, $f_y = 60$ ksi.

3. The calculated moment was converted to an equivalent lateral load, Q_y, by dividing the moment by the moment arm. The moment arm is the height to the point of applied lateral load from the base of the wall.

4. The load at first yield, Q_y, was calculated as 75% of Q_i.

5. Horizontal lines corresponding to the Q_y and Q_i were plotted on both the positive and negative directions.

6. A straight was drawn from the origin to the point where the horizontal line corresponding to Q_y intersects the envelope of the hysteresis loop in both the positive and negative directions.

7. This line was extended to the point where the horizontal line corresponding to Q_i intersects the envelope of the hysteresis loop in both the directions.

8. A straight line was drawn from this point to intersect the X-axis in both directions.

9. The yield displacement, $\Delta_y^{'}$, was calculated as the average of the distances from the origin to the intersection point along the X-axis in both directions. Distances A and B in Figure 4.3.

10. The displacement ductility factor was obtained by dividing the ultimate displacement Δ_u by the calculated yield displacement $\Delta_y^{'}$.

4.4 Test Results

The relation between the applied horizontal load and the top horizontal displacement was plotted to form the hysteresis loops for the samples. The hysteresis loops for the original pier walls as well as the repaired pier walls were plotted. Figures 4.4 to 4.9 are the hysteresis loops formed by the lateral loads vs. top displacements for the original pier walls while Figures 4.10 to 4.15 represent the repaired pier walls. The envelope of the hysteresis loops were also plotted. In order to facilitate the comparisons between the original and the repaired pier walls, the envelope of the hysteresis loops for the original and the repaired pier wall are shown in Figures 4.16. to 4.21. Similarly, Figures 4.22 and 4.23 represent the envelope of the hysteresis loops of all the original and all the repaired pier walls.

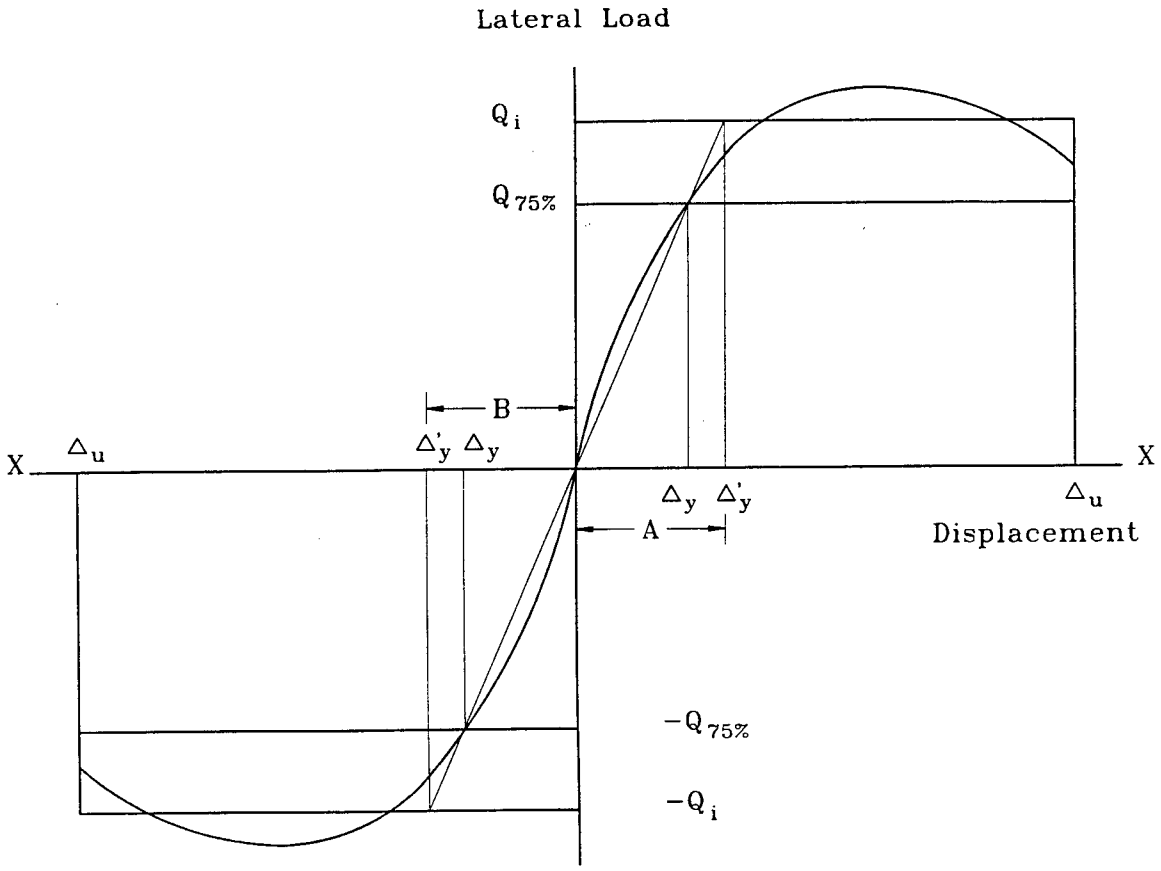

Figure 4.3: Definition of Yield Displacement

Comparing the plots of the original and the repaired samples, the following can be observed:

Stiffness: The envelopes of the hysteresis loops can be utilized in observing the behavior of the repaired pier walls and comparing the lateral stiffness to the original pier wall samples. The lateral response of all six original samples can be grouped in three phases. Phase one is characterized by a distinct initial stiffness. The softening of the initial stiffness is observed in phase two. Phase two can be approximated by two linear segments. In the last phase, a relatively flat, yielding behavior can be observed.

In general, the response of the repaired pier wall samples can also be grouped

in three phases. The stiffness in the initial phase is less than that of the original samples. The repaired pier walls in phase two exhibit a stiffer response compared to the original samples. Unlike the original samples, varying degrees of yielding can be observed in phase three.

It is interesting to note that repaired sample LN, tested without any axial load, exhibits only two phases unlike the three phases observed in all the original as well as the other five repaired samples. The transient second phase, an intermediate stiffness between the first phase and the third phase is not present. The repaired sample LN exhibits an elastic- plastic response.

Strength: All the six repaired pier walls achieved higher strength than the original pier walls. The increase in the maximum lateral strength range from 3.1% to 27.3%.

Ductility: Except for the repaired HP pier wall, all the other repaired samples achieved lateral displacements that are comparable to the original samples. However, the displacement ductility factors of the repaired walls were lower than the original samples. This can be attributed to the value of the new yield displacements being larger than the original yield displacement.

General Observation: Figure 4.22 and Figure 4.23 show that the lateral response of the original walls to be uniform among the L and the H samples. However, the response of the repaired walls are not as uniform among the samples. This can be attributed to the two different repair schemes.

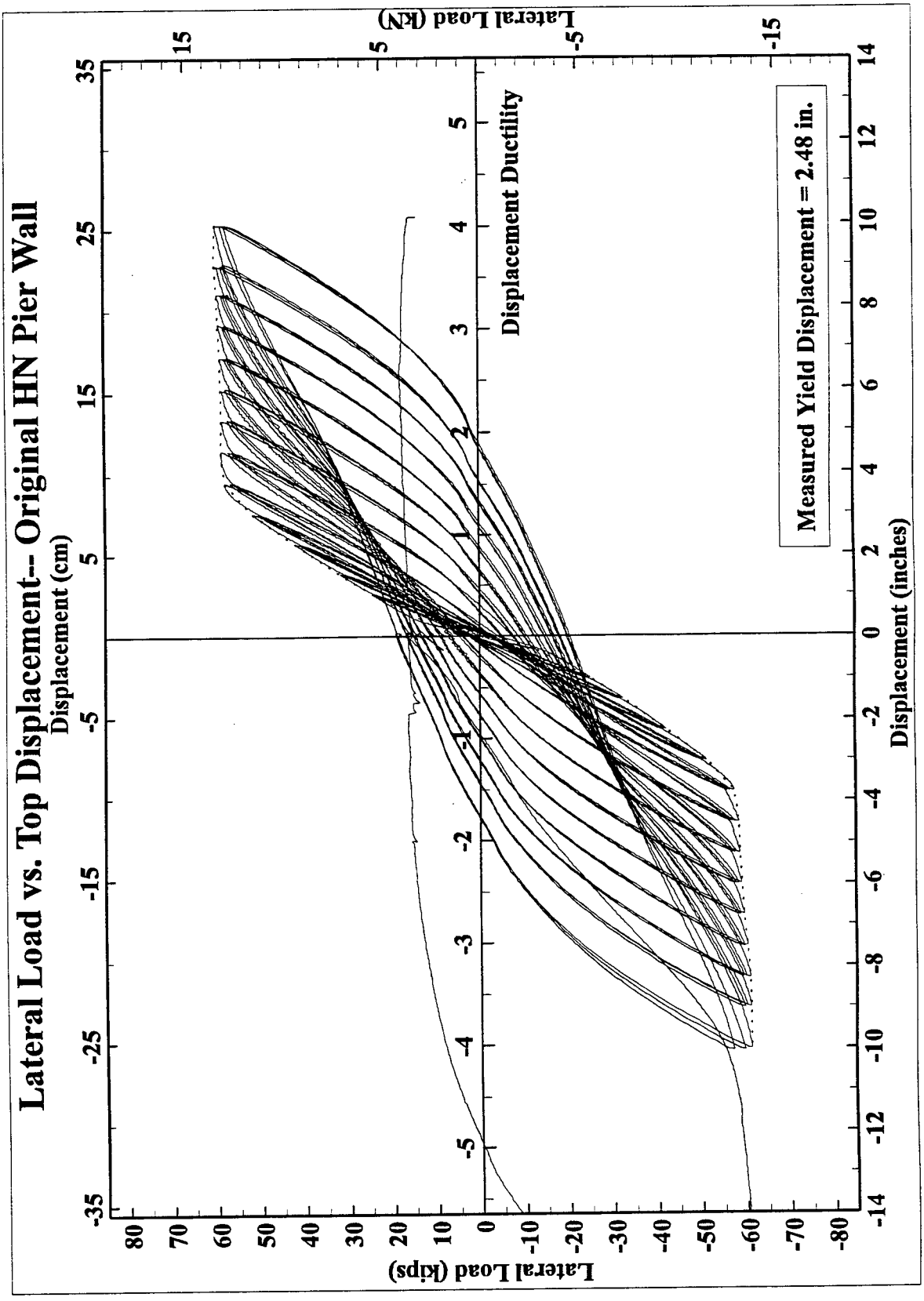

Figure 4.4: Hysteresis Loops of the Original HN Pier Wall

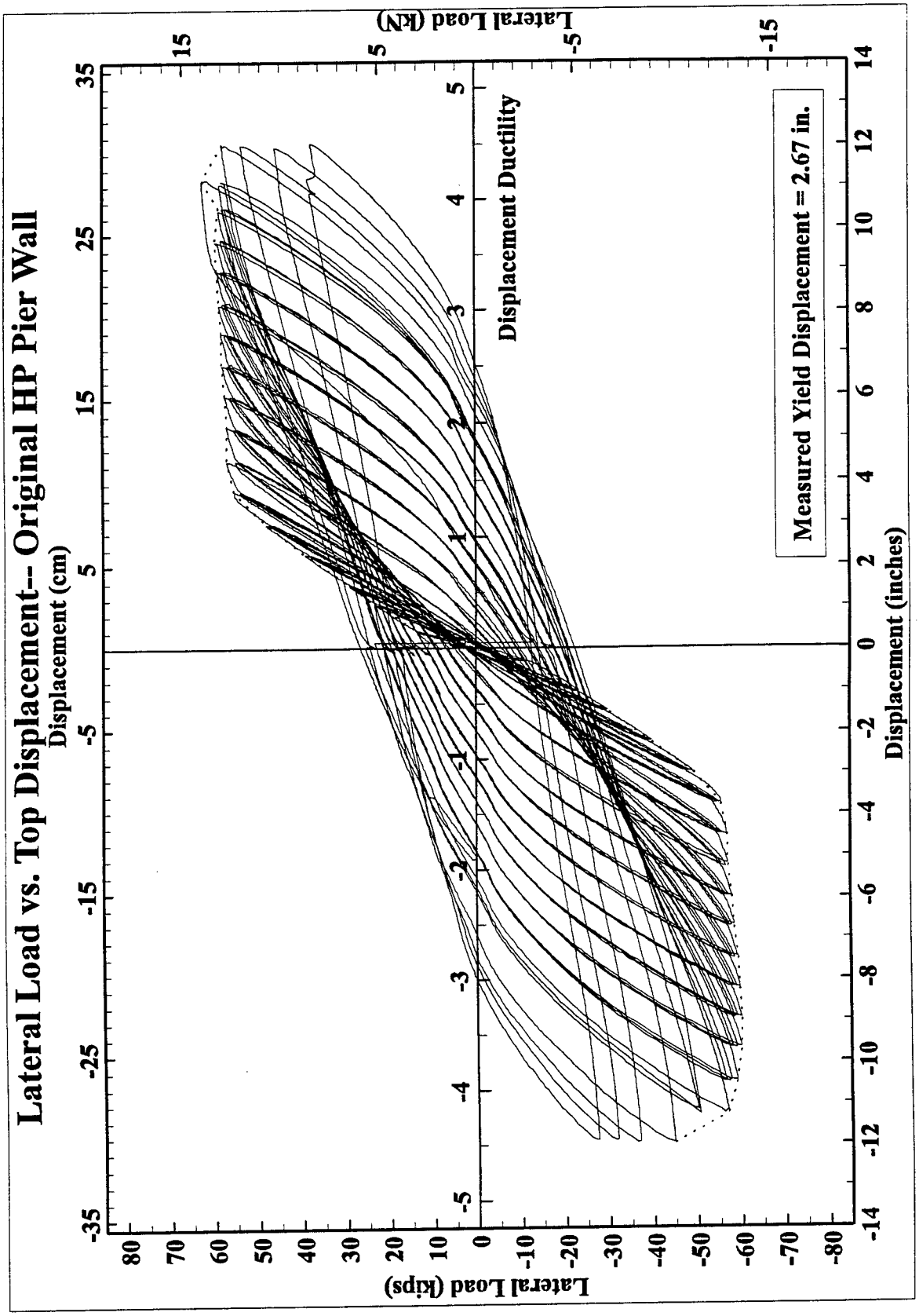

Figure 4.5: Hysteresis Loops of the Original HP Pier Wall

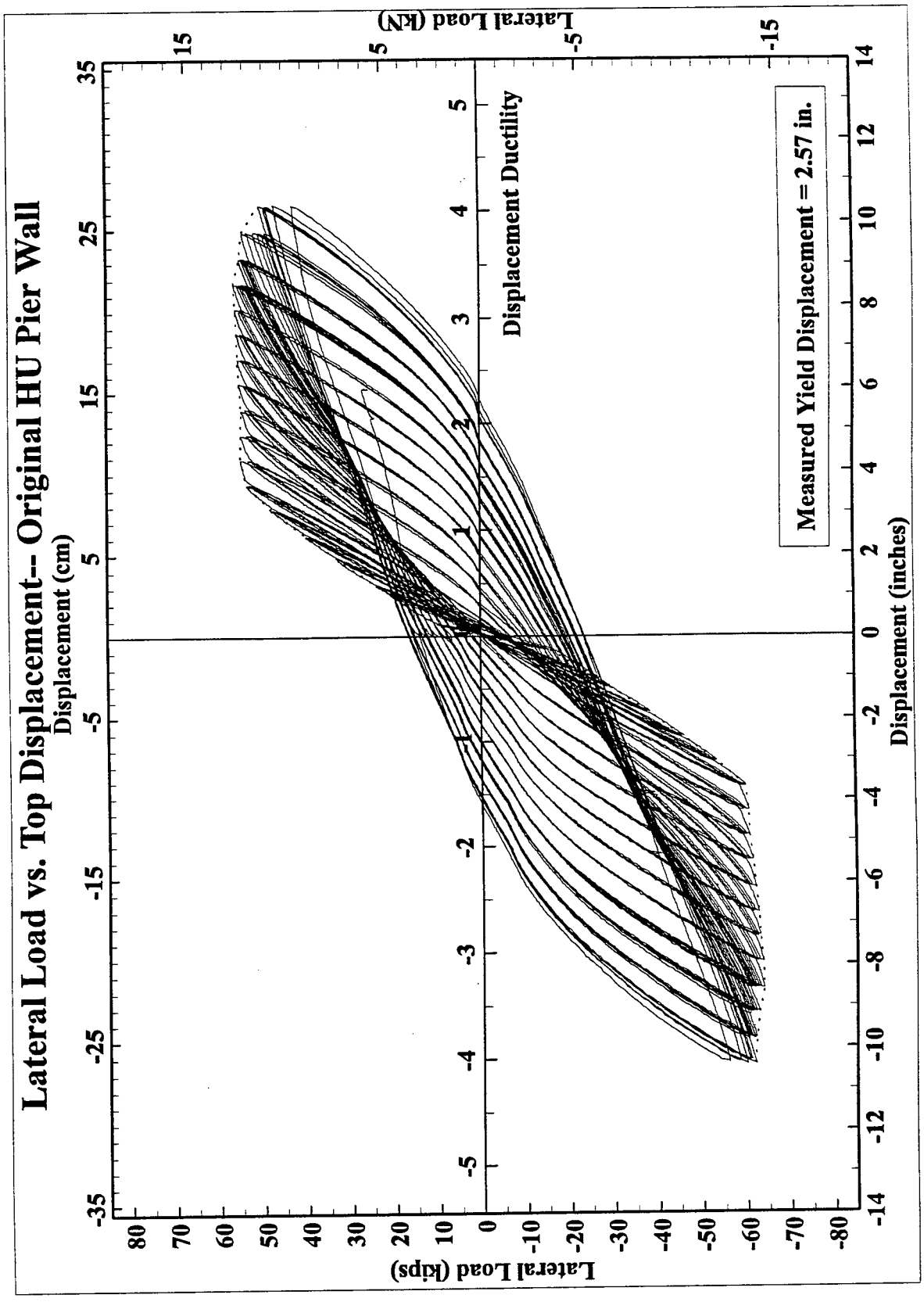

Figure 4.6: Hysteresis Loops of the Original HU Pier Wall

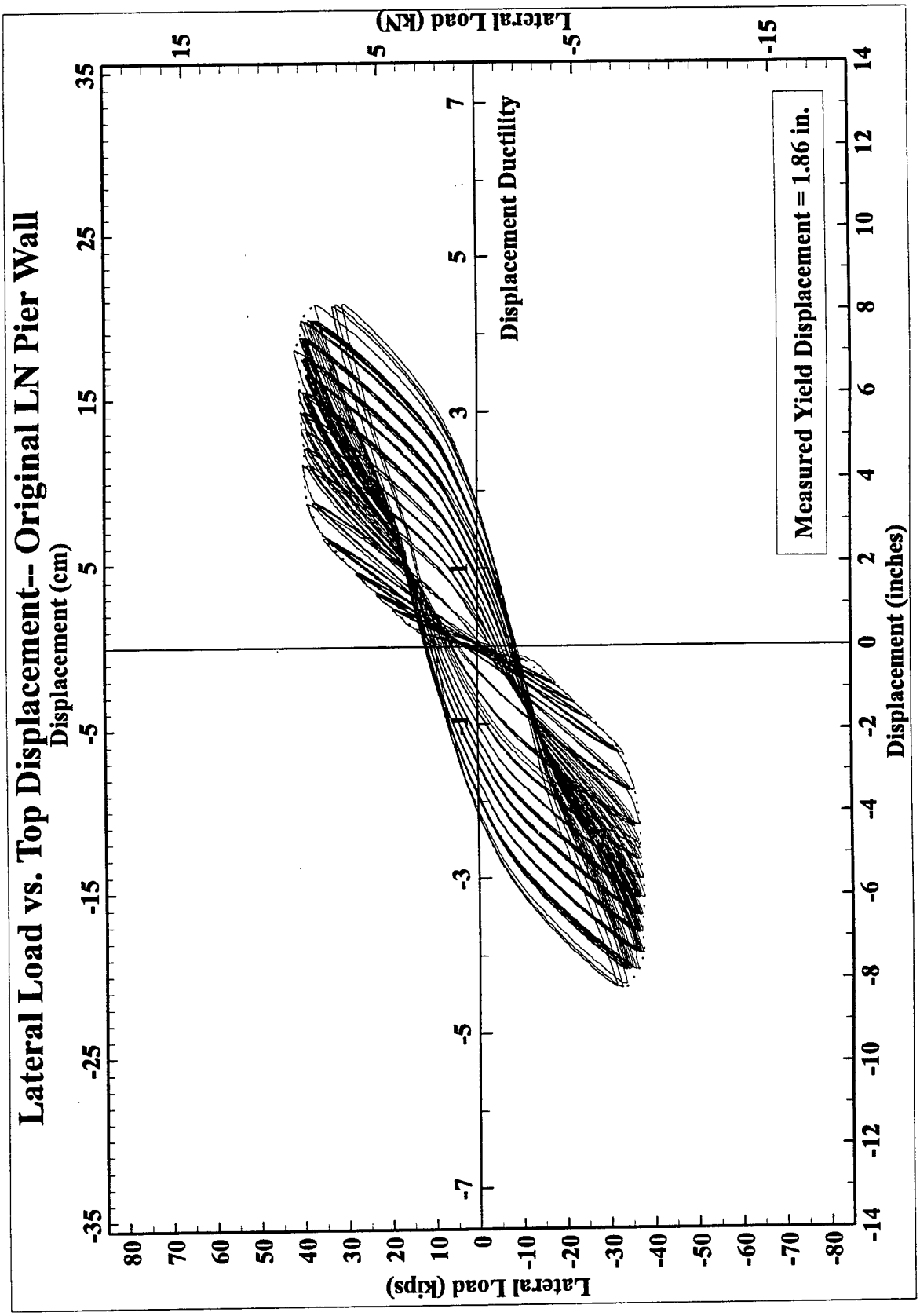

Figure 4.7: Hysteresis Loops of the Original LN Pier Wall

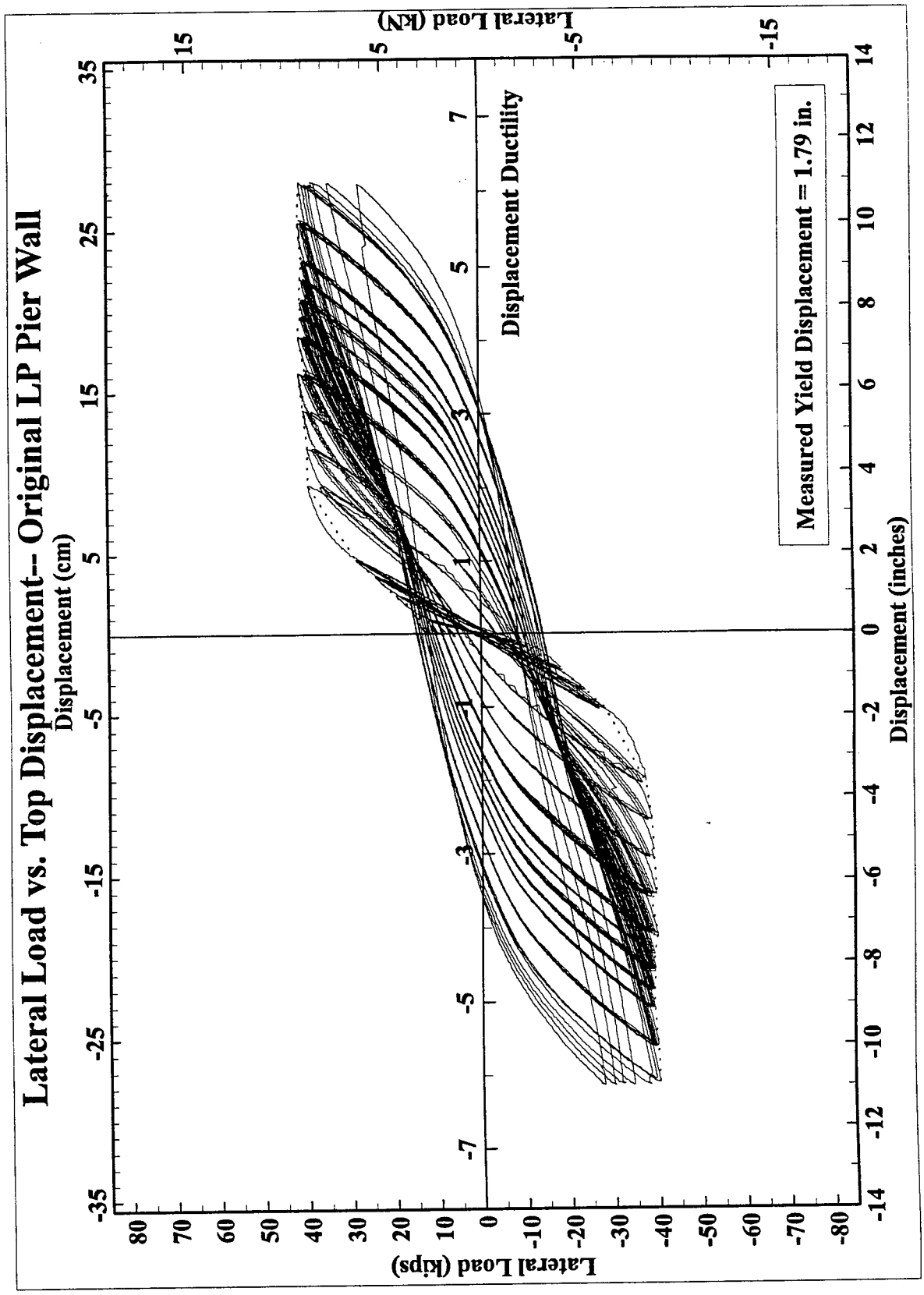

Figure 4.8: Hysteresis Loops of the Original LP Pier Wall

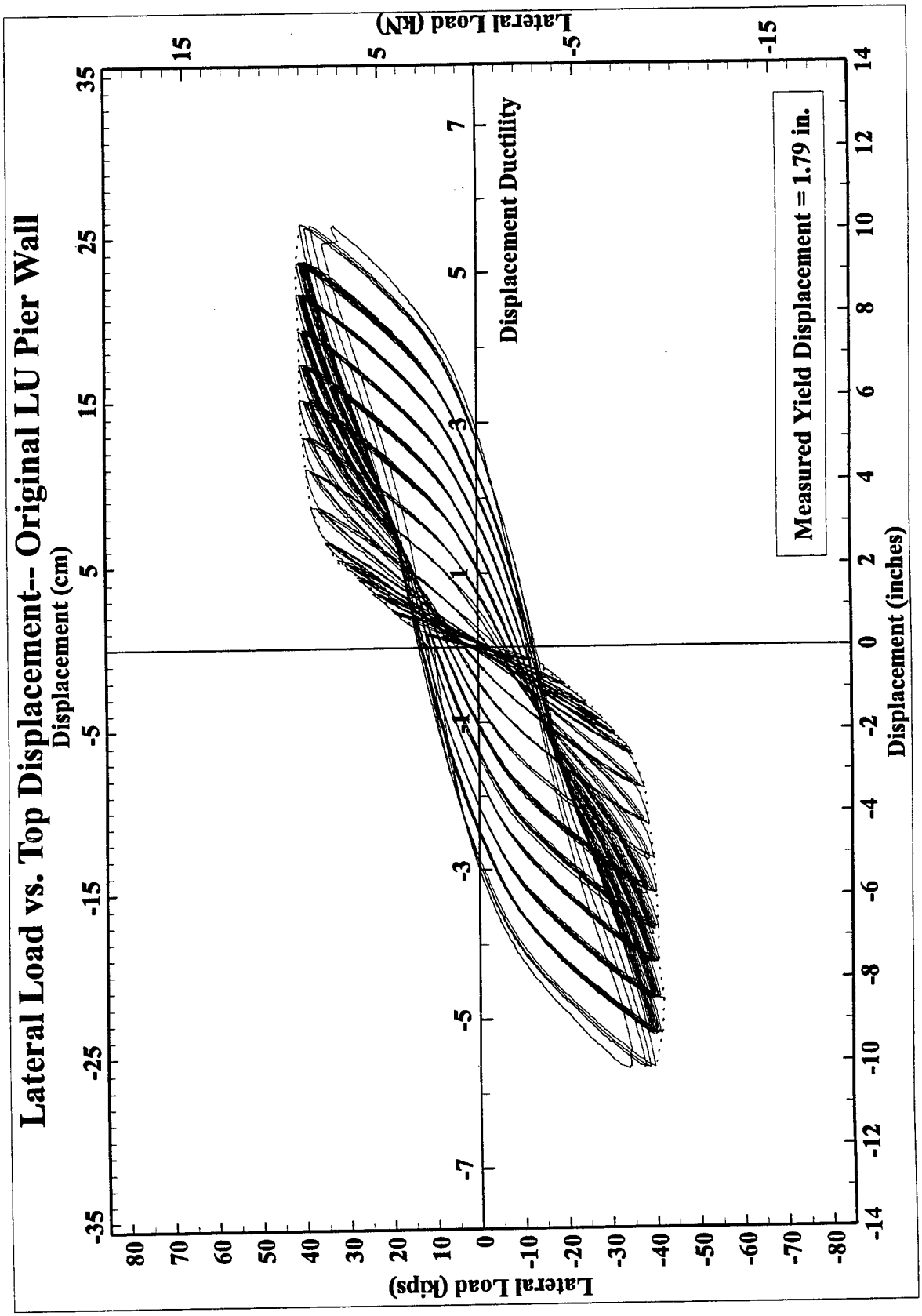

Figure 4.9: Hysteresis Loops of the Original LU Pier Wall

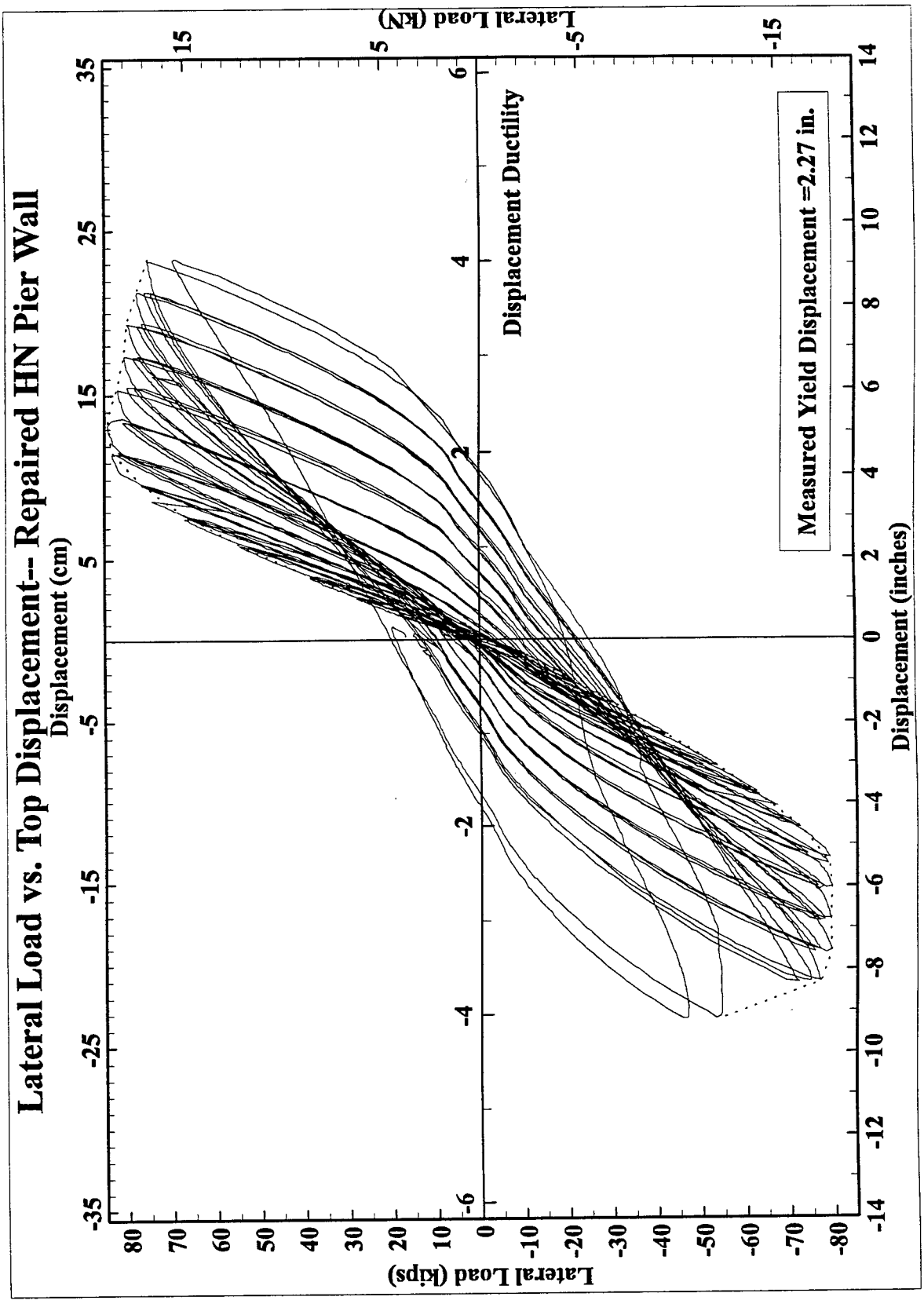

Figure 4.10: Hysteresis Loops of the Repaired HN Pier Wall

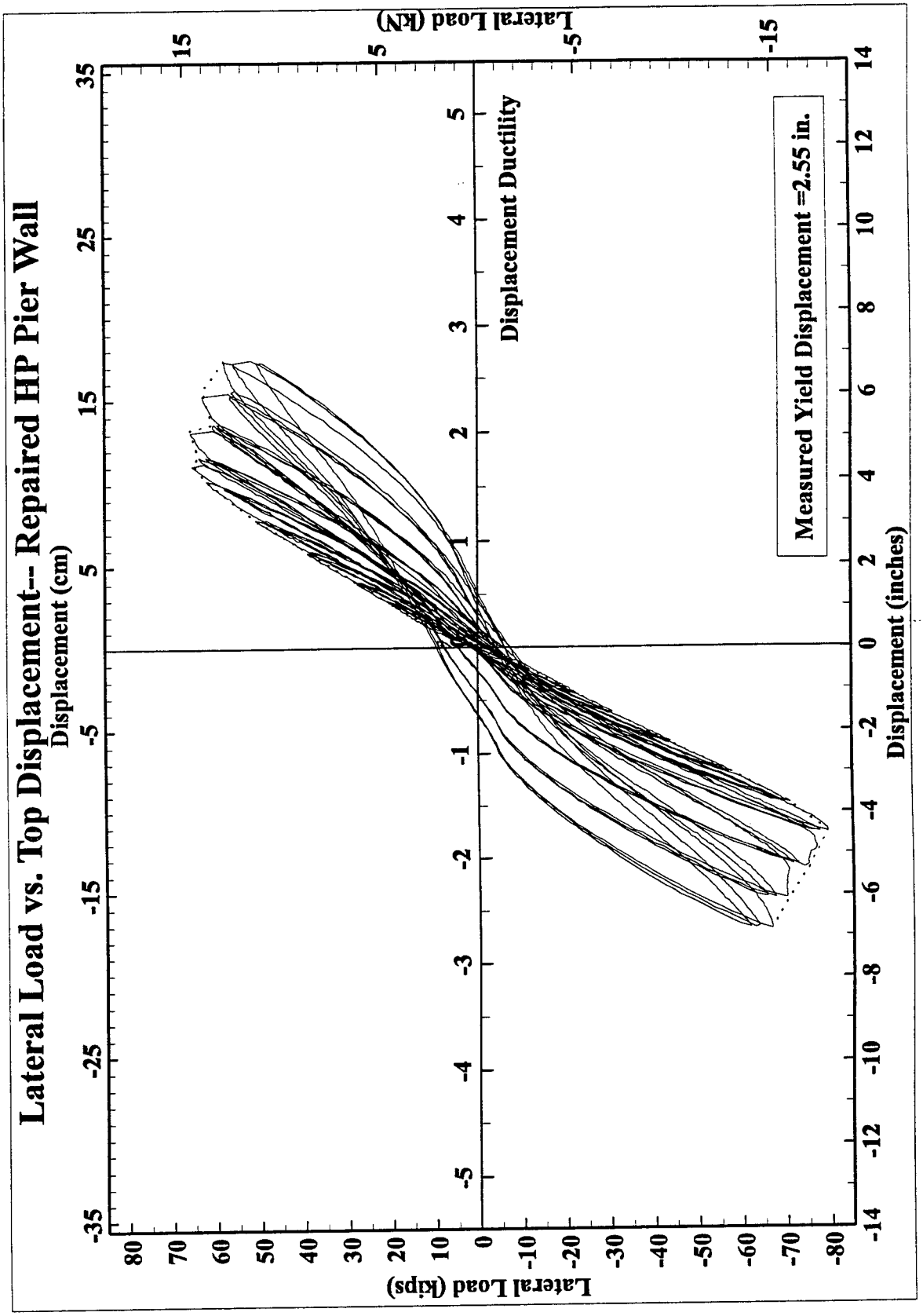

Figure 4.11: Hysteresis Loops of the Repaired HP Pier Wall

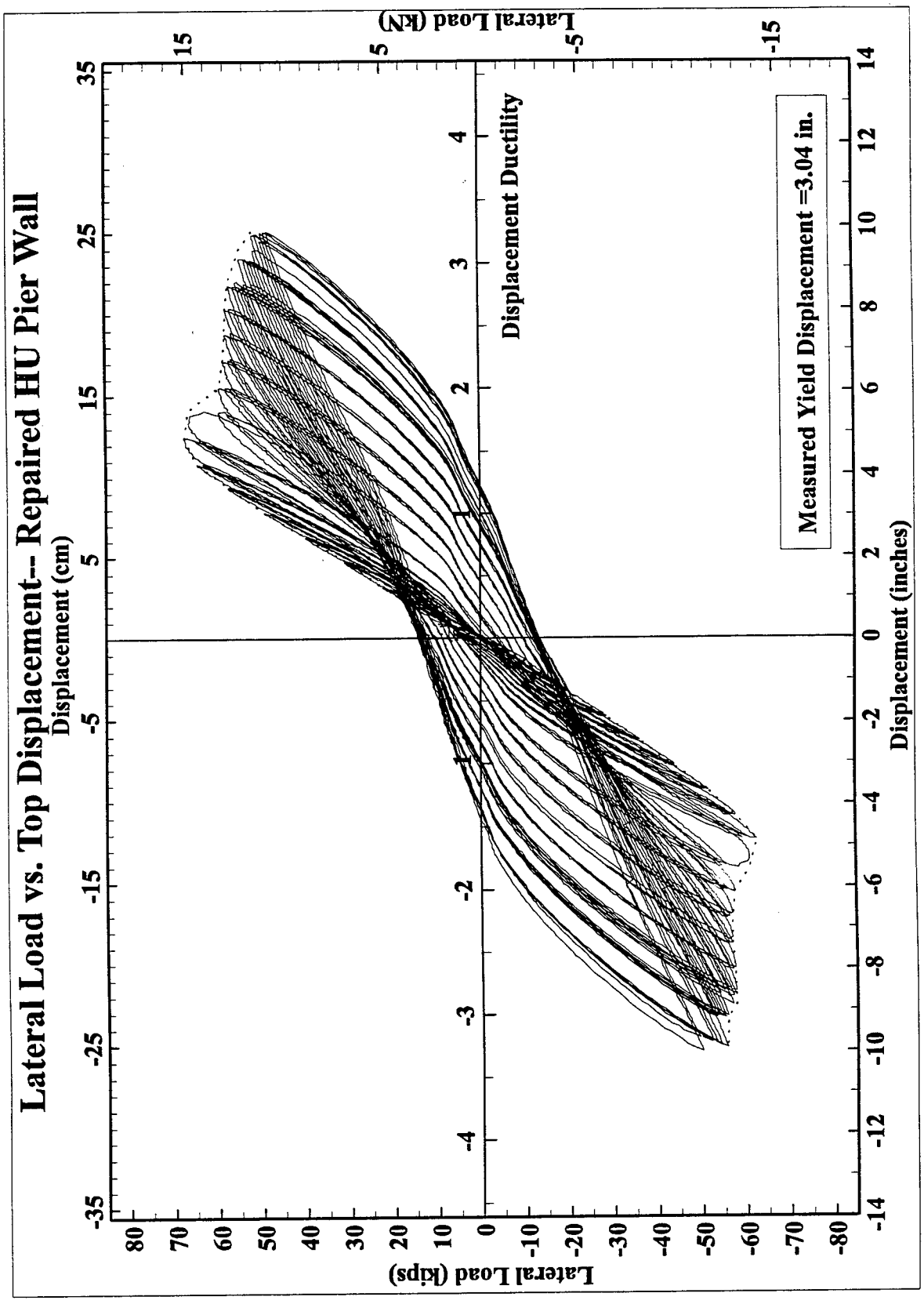

Figure 4.12: Hysteresis Loops of the Repaired HU Pier Wall

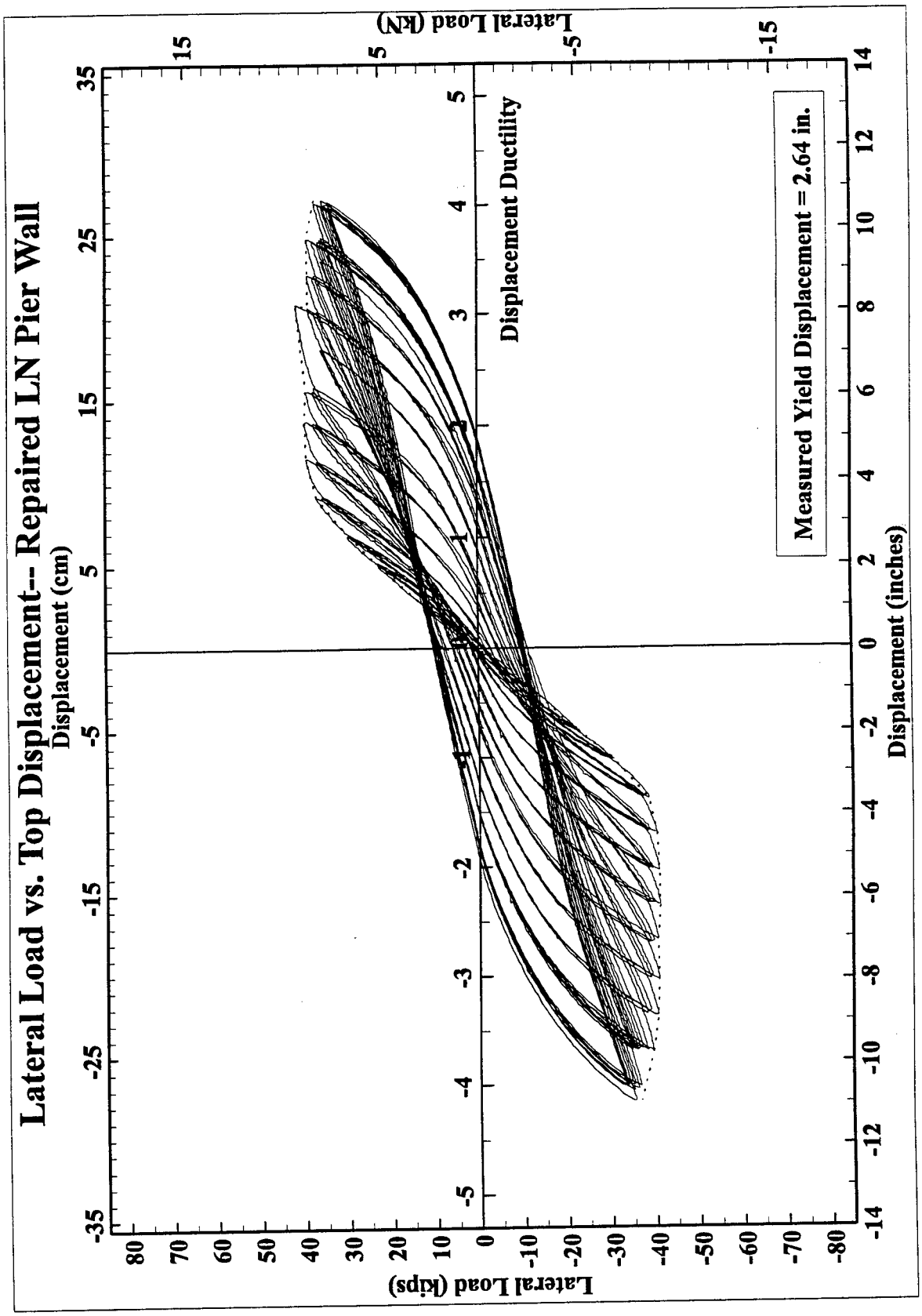

Figure 4.13: Hysteresis Loops of the Repaired LN Pier Wall

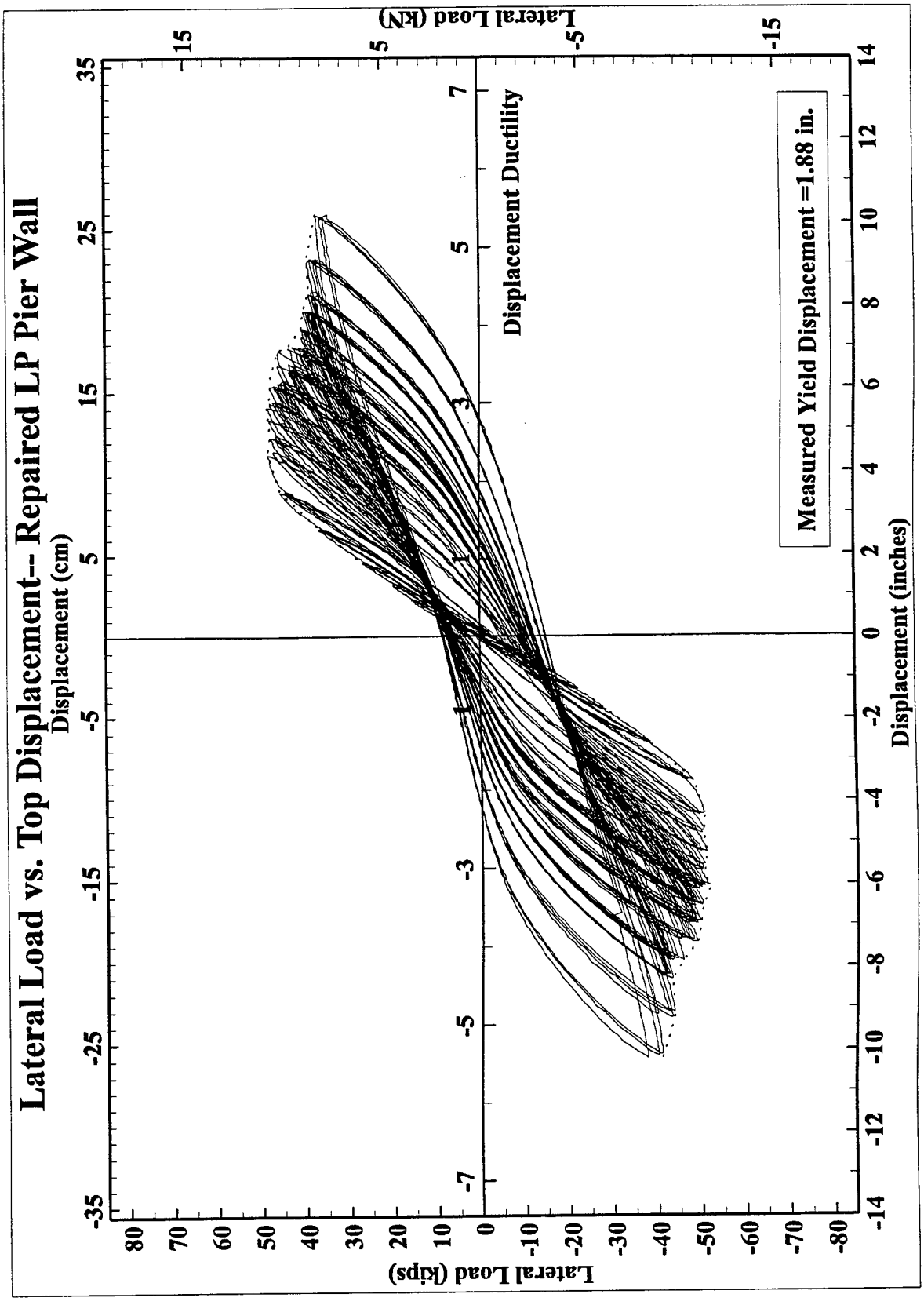

Figure 4.14: Hysteresis Loops of the Repaired LP Pier Wall

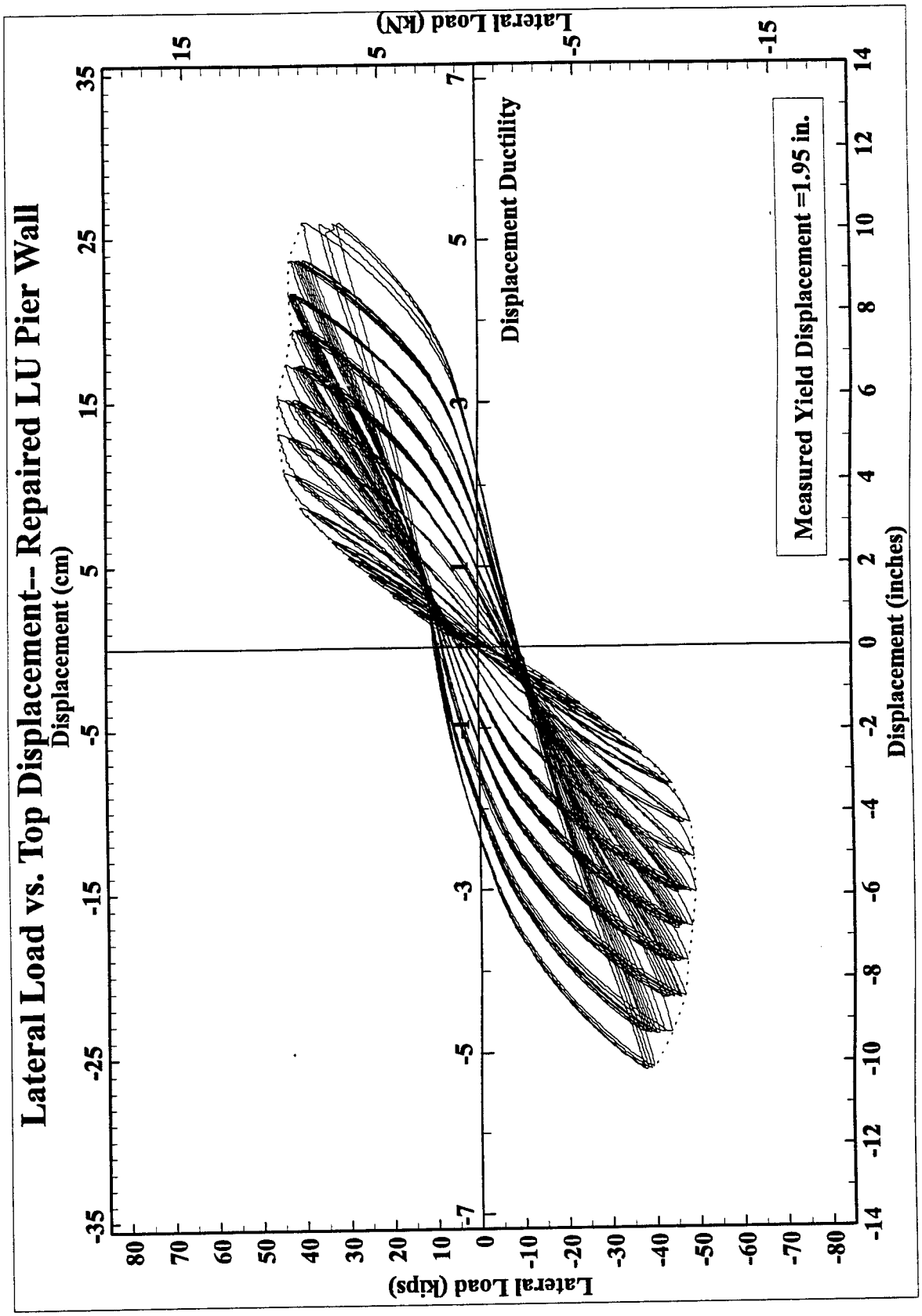

Figure 4.15: Hysteresis Loops of the Repaired LU Pier Wall

Pier Wall	Original Pier Wall			Repaired Pier Wall		
	Max Lateral Load	Lateral Displ	Displ Ductility	Max Lateral Load	Lateral Displ	Displ Ductility
LU	41.9 kips	10.2 in.	5.69	49.0 kips	10.2 in.	5.25
LP	41.3 kips	11.0 in.	6.14	51.5 kips	10.2 in.	5.44
LN	40.3 kips	8.2 in.	4.40	41.6 kips	10.9 in.	4.13
HU	63.8 kips	10.5 in.	4.07	67.2 kips	10.0 in.	3.29
HP*	62.5 kips	12.1 in.	4.51	79.3 kips	6.9 in.	2.69
HN	61.3 kips	10.0 in.	4.05	84.3 kips	9.2 in.	4.04

* Test ended prematurely

Table 4.1: Comparison of Original and Repaired Pier Walls

4.5 Strain Gages

In order to monitor strains in the reinforcements, strain gages were installed at strategic locations. Strain gages were mounted on the vertical reinforcement bars, horizontal reinforcement and the cross-ties. All the strain gages shown in Figures 3.4 to 3.10 had been installed. However, at the start of the test, it was noticed that some of the strain gages were damaged. The damage had occurred while concrete was poured. The pumping and vibrating of the concrete had caused the damage. The data from the surviving strain gages were analyzed. Furthermore, it was found that the strain gages had stopped correctly acquiring data at various stages of the tests. Although, a lot of strain gages had been installed at the beginning of the test to acquire various information, only a few strain gages had survived. Figures 4.24 to 4.28 show the plots of lateral load versus strain for the vertical reinforcements, horizontal reinforcement and the cross-ties at different locations of the repaired pier walls.

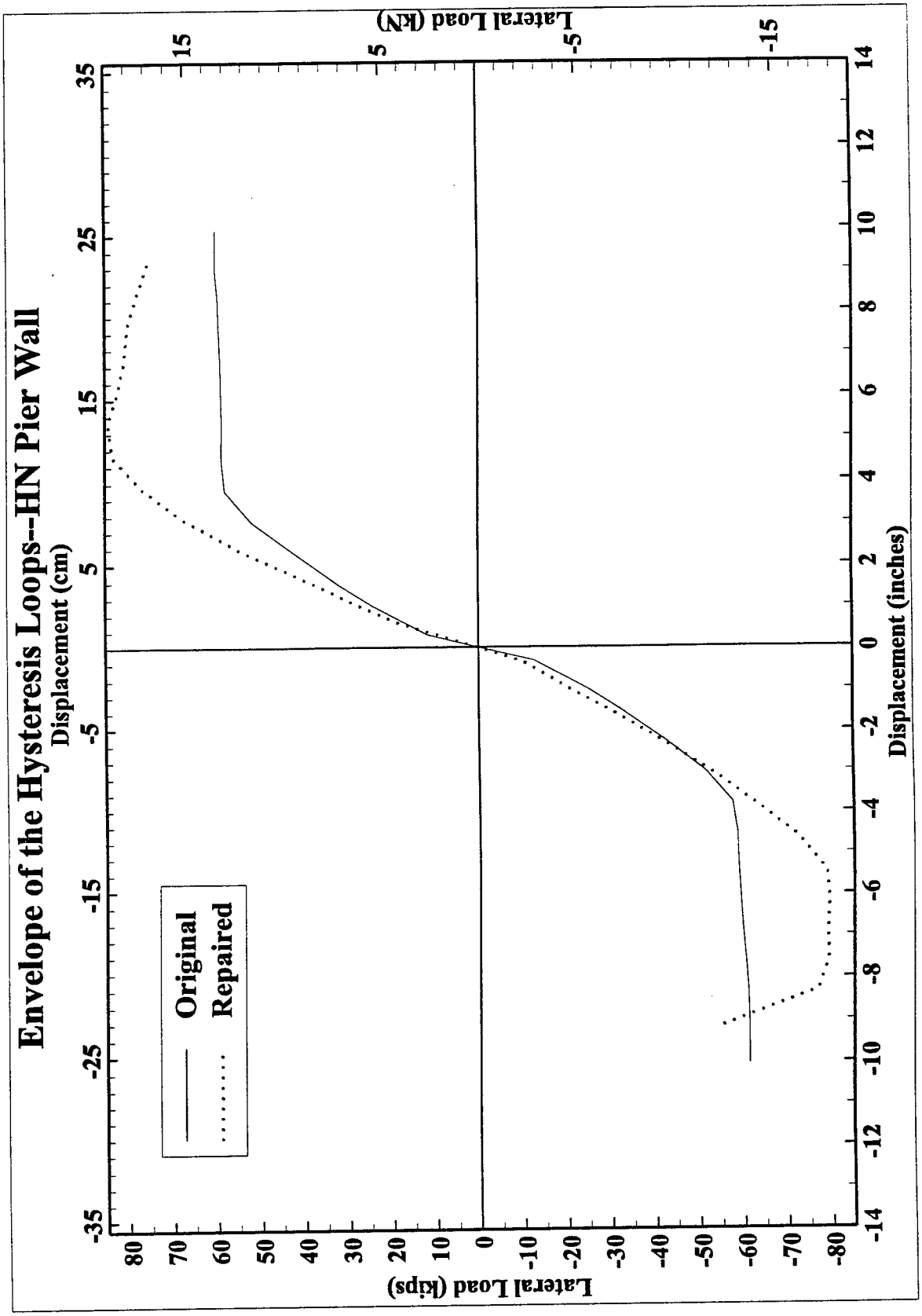

Figure 4.16: Envelope of the Hysteresis Loops: HN Pier Wall

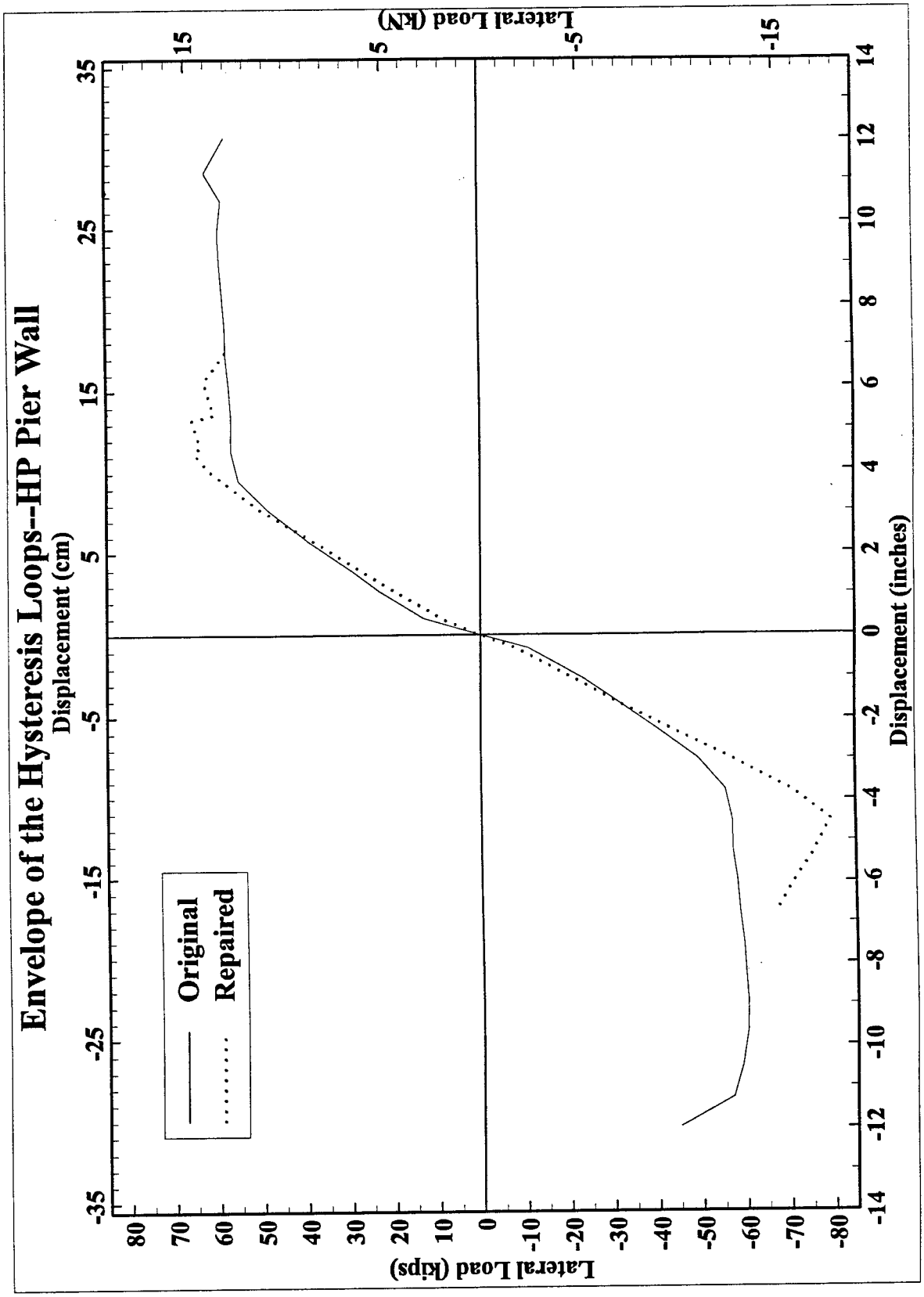

Figure 4.17: Envelope of the Hysteresis Loops: HP Pier Wall

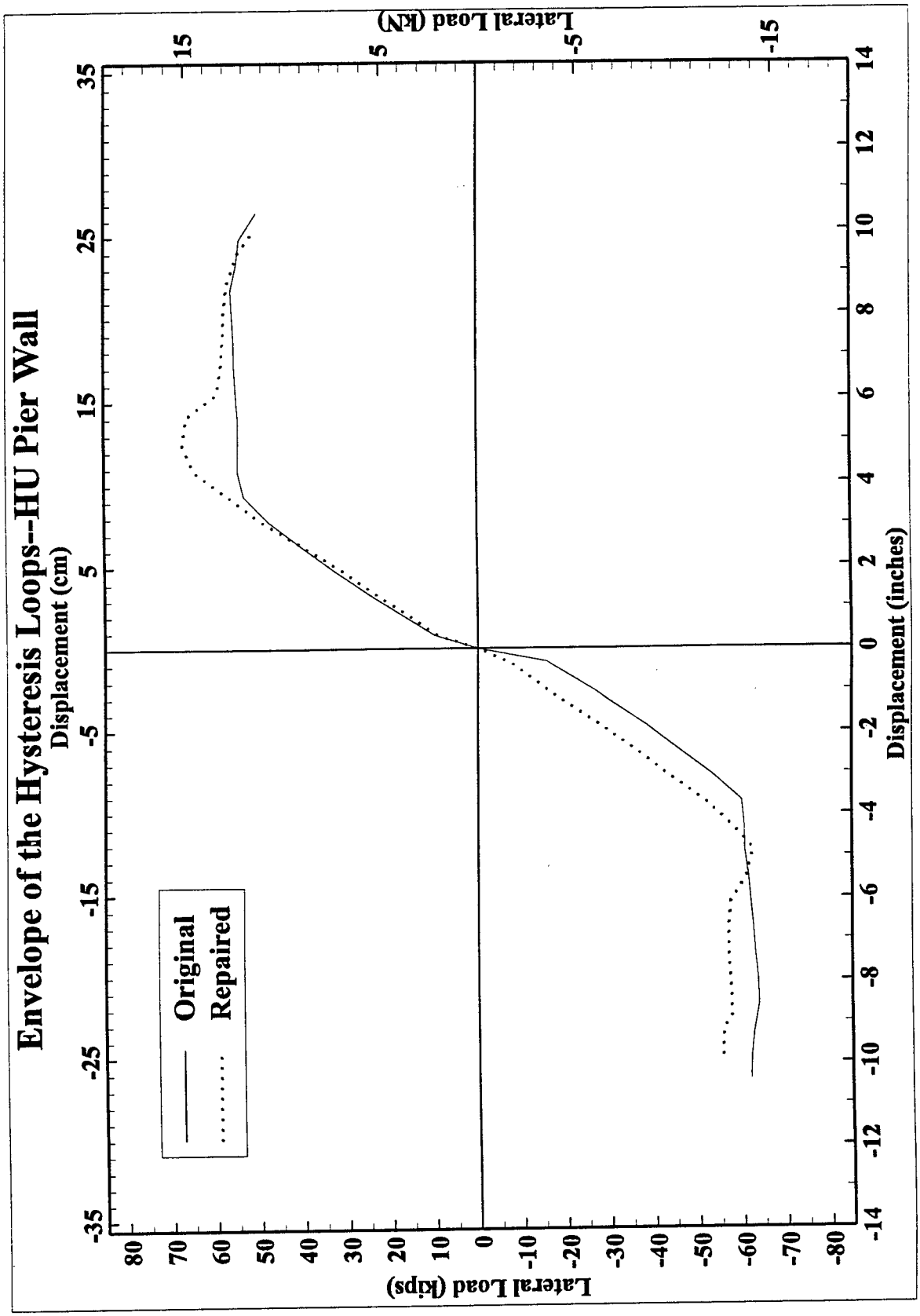

Figure 4.18: Envelope of the Hysteresis Loops: HU Pier Wall

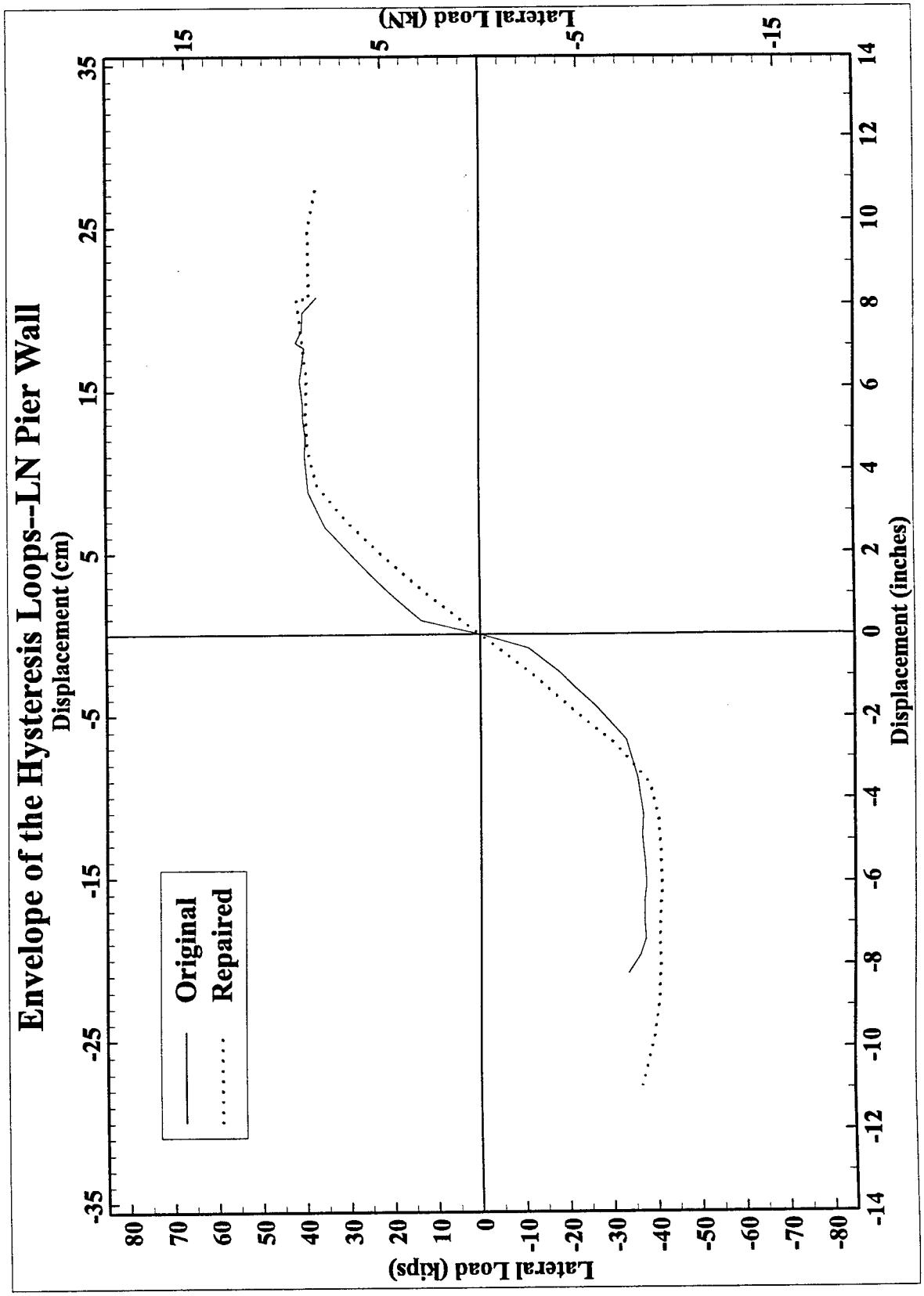

Figure 4.19: Envelope of the Hysteresis Loops: LN Pier Wall

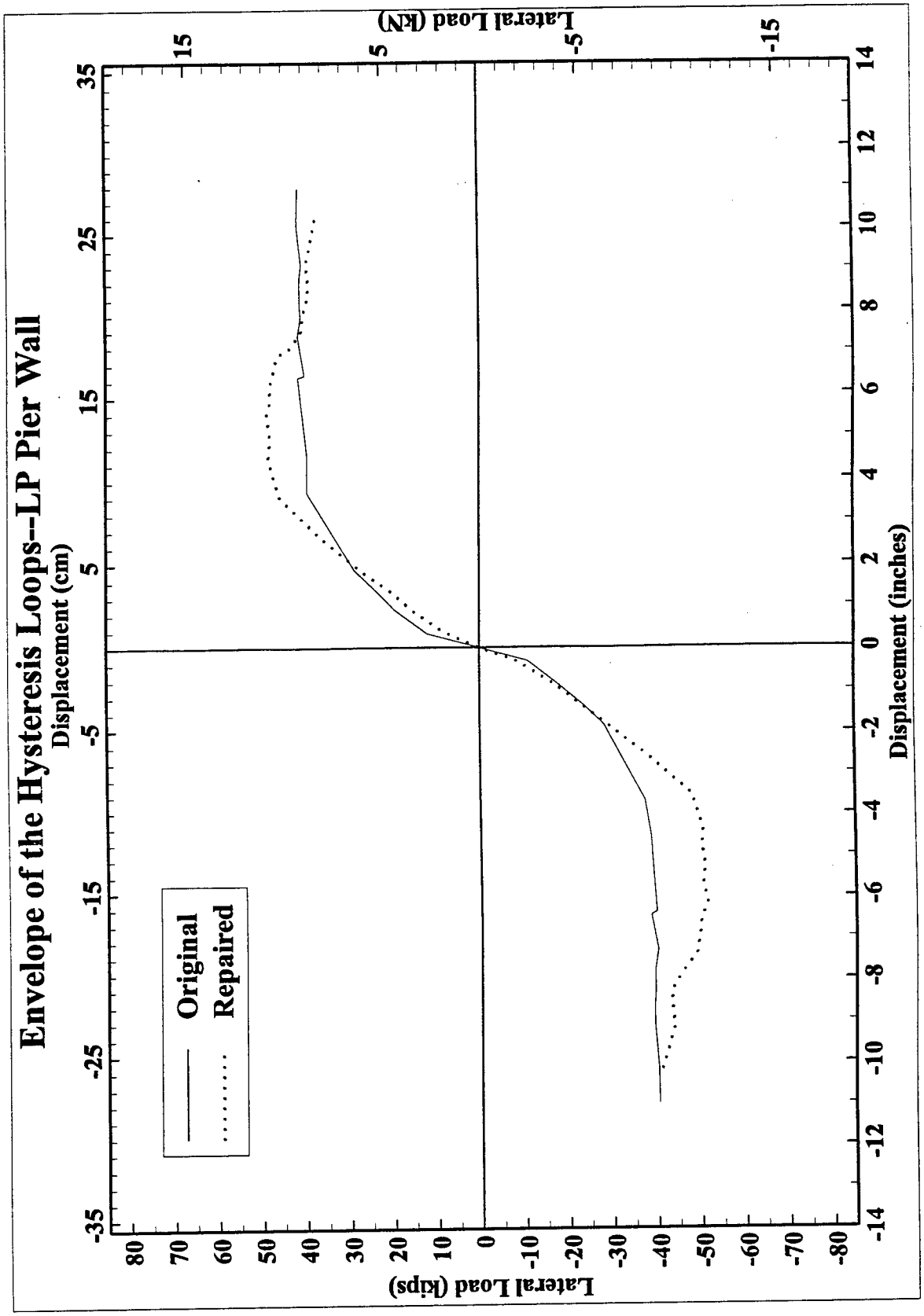

Figure 4.20: Envelope of the Hysteresis Loops: LP Pier Wall

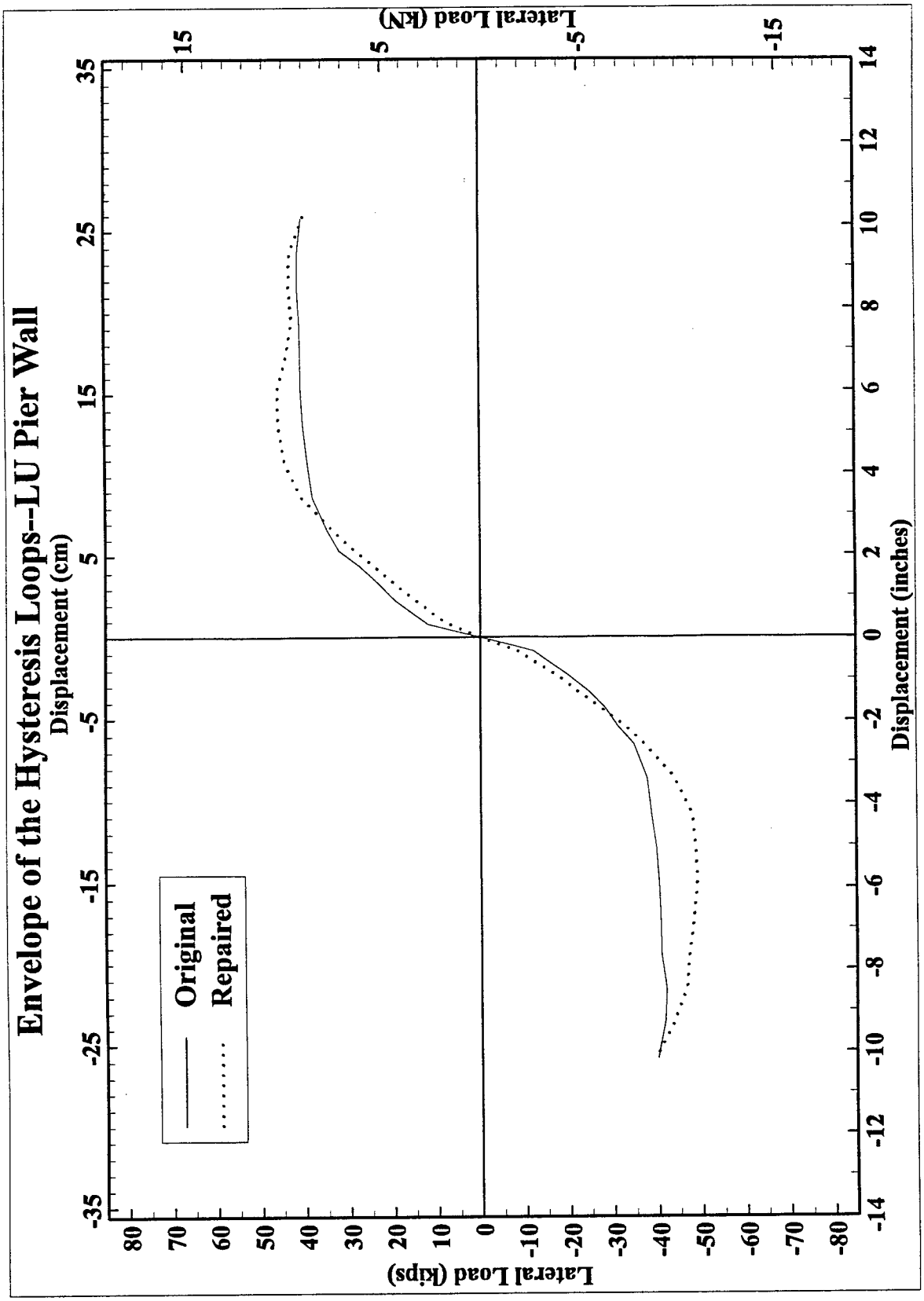

Figure 4.21: Envelope of the Hysteresis Loops: LU Pier Wall

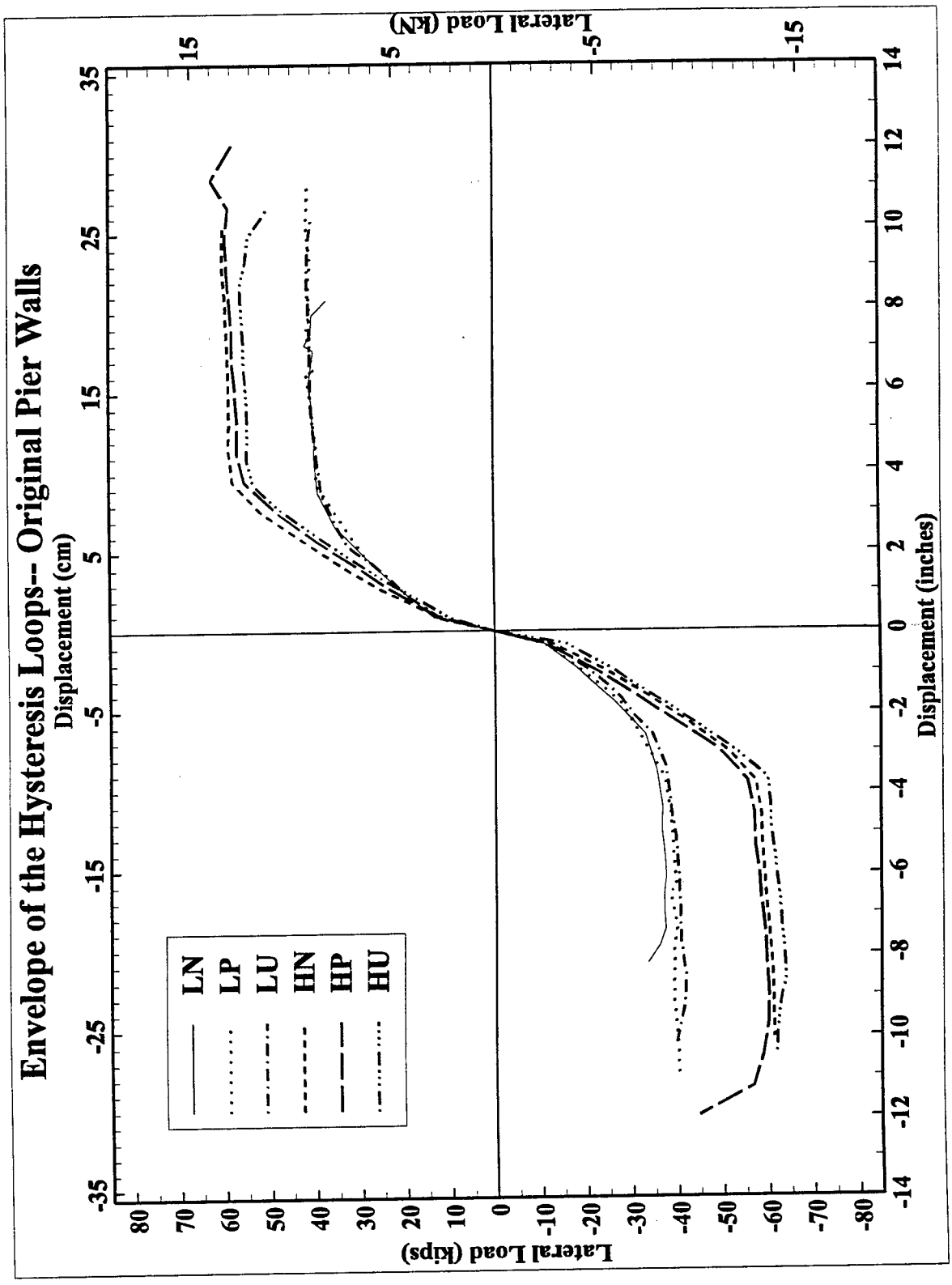

Figure 4.22: Envelope of the Hysteresis Loops: All the Original Pier Walls

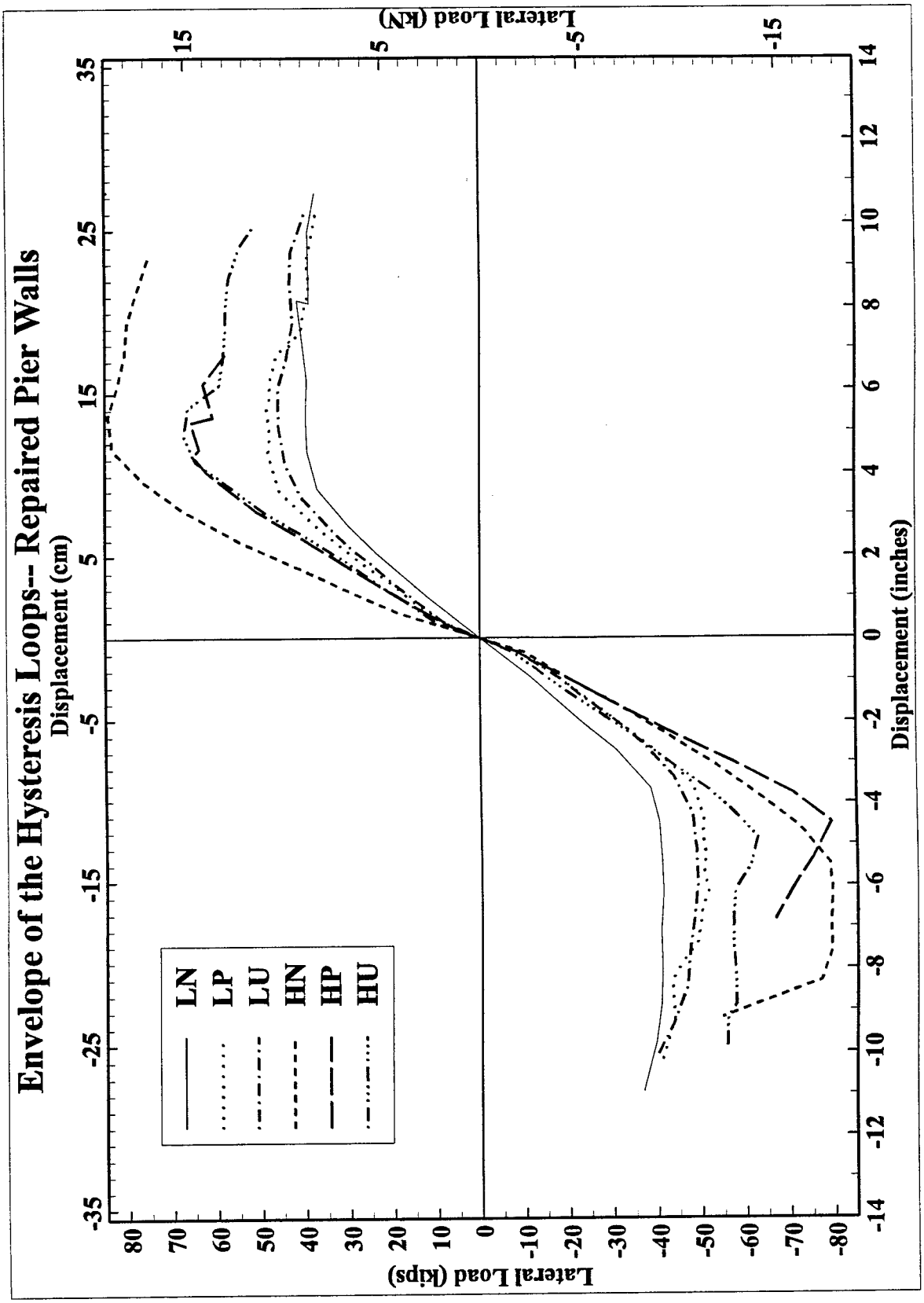

Figure 4.23: Envelope of the Hysteresis Loops: All the Repaired Pier Walls

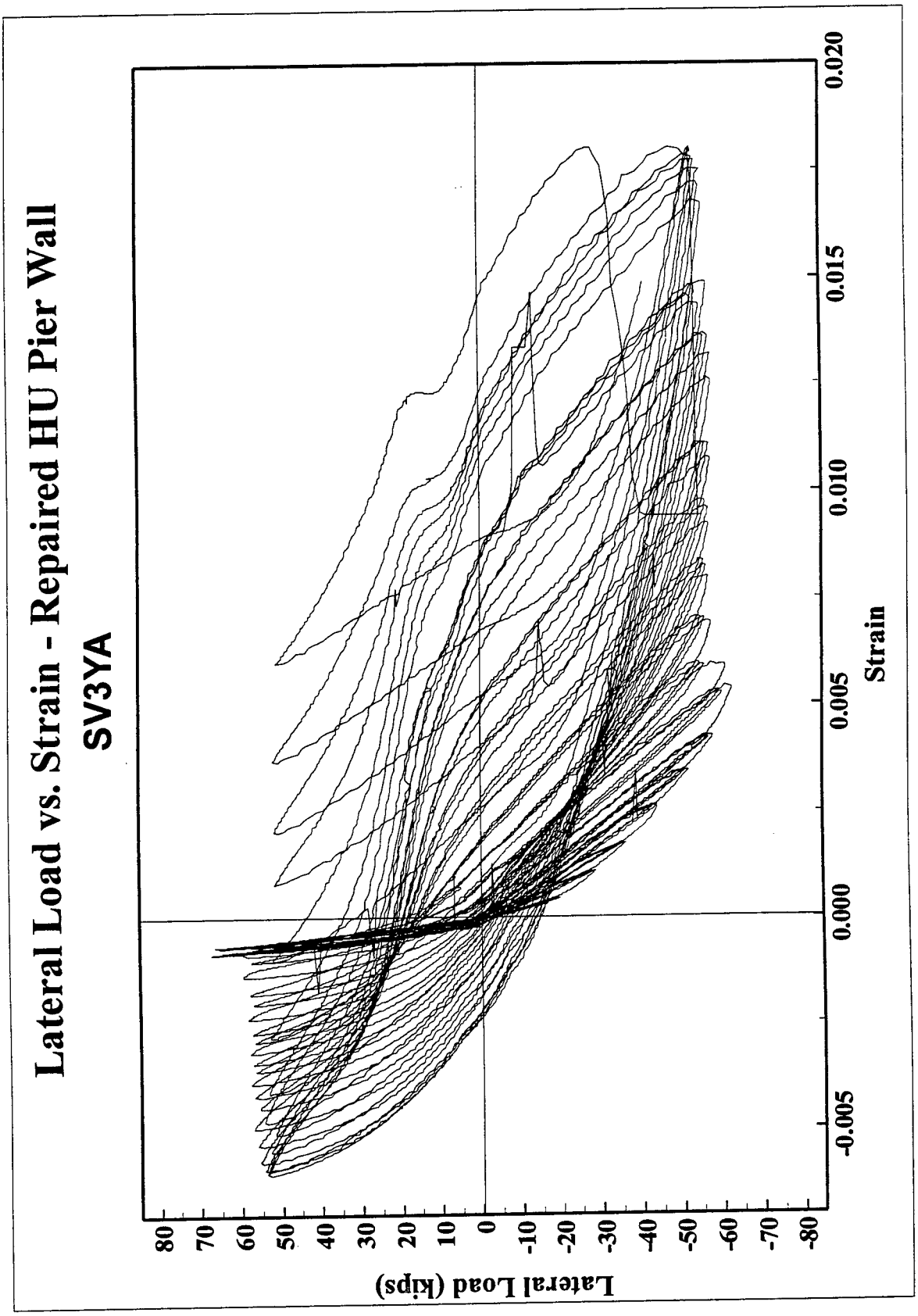

Figure 4.24: Strain in Vertical Reinforcement for Repaired HU Wall-Side A

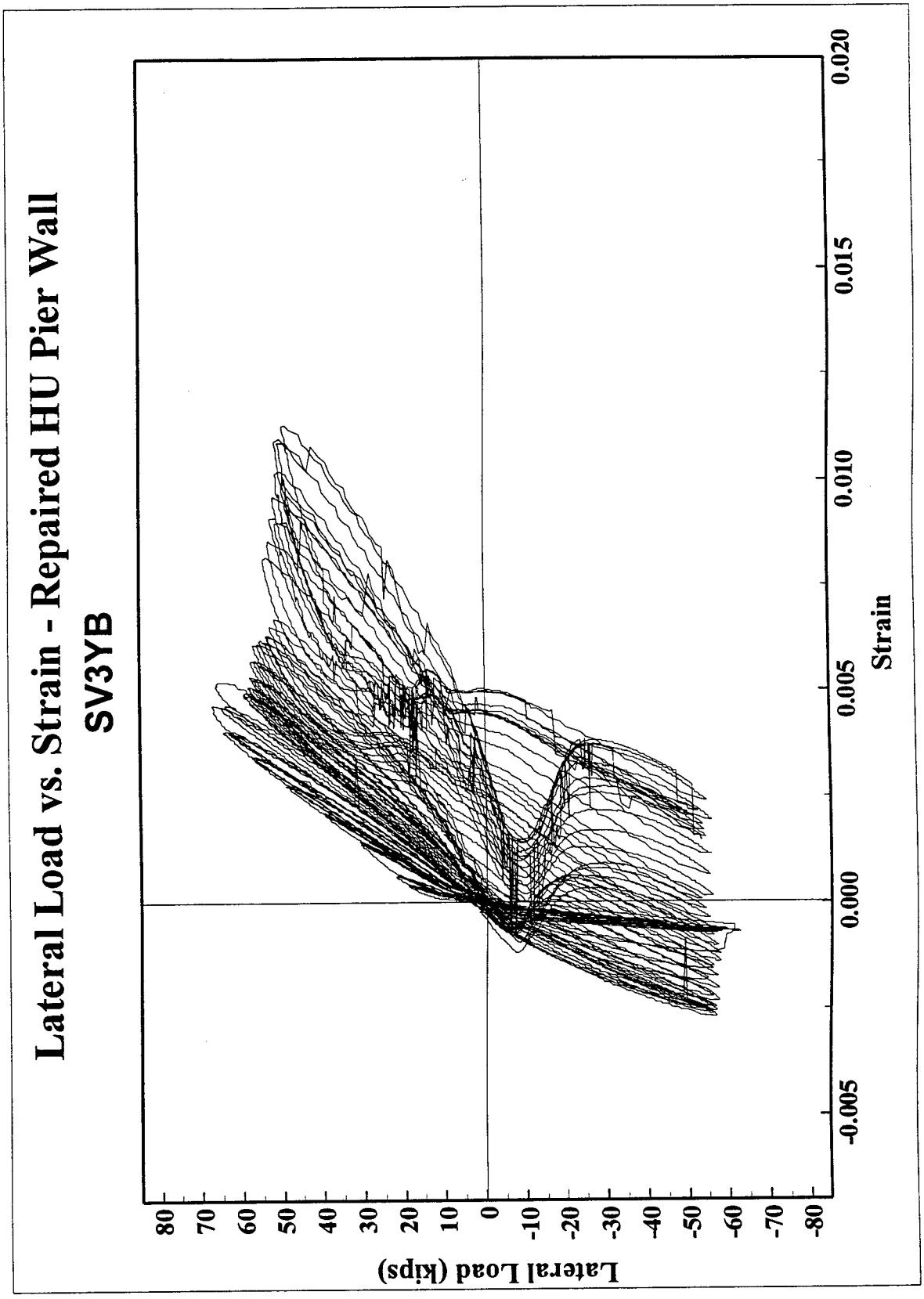

Figure 4.25: Strain in Vertical Reinforcement for Repaired HU Wall-Side B

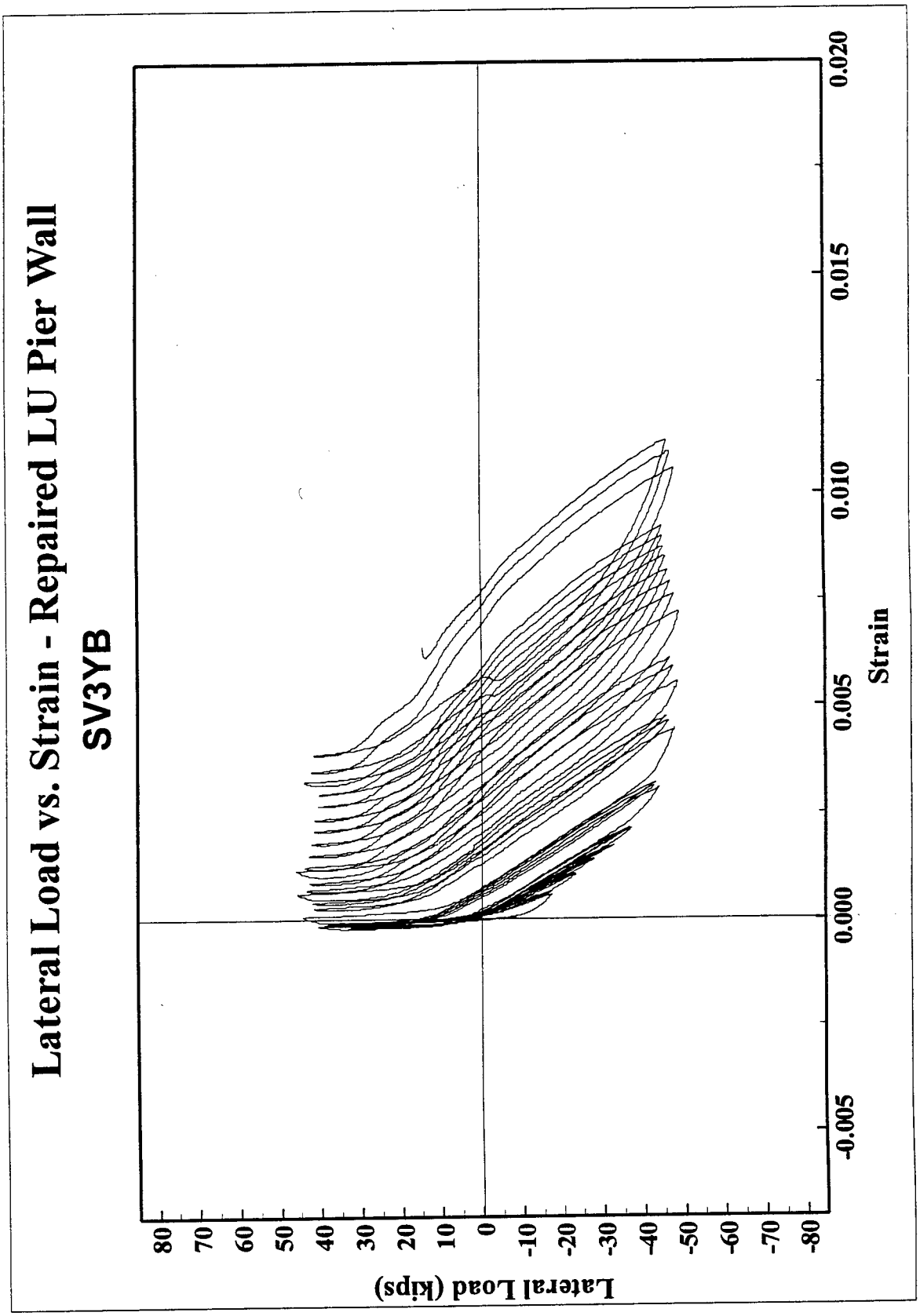

Figure 4.26: Strain in Vertical Reinforcement for Repaired LU Wall-Side B

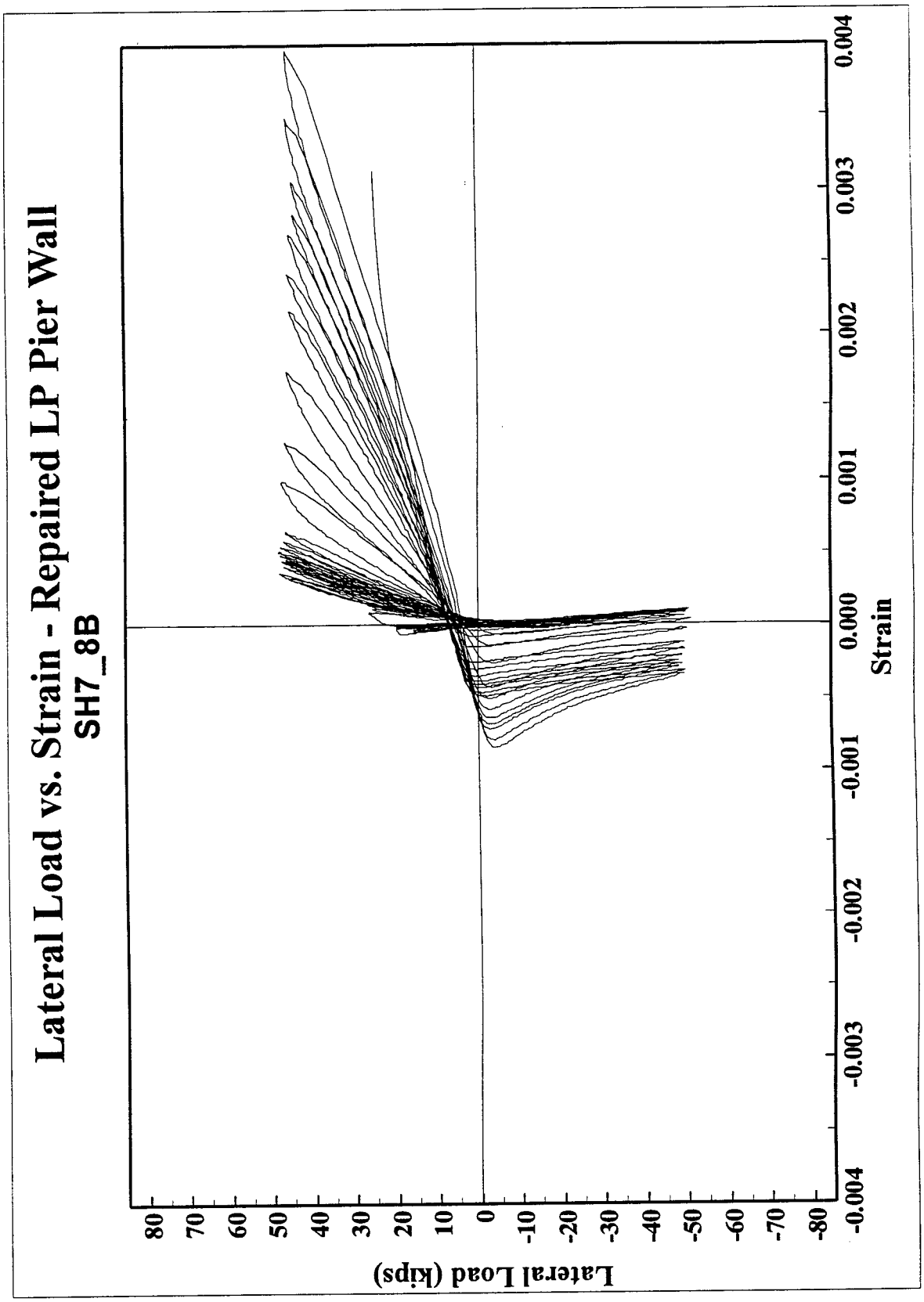

Figure 4.27: Strain in Horizontal Reinforcement from Repaired LP Wall

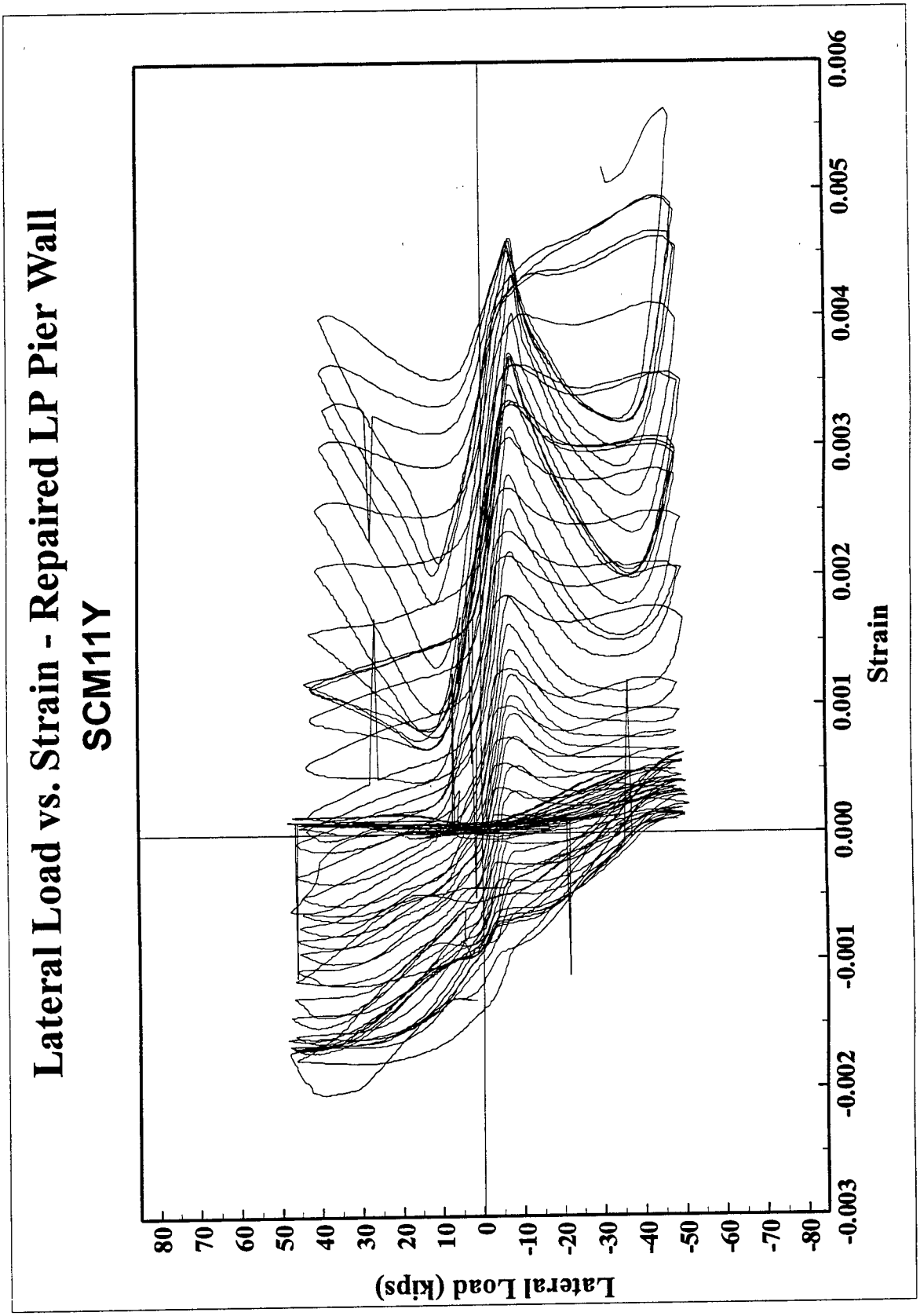

Figure 4.28: Strain in Cross-tie from Repaired LP Wall

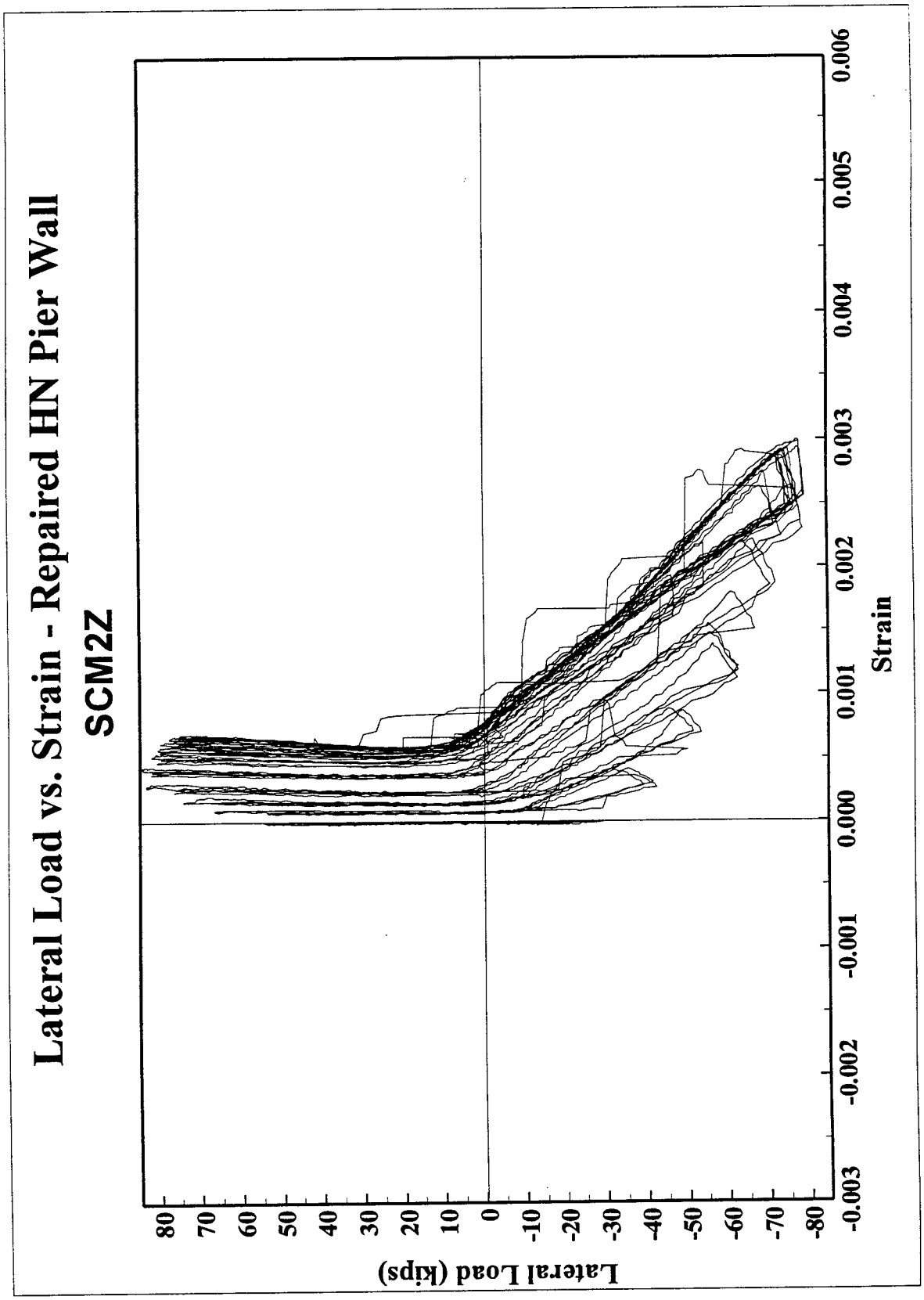

Figure 4.29: Strain in T-Headed Cross-tie

Chapter 5

Experimental Modal Analysis

Experimental modal analyses were performed to determine the dynamic characteristics of the repaired pier wall samples. This vibration technique provides a simple non-destructive means of obtaining a structure's modal parameters such as natural frequencies, damping and mode shapes. For each of the six pier wall samples, a modal analysis was performed before and after the sample was subjected to the reversed cycle lateral loads. The dynamic characteristics were obtained by subjecting each wall to a small amplitude shaker force while measuring the acceleration response at a number of strategic locations on the pier wall. The modal investigation was confined to only the weak-axis direction since the all pier walls were tested about their weak-axis. The results obtained from the modal analysis were used to correlate the stiffness degradation of the pier wall samples.

5.1 Vibration Test Setup

A block diagram of the experimental modal analysis test setup is shown in Figure 5.1. A 30 lb., low frequency shaker mounted on the top of the pier wall provided the excitation during the modal analysis. The shaker was securely attached to the pier wall with four bolts that mated with four nuts that had been imbedded in pre-drilled

holes in the top face of the pier wall. The shaker was used in its horizontal mode to vibrate the wall about the weak-axis. An HP 35665A, two channel dynamic signal analyzer/data acquisition system provided the drive signal to the shaker via an APS power amplifier.

Sine Sweep excitation was used to obtain the first three modes of the pier wall since laboratory experience has shown that this excitation provides the best signal-to-noise ratio in the Structural Engineering Test Hall. A PCB accelerometer was mounted on the shaker mass to monitor its excitation. Another PCB accelerometer was attached to the pier wall to monitor its response. This 'roving' accelerometer was then moved to measure the response at various other strategic positions on the pier wall face as shown in Figure 5.2. It should be noted that no accelerometers were placed at points 11, 12 or 13 at the base of the pier wall since these were used solely as 'fixed' reference points in the modal identification process. Table 5.1 shows the coordinates of the accelerometer response locations on the pier wall.

5.2 Data Acquisition / Data Reduction

Frequency response and coherence function measurements were made at 10 strategic locations on the pier wall's vertical face. The frequency response function is the frequency domain representation of the basic input/output (input = force excitation / output = acceleration response) characteristic of the structural system. The coherence function, which provides the frequency domain representation of the signal-to-noise ratio, serves as a qualitative guide as to the quality of the experimentally acquired data.

The 10 measurement points were chosen so that the pier wall's bending and twisting behavior could represented. The shaker was purposely mounted off-center so that the

symmetric and anti-symmetric modes would be excited. The modal analysis survey was confined to 1 Hz to 60 Hz in the 'before' test condition and 1 Hz to 71 Hz in the 'after' condition.

Consider the pair of frequency response function measurements are shown in Figure 5.3 and Figure 5.4 for pier wall LU. Figure 5.3 represents the 'before' condition whereas Figure 5.4 depicts the 'after' condition. Note that the first three frequencies corresponding to the 'before' condition decrease in the 'after' condition. This behavior, which is typical of all six repaired pier walls in their 'before' and 'after' condition, is what one would expect since the damaged pier wall is less stiff due to the reversed cycle lateral load test. In addition to the expected decrease in frequencies, as a rule the modal damping ratios increased in the 'after' condition. Note the relative sharp resonance peaks in the 'before' condition and the relative blunt resonance peaks in the 'after' condition. Sharp peaks correspond to light modal damping whereas blunt resonance peaks correspond to heavier modal damping.

With few exceptions, the experimental modal analysis of each pier wall produced excellent results with distinct, sharp modal resonances in the frequency response functions for all measurement points of the structure which, in turn, lead to the identification of distinct modes in the frequency band of interest. The use of Sine Sweep as the excitation time history contributed to the acquisition of the excellent frequency response functions.

The modal parameter identification software SMS Modal 3.0 [10] was used to process the experimentally acquired frequency response function data to obtain the modal parameters of the repaired samples. The modal parameters of interest were the frequencies, damping ratios and mode shapes of each wall. The measured frequency response functions were curve fitted to obtain the first three frequencies and their corresponding mode shapes. Since, in general, the modes were well separated, no

Point No.	X Coord.	Y Coord.	Z Coord.
1	0.00	0.00	126.00
2	0.00	16.75	126.00
3	0.00	33.75	126.00
4	0.00	50.25	126.00
5	0.00	67.00	126.00
6	0.00	0.00	63.00
7	0.00	33.50	63.00
8	0.00	67.00	63.00
9	0.00	33.50	95.25
10	0.00	33.50	31.75
11	0.00	0.00	0.00
12	0.00	33.50	0.00
13	0.00	67.00	0.00

Table 5.1: Coordinates of the Measured Points

problems were encountered using the polynomial curve fitting procedure. Using the animation menu of SMS Modal 3.0, it could be seen that, typically, the first and the third modes were bending modes whereas the second mode was a torsion mode. The results are summarized in Table 5.2.

5.3 Stiffness Degradation

The first mode's frequency of each pier wall in the 'before' condition was typically reduced to 30% - 50% in the 'after' condition. Using the repaired LU pier wall as an example, a pier wall's stiffness degradation was determined from the vibration tests by using the relationship

$$(K_2/K_1) = (\omega_2/\omega_1)^2 = (2.9 \text{ Hz}/9.1 \text{ Hz})^2 = 0.10 \Longrightarrow 90\% \text{ stiffness degradation}$$

where K_1 and ω_1 represent the stiffness and frequency of the repaired pier wall before the test and K_2 and ω_2 are the stiffness and frequency of the walls after the cyclic test. It was assumed that the pier wall mass before and after cyclic testing remained

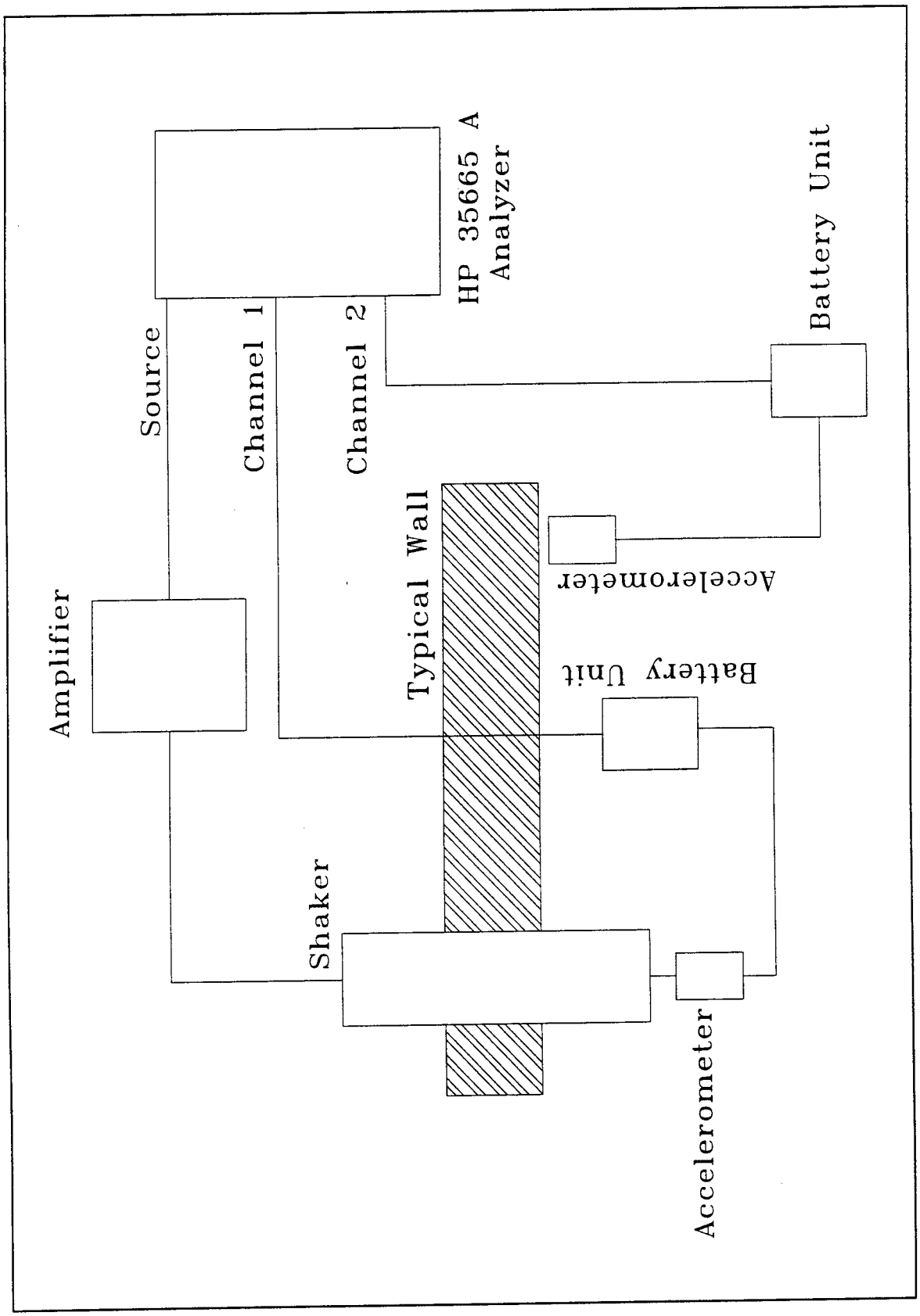

Figure 5.1: Block Diagram - Experimental Modal Analysis Test Setup

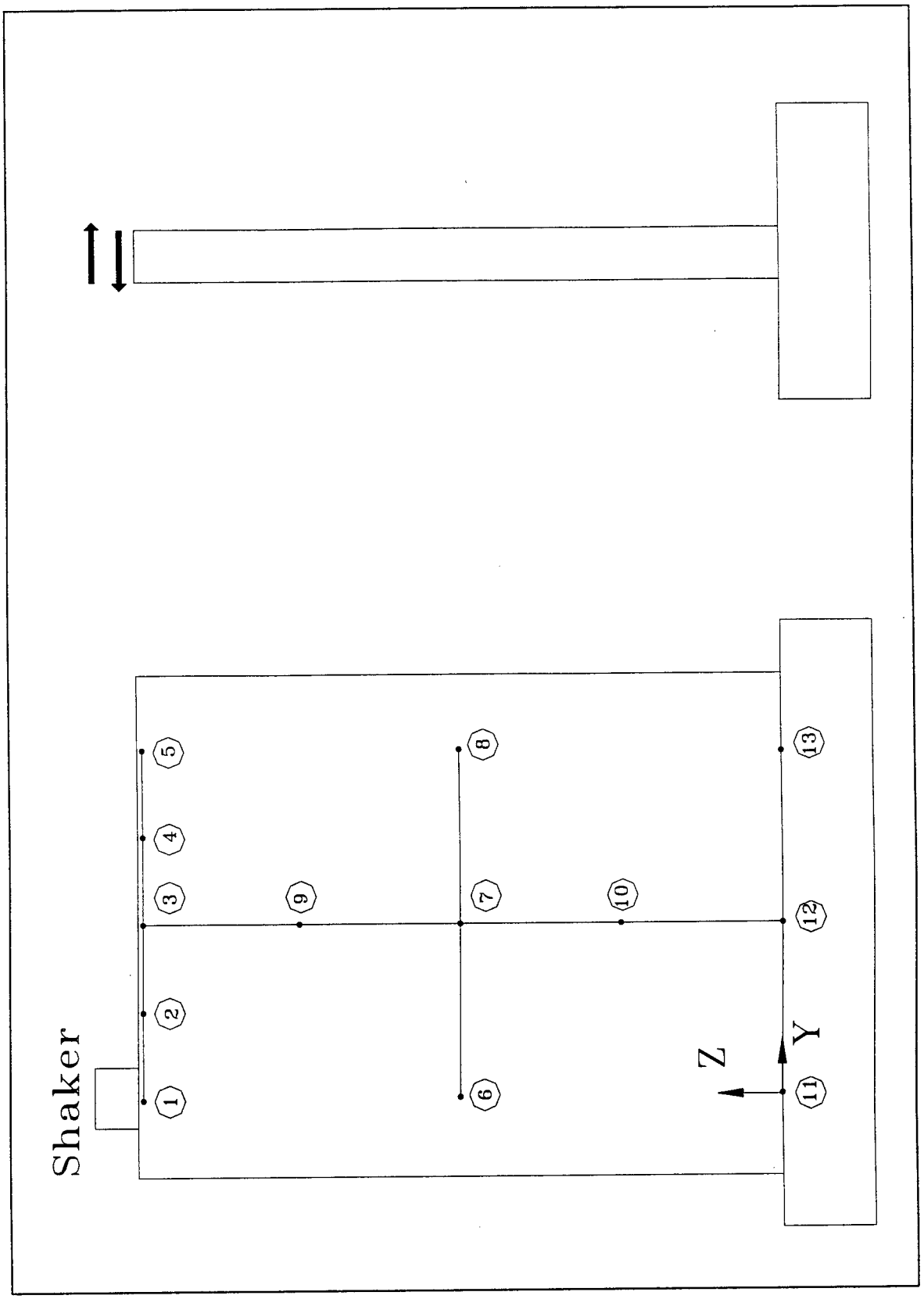

Figure 5.2: Location of the Measured Points

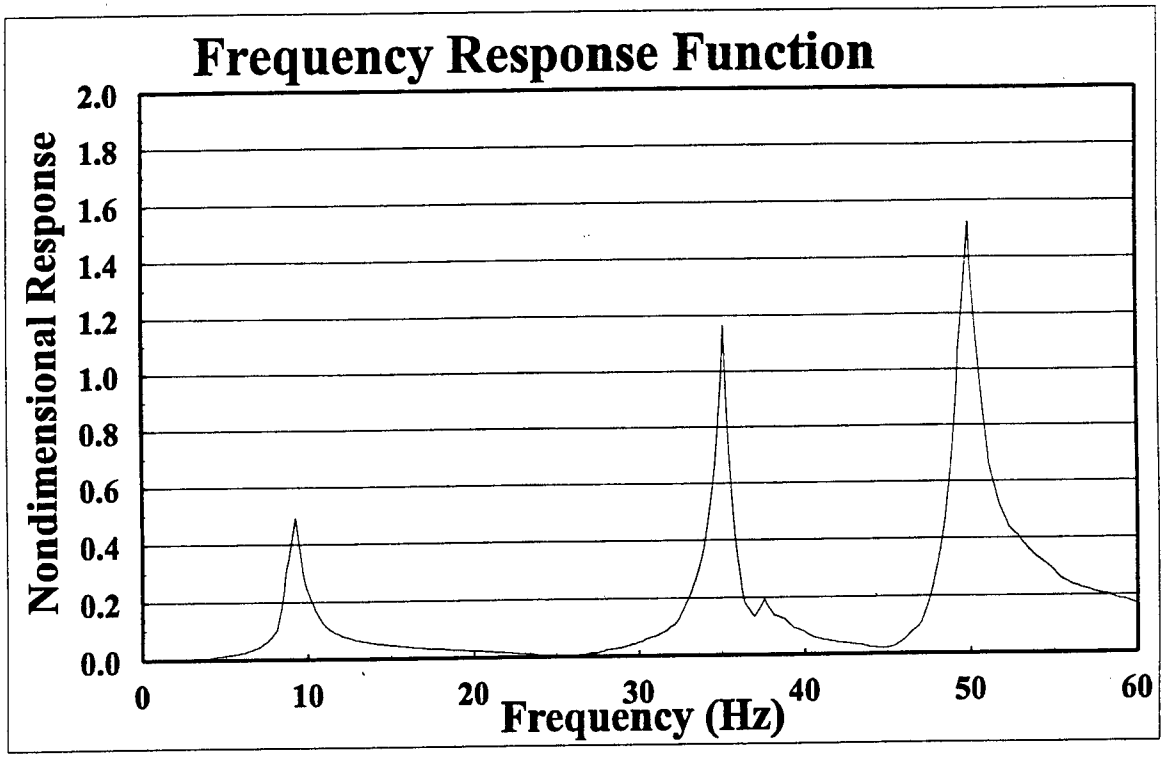

Figure 5.3: FRF of Point 1 -LU Wall- 'Before' Test Condition

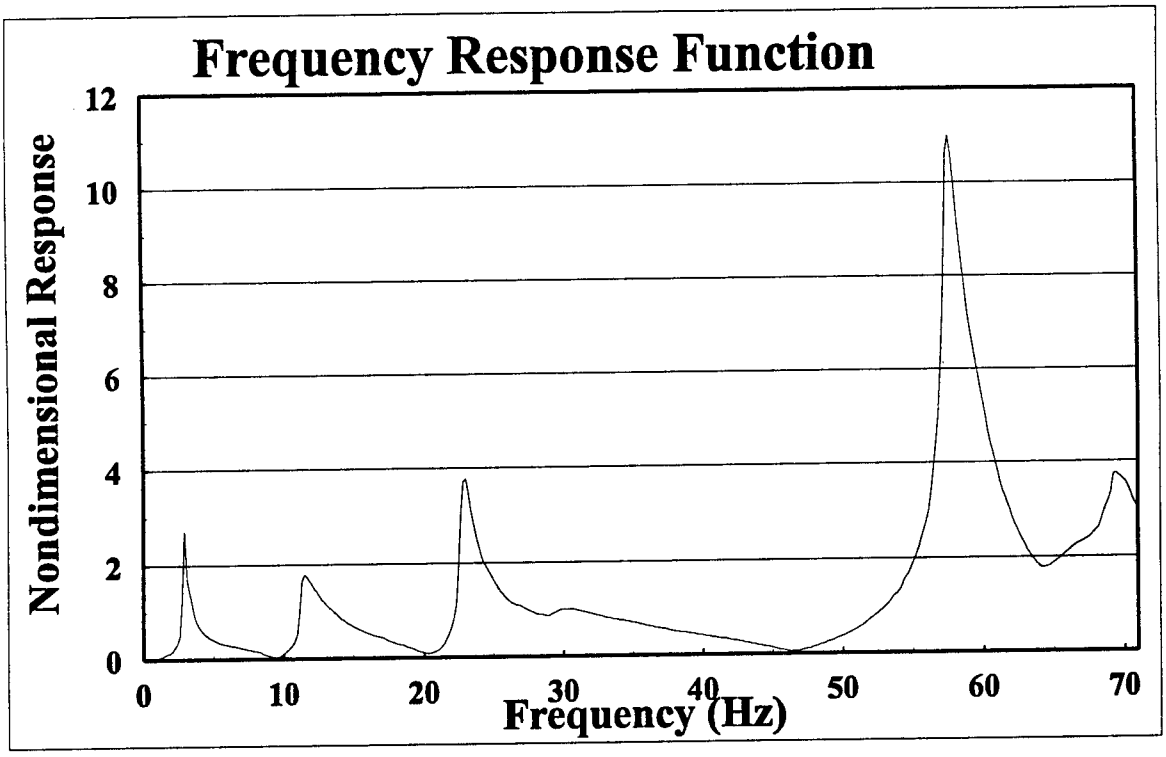

Figure 5.4: FRF of Point 1 -LU Wall- 'After' Test Condition

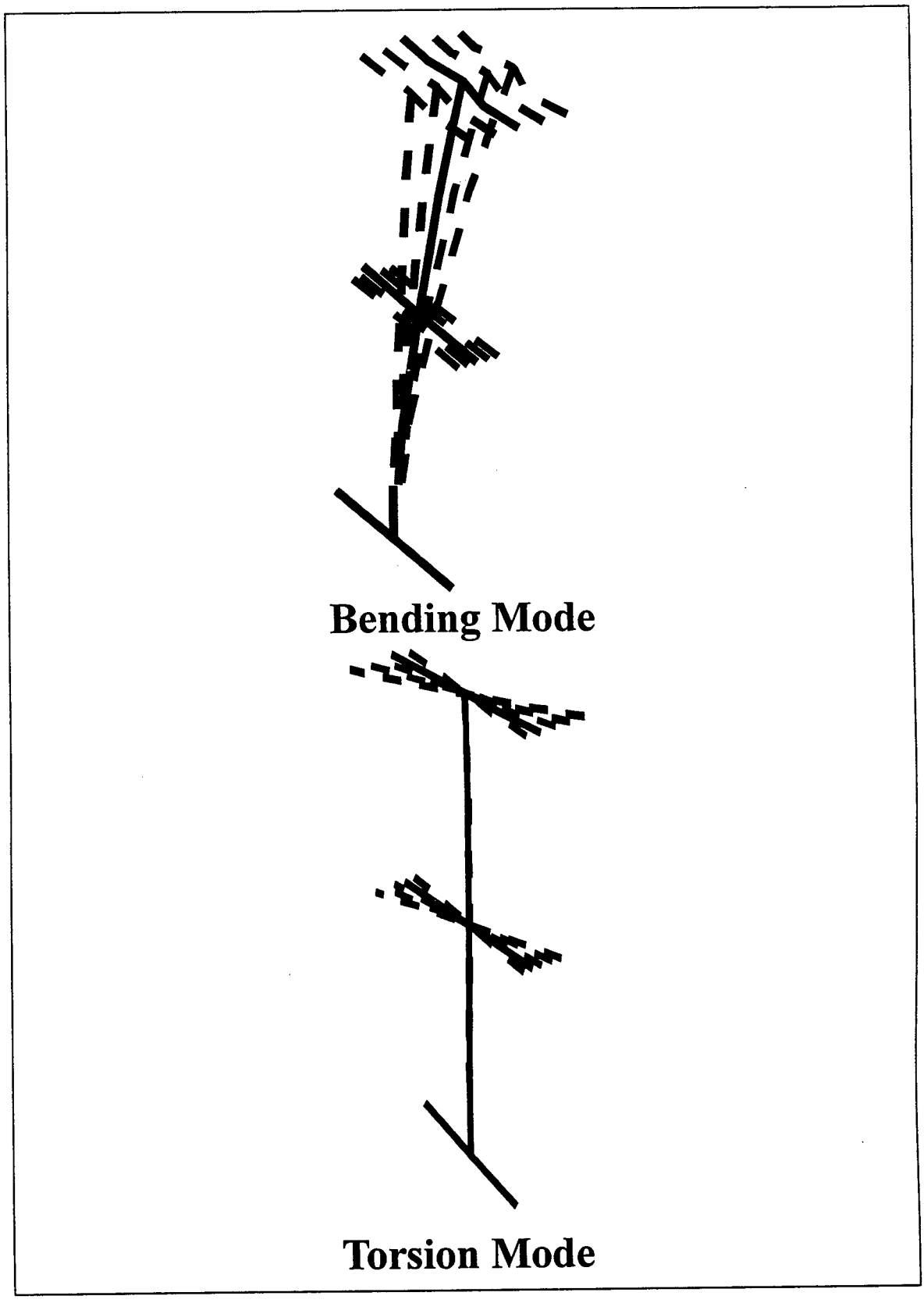

Figure 5.5: Animated Mode Shapes

Pier Wall	Mode No.	Before Testing		After Testing	
		Freq. (Hz)	Damping %	Freq. (Hz)	Damping %
LU	1	9.06	2.72	2.87	5.07
	2	34.98	0.76	11.36	5.09
	3	49.80	1.05	22.90	1.88
LP	1	8.17	2.72	3.32	3.86
	2	32.57	1.33	11.93	2.78
	3	48.05	1.35	24.40	2.13
LN	1	7.83	2.39	3.20	3.29
	2	31.30	1.87	10.61	3.49
	3	42.62	1.48	21.09	2.49
HU	1	8.56	1.93	4.24	2.14
	2	32.09	0.89	13.12	2.80
	3	36.42	1.41	27.20	1.67
HP	1	9.37	4.39	4.35	2.90
	2	30.85	0.89	17.32	1.54
	3	40.79	1.96	32.56	1.14
HN	1	10.39	1.94	4.66	1.22
	2	34.78	1.10	15.92	1.42
	3	50.87	1.11	31.20	1.02

Table 5.2: Modal Properties of Repaired Pier Walls - First Three Modes

the same since most of the concrete cover spalling occurred near its base and therefore did not affect the effective mass in the first mode of vibration.

As an independent check of the stiffness degradation, the stiffness was calculated from the slopes of the Lateral Load vs. Displacement curves shown in Figures 4.9 to 4.14. Again using pier wall LU as an example, K_1 obtained from the first displacement cycle was found to be 22.6 kips/in. whereas K_2 obtained from the last displacement cycle was found to be 2.1 kips/in. Accordingly, the stiffness degradation obtained from the ratio $K_2/K_1 = 0.09$ was consistent with the experimental modal analysis results. The results of all the six repaired pier wall are presented in Table 5.3.

Experimental modal analysis is a useful tool that can be used to estimate the

Pier Wall	ω_1 (Hz)	ω_2 (Hz)	$(\omega_2/\omega_1)^2$	K_1 (kips/in)	K_2 (kips/in)	K_2/K_1	ξ_1 (%)	ξ_2 (%)
LU	9.1	2.9	0.10	22.6	2.1	0.09	2.7	5.1
LP	8.2	3.3	0.17	21.7	2.4	0.11	2.7	3.9
LN	7.8	3.2	0.17	13.0	2.5	0.19	2.4	3.3
HU	8.6	4.3	0.25	22.7	5.2	0.23	1.9	2.1
HP	9.4	4.4	0.22	23.5	5.4	0.23	4.4	2.9
HN	10.4	4.7	0.20	29.4	5.2	0.18	1.9	1.2

ω_1 = Fundamental mode frequency of repaired pier wall before cyclic tests
ω_2 = Fundamental mode frequency of repaired pier wall after cyclic tests
K_1 = Lateral stiffness of repaired pier wall before cyclic tests
K_2 = Lateral stiffness of repaired pier wall after cyclic tests
ξ_1 = Damping ratio in the fundamental mode of repaired pier wall before cyclic tests
ξ_2 = Damping ratio in the fundamental mode of repaired pier wall after cyclic tests

Table 5.3: Pier Wall Stiffness Degradation

dynamic characteristics of a structure. Modal properties, such as frequencies, mode shapes and damping, can be estimated. Data obtained from the modal analysis clearly demonstrate the frequency shifts in the pier walls. Frequency shifts from a higher frequency to a lower frequency as a result of damage to the structure was well documented. The damping ratios from the different modes may be used in a finite element analysis. Similarly, data from the mode shapes help separate a bending mode from a torsion mode.

Chapter 6

Full-Scale Pier Walls

6.1 Introduction

6.1.1 Project Scope

Various half-scale pier wall tests have been conducted at UCI. In the half-scale tests, the steel reinforcement and concrete aggregate were scaled. To understand the effects of scaling in cyclic loading tests, two new full-scale pier walls were built to modern design standards to reflect in-situ conditions. The full-scale samples allow correlation of the half-scale test results to pier walls of modern design.

6.1.2 Objectives

Several half-scale pier wall samples have shown that the cross-ties' performance was not satisfactory as their ends opened under the lateral forces exerted by the buckling of the vertical reinforcement. The objective of this task was to study this phenomena further and provide practical design recommendations. More specifically, the research investigates the following:

- Build and test two full-scale pier walls representative of in-situ field conditions with a vertical reinforcement ratio $\rho = 1.3\%$ for both samples.

- Study the effects of scaling reinforcement between the half-scale samples and the full-scale samples.
- Compare the performance of standard cross-ties to enhanced cross-ties in full-scale samples.

6.2 Dimensions and Reinforcement Details

Each of the previous half-scale samples had a height of 127 inches, a width of 96 inches and a thickness of 10 inches. The full-scale samples had the same width, 96 inches, as the half-scale samples but the height and the thickness was increased to 207 inches and 20 inches respectively. Experience has shown that the width of the wall does not significantly affect the stiffness provided it is greater than four times the thickness of the wall.

Two full-scale pier walls, designated as Samples 1 and 2, were designed with reinforcement details as shown in Figure 6.1 and Figure 6.2. The vertical reinforcement ratio in Sample 1 and Sample 2 was 1.3%. Grade 60 #9 reinforcement bars were used as the vertical steel in both the samples whereas both #3 and #4 Grade 60 reinforcement bars were used as the cross-ties in the samples. Sample 1 was built using a #4 reinforcement bar as the cross-tie giving the horizontal steel reinforcement ratio of 0.67% in the plastic hinge zone and 0.31% in the upper portion of the wall. However, the cross-tie configuration for Sample 2 was different in the plastic hinge zone. A pair of #3 reinforcement bars, with alternating 90 and 135 degree hooks, were used as the cross-ties. This configuration made the horizontal reinforcement ratio for Sample 2 to be 0.73% in the plastic hinge zone. However, the cross-tie configuration in the upper portion of the wall was the same as that of Sample 1.

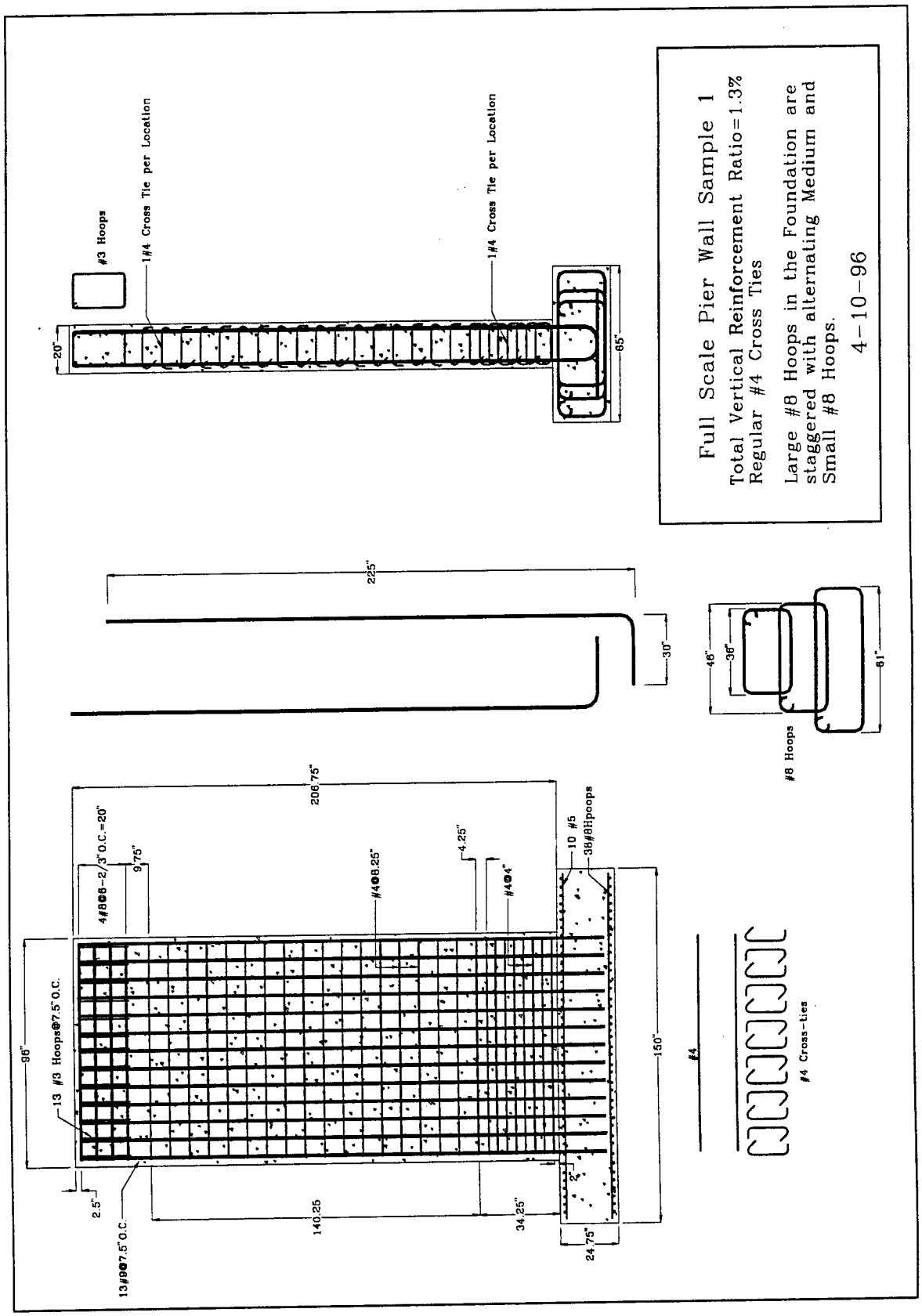

Figure 6.1: Full-Scale Sample 1

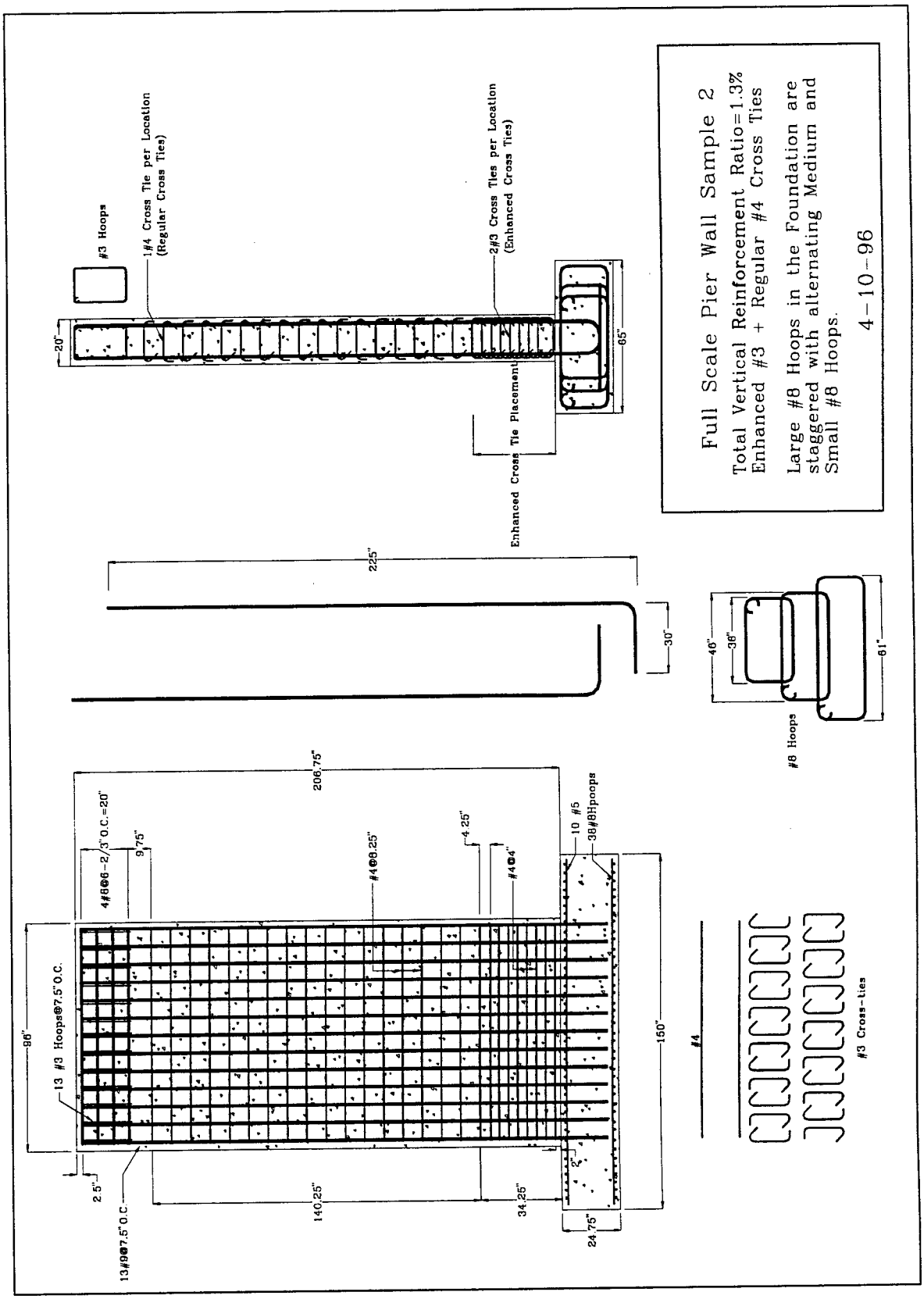

Figure 6.2: Full-Scale Sample 2

Reinforcement Type	Used As	Yield Stress (ksi)	Ultimate Tensile Strength (ksi)
#5	Straight Bars	NA	NA
#8	Hoops	NA	NA

Table 6.1: Material Properties of Steel: Footing Reinforcements

Reinforcement Type	Used As	Yield Stress (ksi)	Ultimate Tensile Strength (ksi)
#3	Cross-ties	71,323	104,678
#3	Hoops	66,938	104,172
#4	Cross-ties	64,000	104,000
#4	Horizontal Bars	70,500	111,000
#8	Horizontal Bars	66,000	106,000
#9	Vertical Bars	NA	NA

Table 6.2: Material Properties of Steel: Wall Reinforcements

6.3 Concrete and Steel Material Properties

All the steel reinforcement conformed to ASTM A615 New Billet Steel Standards and was of Grade 60. The material properties of the reinforcement used in the footings are summarized in Table 6.1. Similarly, Table 6.2 lists the material properties of the reinforcement used in the walls of the full-scale samples. The values tabulated in Tables 6.1 and 6.2 were obtained from the supplier, Rebar Engineering.

A concrete mix with 1 inch aggregate and a nominal strength $f_c' = 4000$ psi was used in constructing the footings and the walls of both full-scale samples. A 6.38 sack mix was utilized in obtaining a nominal concrete strength of 4000 psi. The mix proportions were as follows:

Batch No.	Slump (inches)	Sample	Tested on (Day)	f_c'(psi) for Sample No.			Mean (psi)
				1	2	3	
			7^{th}	2410	3180	3110	2900
			28^{th}	3010	2790	3470	3240
F-1	NA	Sample 1	224^{th}	4950	5130	5130	5070
			7^{th}	2480	1950	2830	2420
			28^{th}	3540	2650	3540	3240
F-2	NA	Sample 2	235^{th}	4880	4630	4700	4740

Table 6.3: Compressive Strength of Footings–Two Batches of Concrete

Type II Cement	520 pounds/yard^3
Water	308.58 gallons/yard^3
San Gab Sand	1369 pounds/yard^3
San Gab 1 in. Aggregate	1275 pounds/yard^3
San Gab 3/8 in. Aggregate	475 pounds/yard^3
Pozzolan	80 pounds/yard^3
Water Reducing Admixture (WRDA-79)	30.00 fluid ounces/yard^3
w/c	0.514
Expected Slump	6 inches

Two different batches of concrete were poured in the footings. The two different batches were designated as F-1 and F-2. F-1 was used to construct the footing of Sample 1 whereas F-2 was used for the footing in Sample 2. The compressive strength of these two batches of concrete, obtained using standard cylinder samples at various times, are shown in Table 6.3. Due to the large size of the full-scale sample, two different batches of concrete had to be poured. The two different batches were designated W-B and W-T. W-B was utilized in constructing the lower half portions of both full-scale walls whereas the upper half portions of both full-scale walls utilized W-T. The slump and the compressive strength at various stages are shown in Table 6.4.

Batch No.	Slump (inches)	Sample	Tested on (Day)	f_c'(psi) for Sample No.			Mean (psi)
				1	2	3	
			7^{th}	3410	3500	3890	3620
			28^{th}	4240	4350	4490	4360
			78^{th}	5380	5730	5130	5410
W-B	4	Sample 1 & 2	89^{th}	5200	4780	5380	5120
			7^{th}	3010	3040	3040	3030
			28^{th}	4240	3890	3780	3970
			78^{th}	5130	4850	4420	4820
W-T	3	Sample 1 & 2	89^{th}	4880	4630	4700	4740

Table 6.4: Compressive Strength of Walls–Two Batches of Concrete

6.4 Honey-Combing

Upon removal of the formwork, slight honey-combing could be seen in some portions of the full-scale walls. After consulting with Caltrans, it was recommended to use Set 45 to repair the affected areas. Set 45 is used by Caltrans to repair such problems. The concrete surrounding the honey-combed area was removed and patched with a mixture of Set 45 and pea-gravel.

6.5 Instrumentation

The location of the string potentiometers for Sample 1 and Sample 2 is shown in Figures 6.3 and 6.4. Eight string potentiometers were installed to measure lateral displacements in Sample 1. Eight string potentiometers were also installed in Sample 2, however, three were installed at the top of the wall. Two were installed at each end of the wall to monitor relative displacements while one was installed in the middle to obtain lateral displacements at the top of the wall.

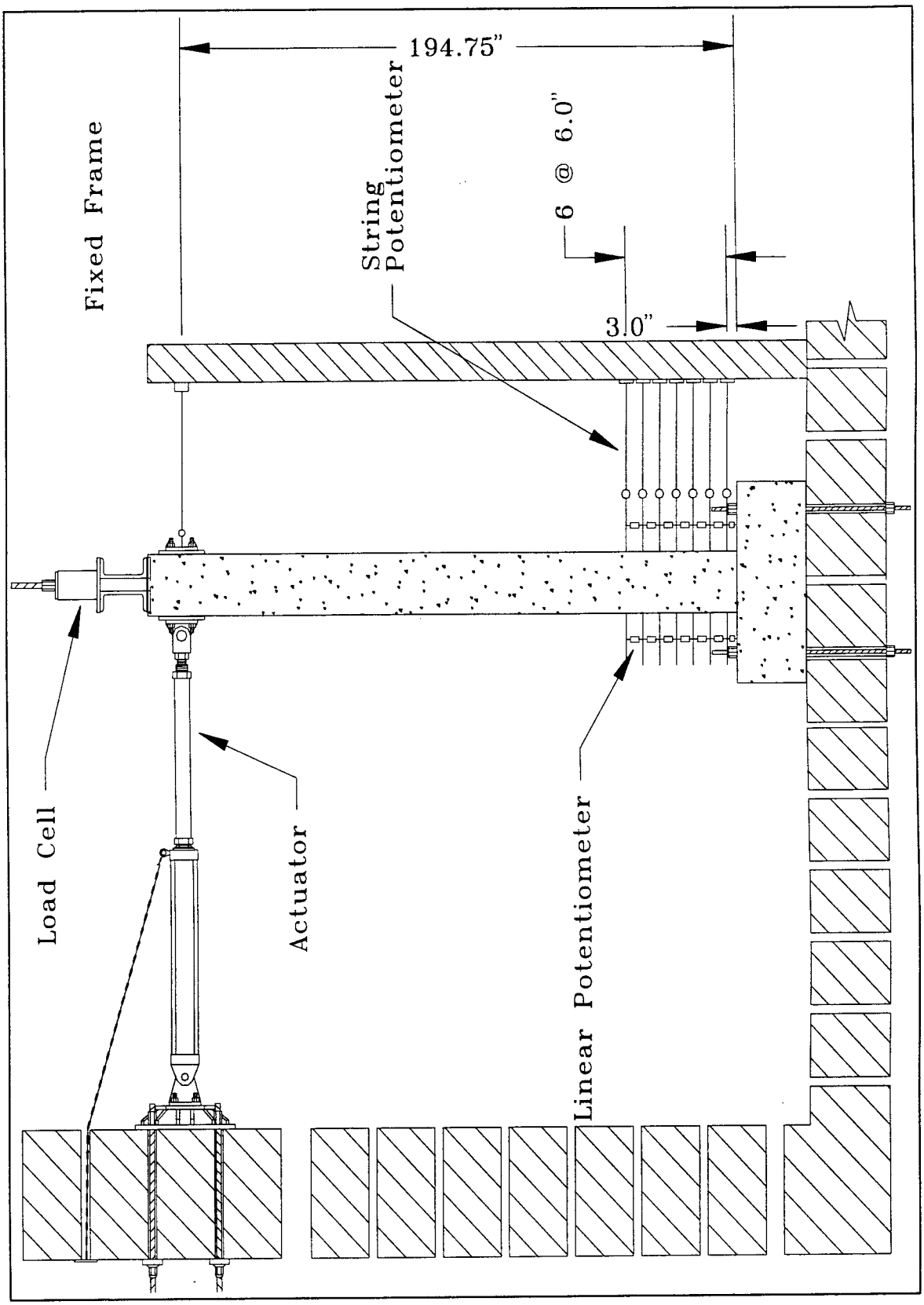

Figure 6.3: Instrumentation: Sample 1

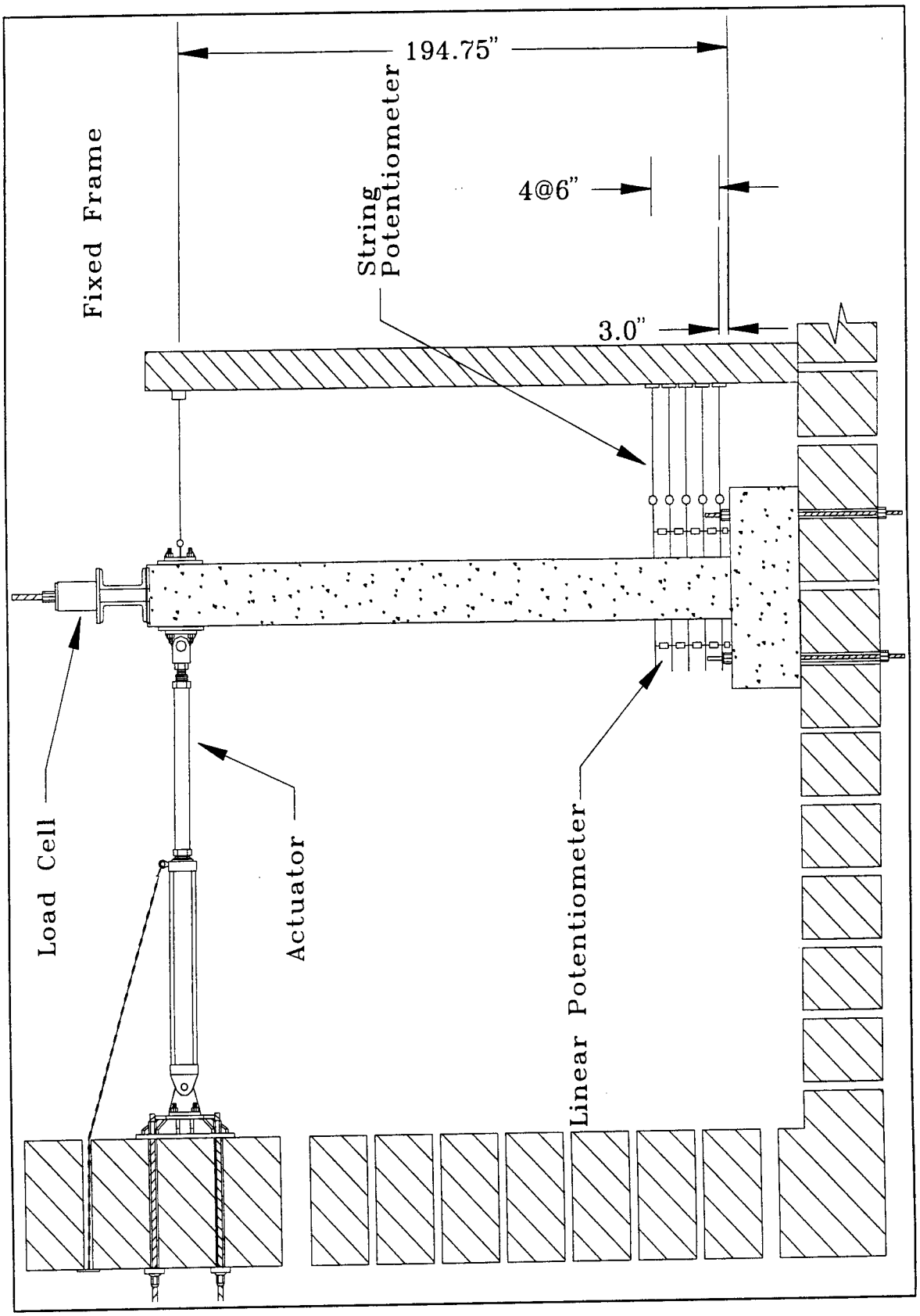

Figure 6.4: Instrumentation: Sample 2

6.6 Test Procedure

As with the original walls, Samples 1 and 2 were subjected to reversed cyclic loading. The same test set-up, as described in Section 3.3 of this report, was used for the test. Since a larger axial load was applied, a larger steel bar, 2.25 inch in diameter, and a larger hinge to accommodate the steel bars was used at each end of the wall. Initially, Sample 1 was tested with one actuator in the middle of the wall. However, when the displacements exceeded the stroke length of the actuator, two longer stroke actuators at each end of the wall were used. Anticipating displacements larger than 16 inches, Sample 2 was tested with two longer stroke actuators at each end of the wall. The plan view of the test set-up is shown in Figure 6.5.

The same test procedure used in testing the original pier walls was utilized. The test procedure was as follows:

1. The two 2.25 inch diameter steel bars were tensioned to produce axial loads approximately equal to 5% of the calculated axial load capacity of the wall. The 5% axial load was calculated to be 400 kips based on the nominal strengths of concrete and steel.

2. The hydraulic actuator jack was driven to the first displacement level and a yield displacement value is measured. The procedure is described in Section 4.3.

3. The sample was cycled three times at the initial lateral displacement level.

4. The actuator load was increased to produce the displacement level equal to the measured yield displacement. The sample was cycled three times at this new displacement level.

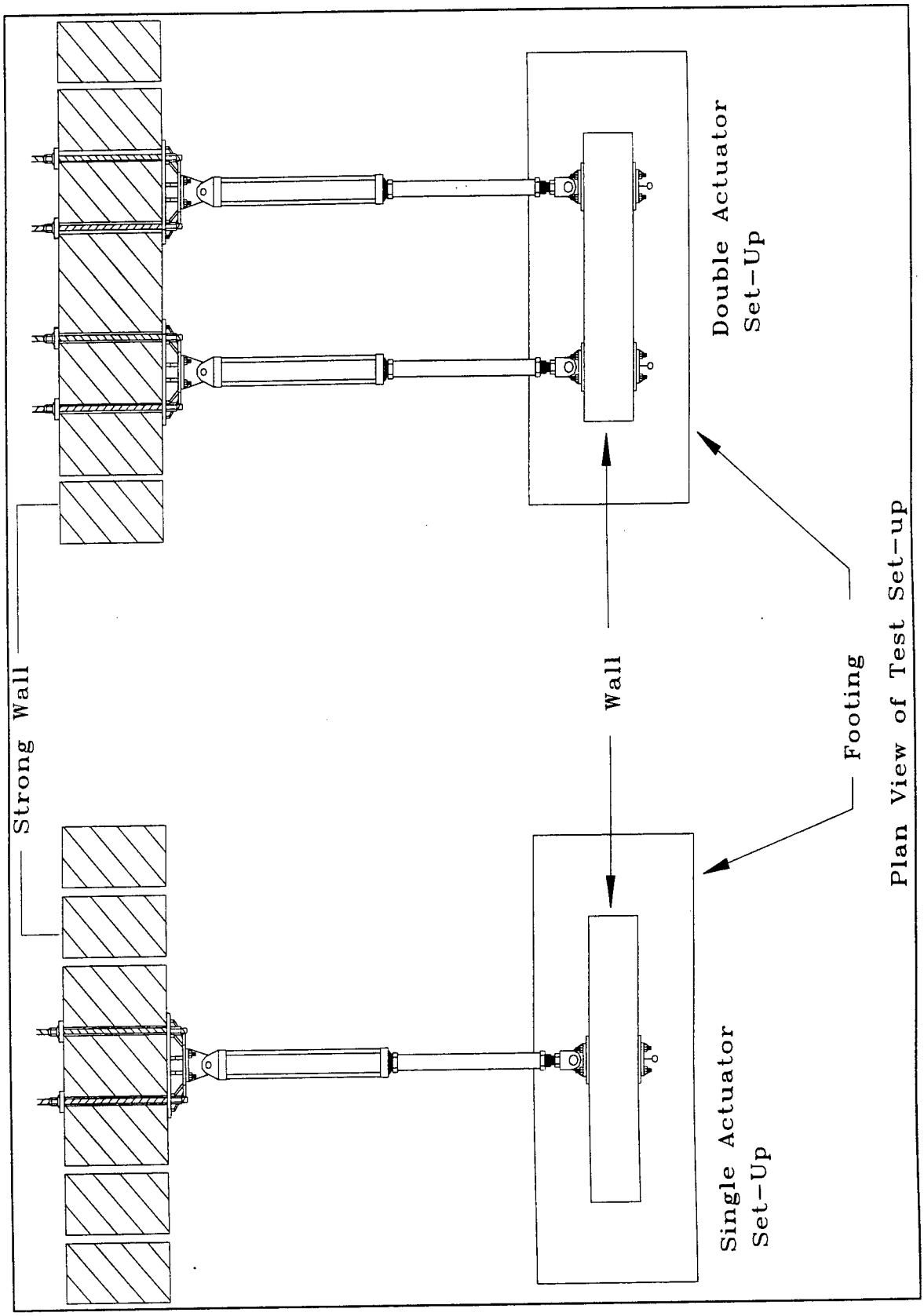

Figure 6.5: Plan View of the Test Set-Up: Full-Scale Samples

Level No.	Sample 1			Sample 2		
	Load(kips)	Δ (in.)	Cycles	Load(kips)	Δ (in.)	Cycles
1	58.3		3	58.3		3
2		2.35	3		2.48	3
3		3.53	3		3.72	3
4		4.71	3		4.96	3
5		5.89	3		6.20	3
6		7.10	3		7.44	3
7		8.28	3		8.68	3
8		9.46	3		9.92	3
9		10.64	3		11.16	3
10		11.82	3		13.64	3
11		13.00	3		14.88	3
12		14.18	3		16.12	3
13		15.36	3			
14		15.89	3			
15		16.54	3			

Table 6.5: Applied Maximum Displacements at Each Level

5. The displacement levels were increased by a third of the measured yield displacement and cycled three times at that displacement level.

6. At the end of each displacement level, the test was briefly stopped to observe the crack development and to save the logged data.

7. Steps 5 and 6 were repeated. Table 6.5 shows the test protocol.

8. The test was stopped when the sample lost more than 20% of its lateral load strength.

6.7 Strain Gages

In order to monitor the strains in the reinforcement bars, strain gages were mounted at various strategic places. The placement and the designation of the strain gages

for the vertical reinforcement and the cross-ties is shown in Figures 6.6 and 6.7 for Sample 1. Similarly, the position and the designation of the strain gages for Sample 2 is shown in Figure 6.8 and Figure 6.9.

6.8 Test Results

The hysteresis loops formed by the lateral loads and the top displacements for Sample 1 and Sample 2 are shown in Figure 6.10 and Figure 6.11. The yield displacement of Sample 1 and Sample 2 was measured to be 2.35 inches and 2.48 inches respectively. The procedure used to obtain these values is described in Section 4.3.

It can be seen from Figure 6.10 that the loads in the last level of the hysteresis loops dropped significantly. The first 16.0 inches of displacement was obtained using a single actuator that had a maximum stroke length of 16 inches. When the displacement level reached 16 inches, the test was stopped. The test was re-setup with two longer stroke actuators since the lateral load had not decreased by 30%. However, when Sample 1 was re-tested seven days later, it was found that the lateral loads had decreased significantly. This can be seen in Figure 6.10.

The displacement differences at each end of the wall had been negligible using the two actuators for Sample 1. Accordingly, Sample 2 was tested with two longer stroke actuators anticipating the displacement levels would exceed 16 inches. The displacements at each end of the walls were measured to monitor the displacement differences between the two ends. The test was stopped when the lateral load had dropped by 33%. The maximum displacement difference at each end was measured to be 3.2 inches. The 3.2 inch displacement value corresponds to a rotation of 1.95°. In both Sample 1 and Sample 2, the displacement at the center of the wall was used to plot the hysteresis loops. The envelope of the hysteresis loops for Sample 1 and

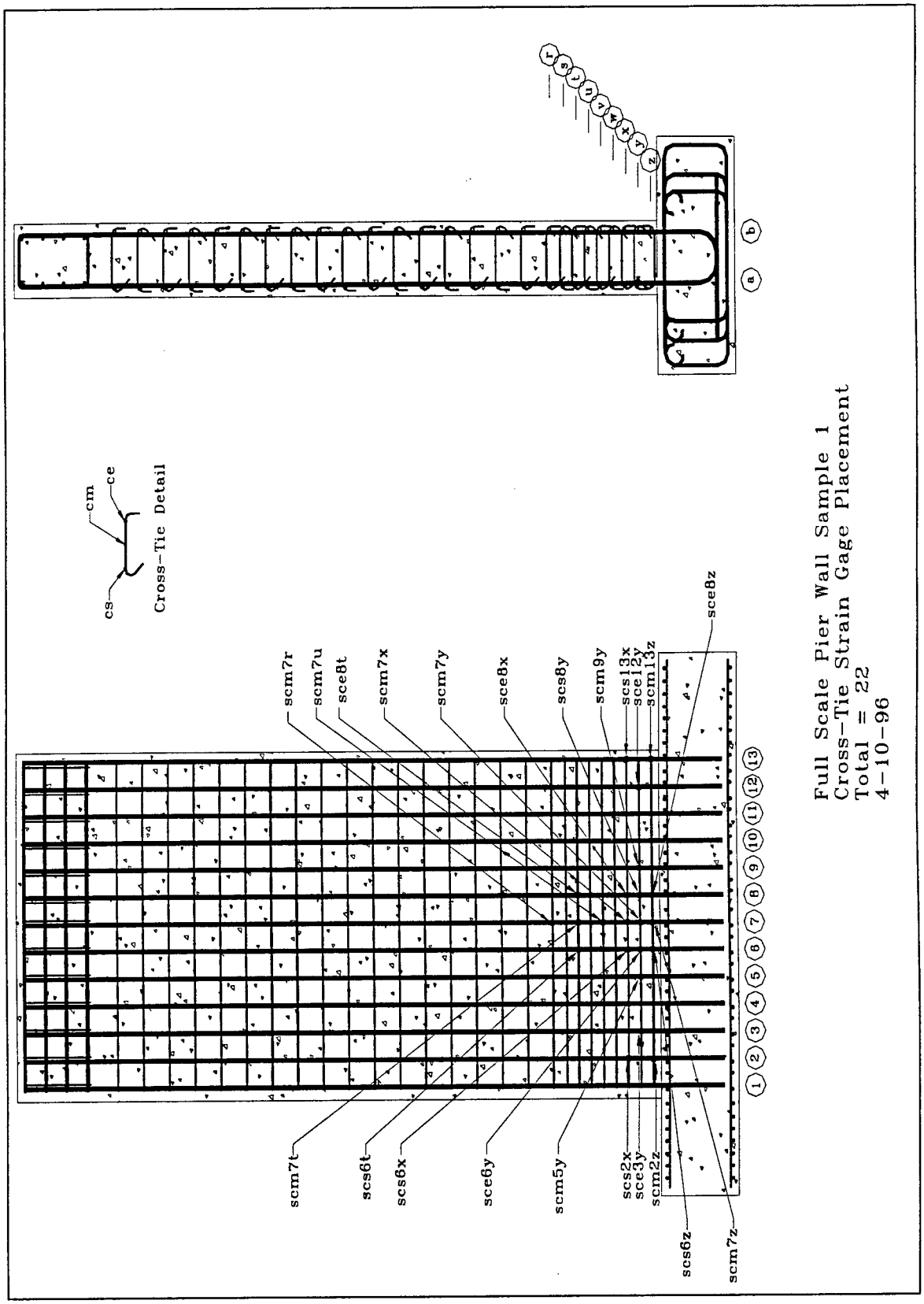

Figure 6.6: Location of Cross-tie Strain Gages: Sample 1

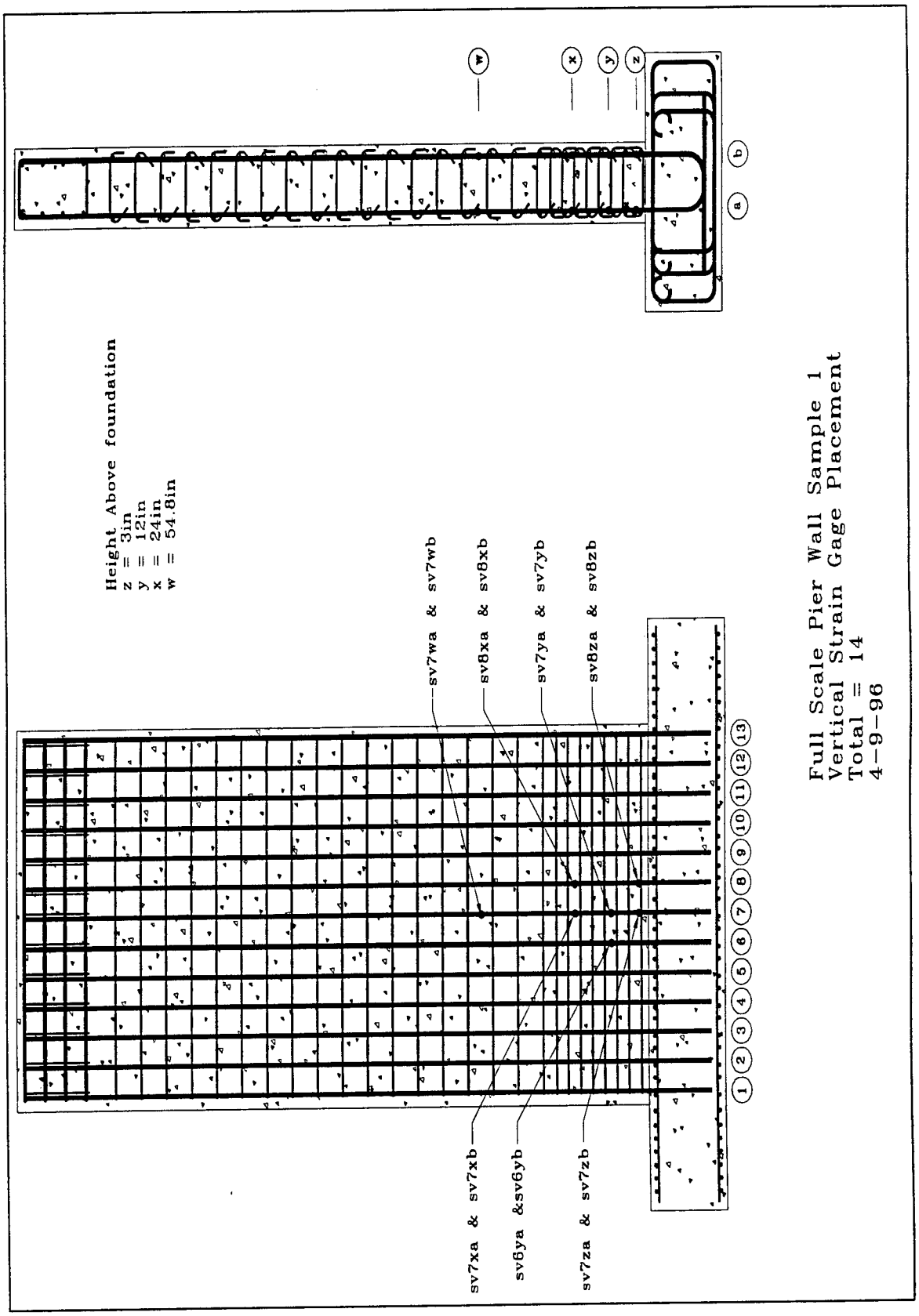

Figure 6.7: Location of Vertical Reinforcement Strain Gages: Sample 1

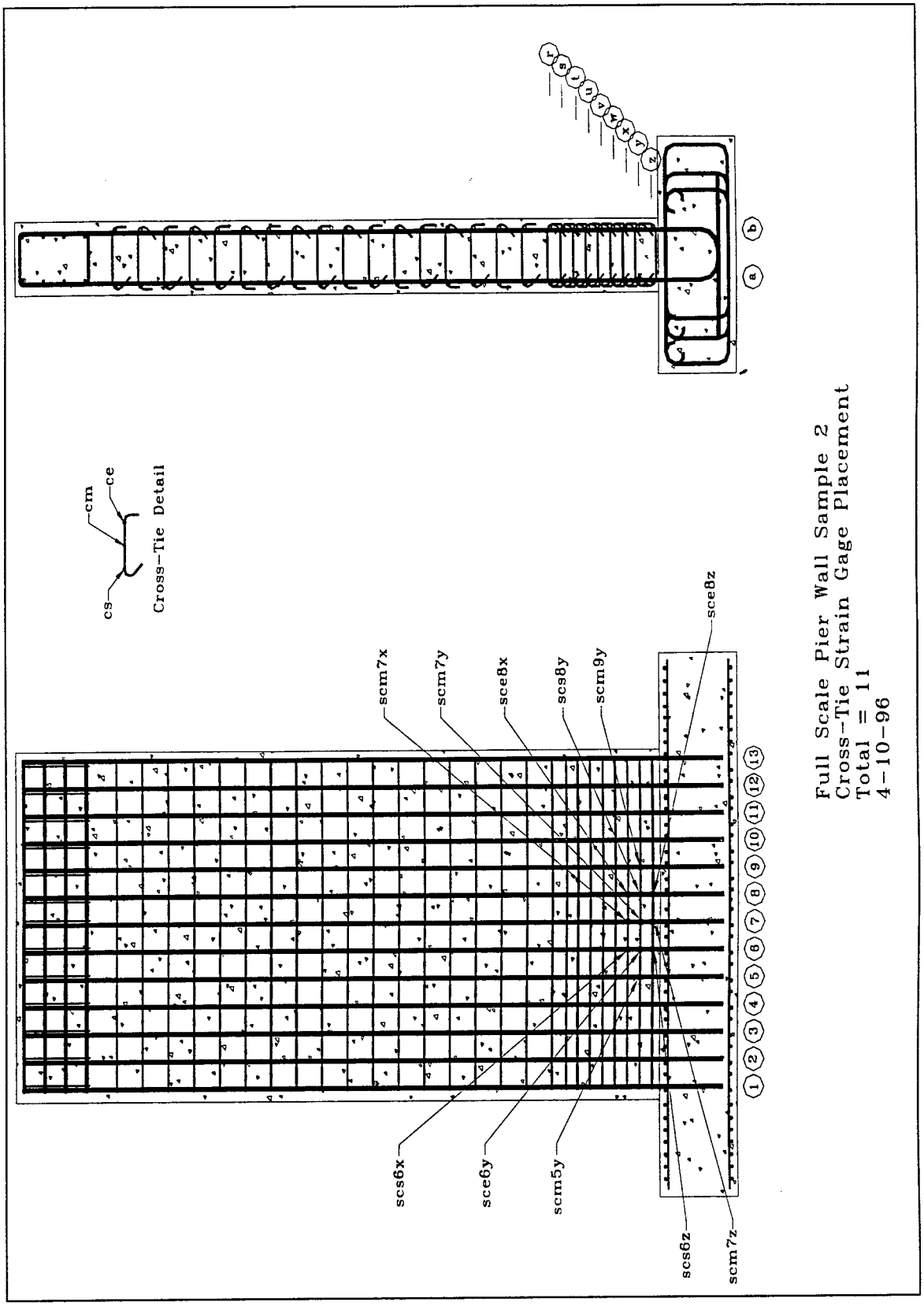

Figure 6.8: Location of Cross-tie Strain Gages: Sample 2

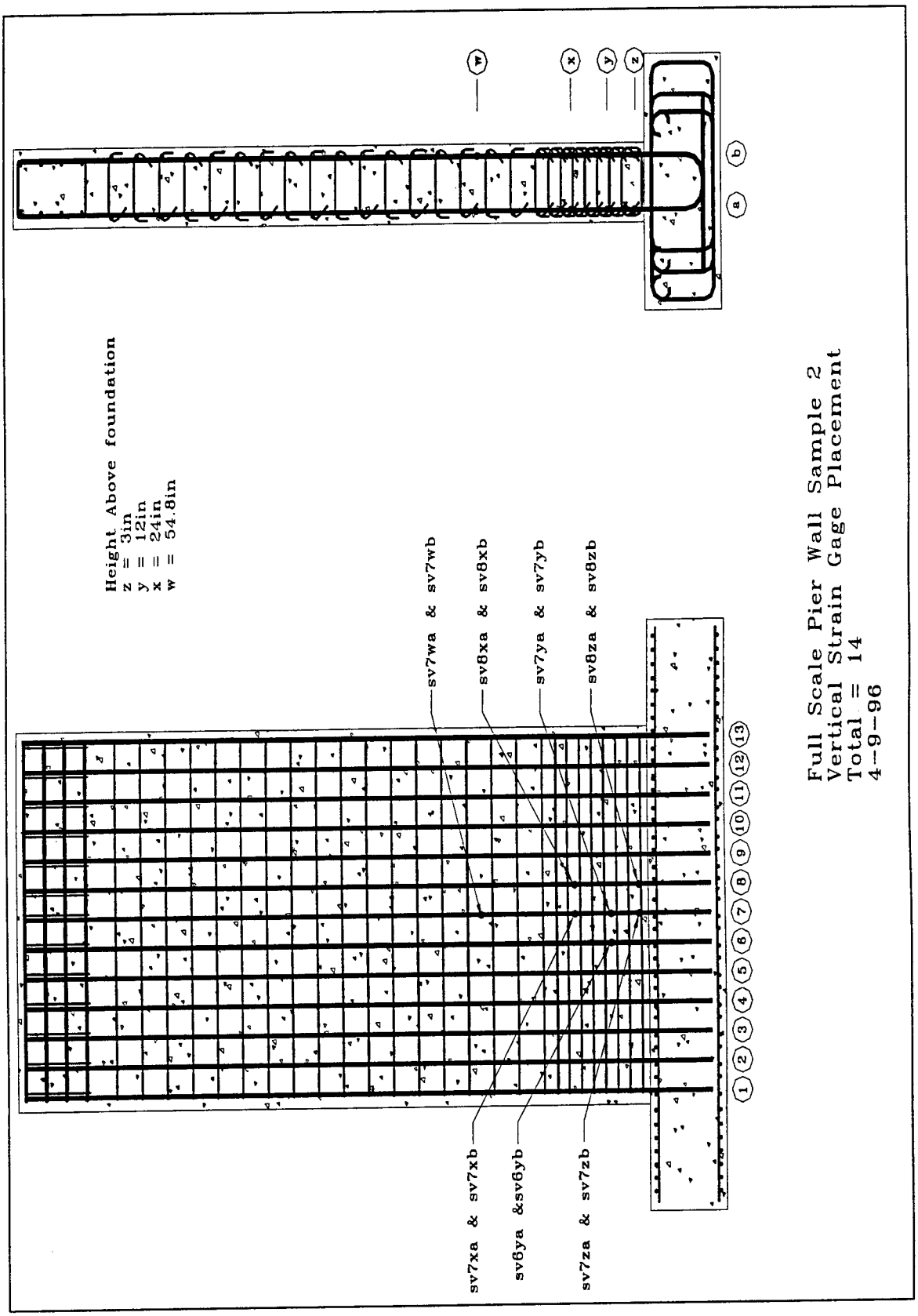

Figure 6.9: Location of Vertical Reinforcement Strain Gages: Sample 2

Sample 2 is shown in Figure 6.12.

The failure patterns in both full-scale samples were similar. The concrete cover at one of the corners of the full-scale walls spalled exposing the vertical reinforcement bar at that corner. Once the concrete cover had spalled off, the vertical reinforcement bar started to buckle as the load level increased. A similar pattern could be observed at the other corners as well.

From the experimental program it was noted that horizontal reinforcement, similar to the 'U' shaped horizontal hoop shown in Figure 6.13, should be provided at each end of the pier wall. The hoops should be placed at the same level as the horizontal reinforcement bars to prevent the premature buckling of vertical reinforcement bars at the corners of the pier wall.

Strength: The actual observed maximum strength in Sample 1 was 28% more than the nominal value calculated based on the ACI definitions. Similarly, in Sample 2 this value was 22% greater.

Ductility: Both full-scale walls reached a displacement ductility factor greater than 6.0.

Cross-tie: None of the 135° legs of cross-ties in either wall opened. Sample 1, with a single #4 cross-tie, obtained a slightly higher displacement ductility factor than Sample 2 which had a pair of alternating #3 cross-ties. The spacing of the horizontal bar in the plastic hinge zone was at 4.0 inches for both the samples. This close spacing increased the buckling load of the vertical reinforcement bars. From experience it was noted that as the load level increases, the vertical reinforcement bars tend to buckle and deform laterally bearing against the cross-ties. It is believed that this causes the cross-ties to open if the imbedded depth is not sufficient. However, in both full-scale walls, the spacing of the horizontal reinforcement bars were close. Therefore, none of the cross-ties in both the walls opened. Had the spacing of the

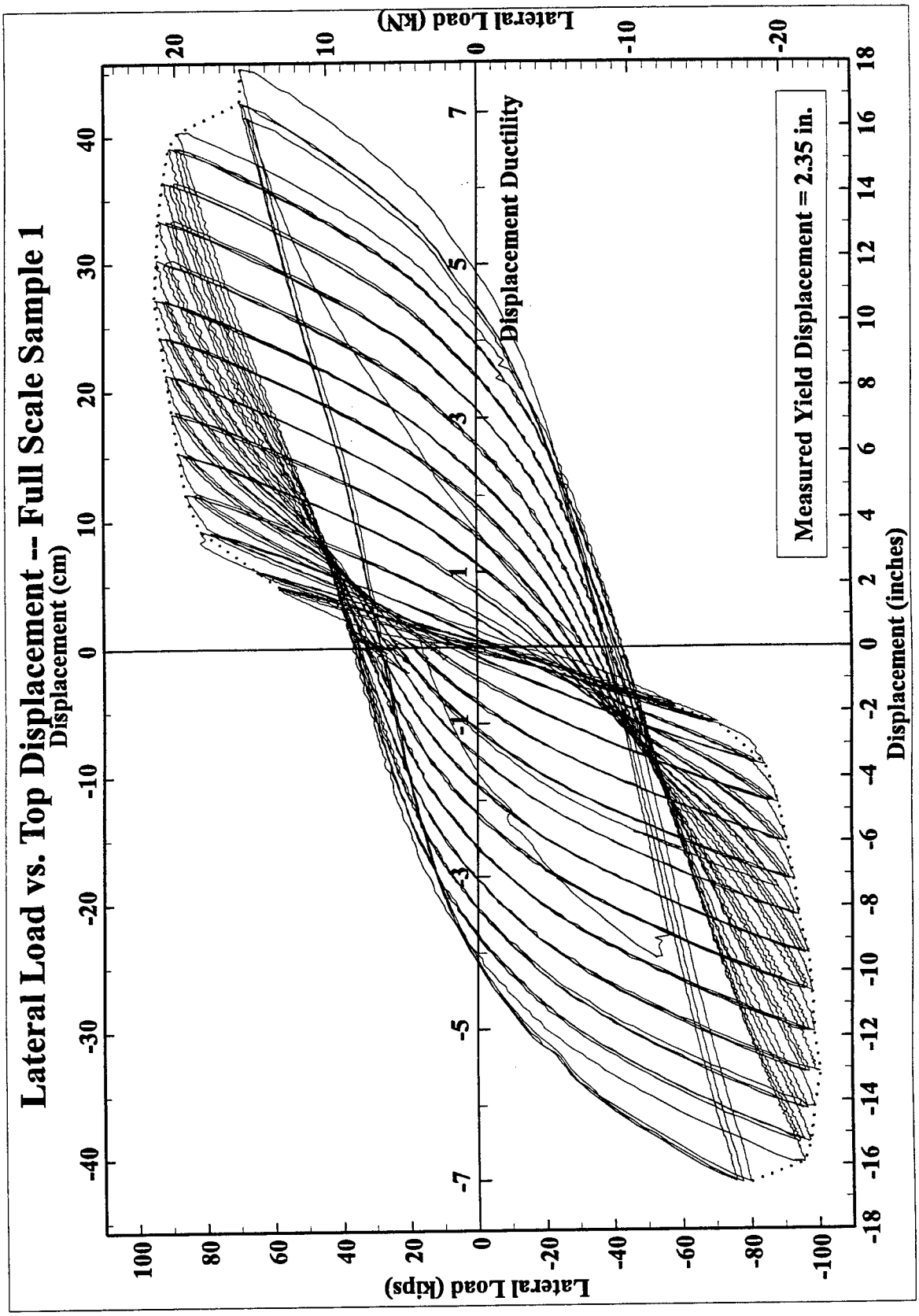

Figure 6.10: Hysteresis Loops for Full-Scale Sample 1

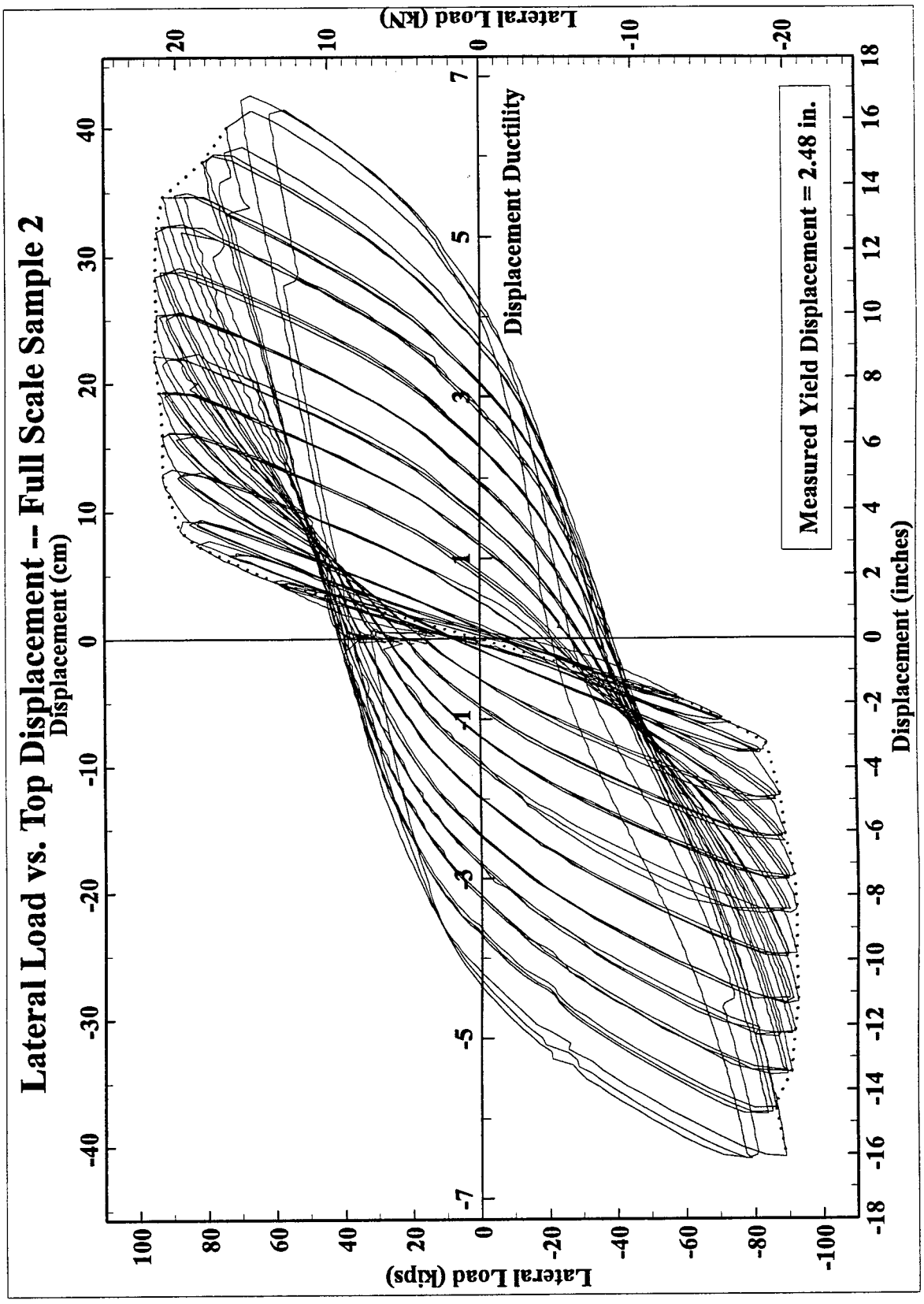

Figure 6.11: Hysteresis Loops for Full-Scale Sample 2

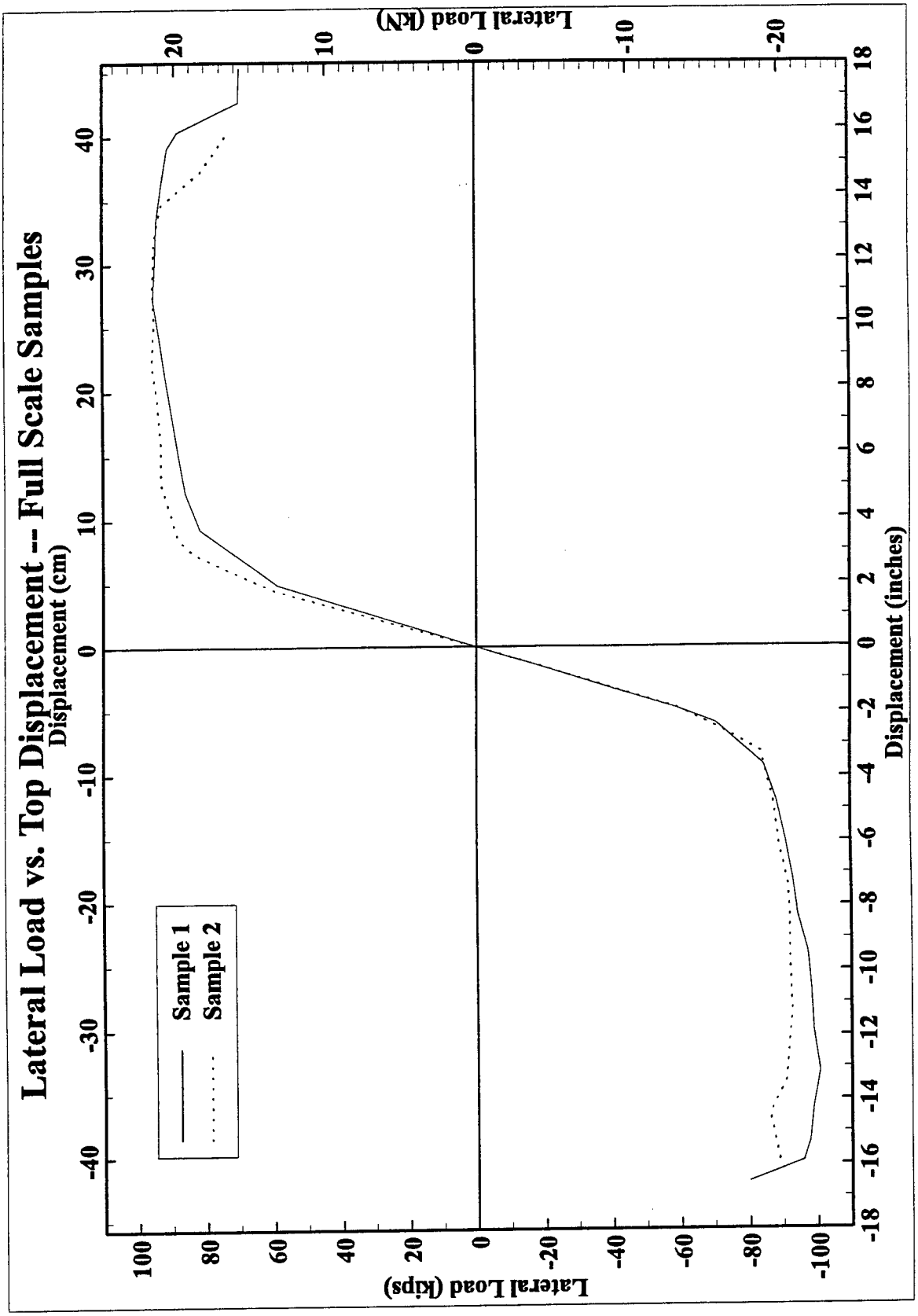

Figure 6.12: Envelope of the Hysteresis Loops: Sample 1 and Sample 2

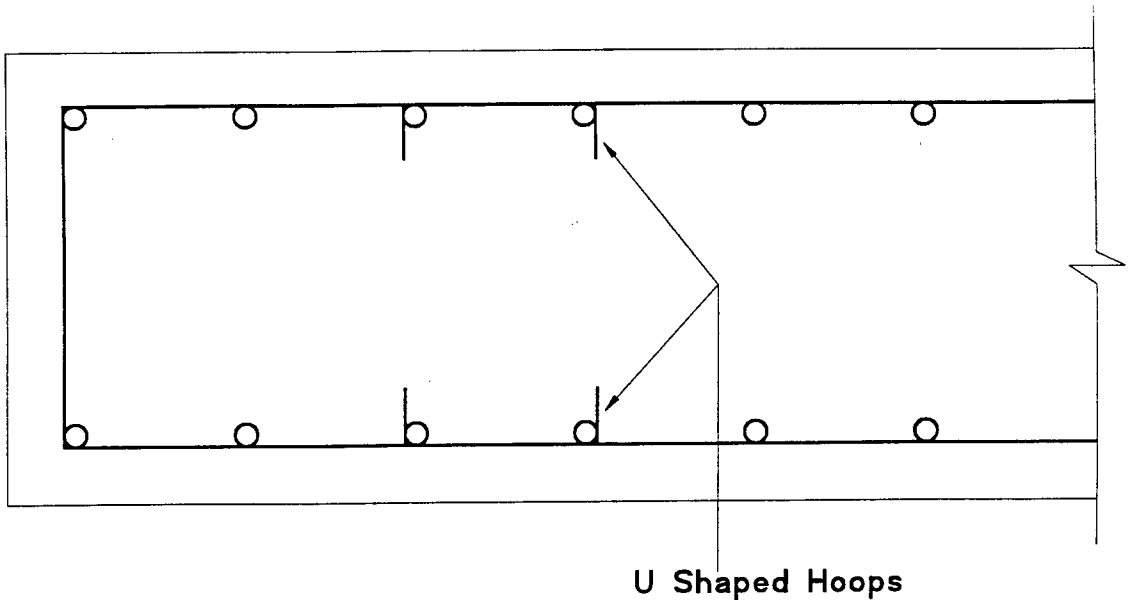

Figure 6.13: 'U' Shaped Horizontal Hoop

horizontal reinforcement bar been increased, the performance difference between an alternating pair of cross-ties and a regular pair of cross-ties could have been better observed.

6.9 Comparison Between Half-Scale and Full-Scale Samples

The half-scale and the full-scale samples behaved similarly. In both the half-scale and the full-scale pier walls, the damage was limited to the plastic hinge region of the pier wall directly above the footing. In the full-scale samples, there was evidence of yield penetration into the footings. The yield penetration was less evident in the half-scale samples. This can be attributed to the larger #9 bars used in the full-scale pier walls.

A comparison of the 'L' half-scale pier walls and the full-scale pier walls is shown in Figure 6.14. The y-axis is non-dimensionalized by taking the ratio of the lateral load to the computed nominal lateral load for the section. This non-dimensional

Pier Wall	Mode No.	Before Testing		After Testing	
		Freq. (Hz)	Damping %	Freq. (Hz)	Damping %
Sample 1	1	8.434	1.275	2.911	2.532
	2	42.488	0.611	10.109	1.748
	3	52.851	1.534	19.000	2.766
Sample 2	1	8.193	1.526	2.719	2.616
	2	42.428	0.572	12.124	2.566
	3	49.851	2.113	24.145	2.297

Table 6.6: Modal Properties of Full-Scale Walls: First Three Modes

lateral load is plotted against displacement ductility of the pier walls which is already non-dimensional. The half-scale walls show a very good comparison with full-scale walls. Note that the LN wall has no cross-ties and thus shows a lower ductility than the rest of the walls. To further elucidate the comparison, Figure 6.15 shows the non-dimensional moment plotted against measured curvature. The curvature measurements are not very accurate, but enough to show a good comparison of the half-scale walls with full-scale pier walls.

6.10 Modal Analysis

As in the repaired walls, experimental modal analysis was performed on the full-scale samples. Modal analysis was done before and after the samples were tested. Initially, before the samples were tested under cyclic loading, the test was confined to a frequency range of 3 Hz to 63 Hz to obtain the first three modes of the samples. Since the lateral stiffness had dropped at the conclusion of the lateral test, the post-test frequency range was reduced to a range of 1.5 Hz to 41.5 Hz. The results of the tests are summarized in Table 6.6.

As in the repaired pier walls, the stiffness degradation was evaluated using hys-

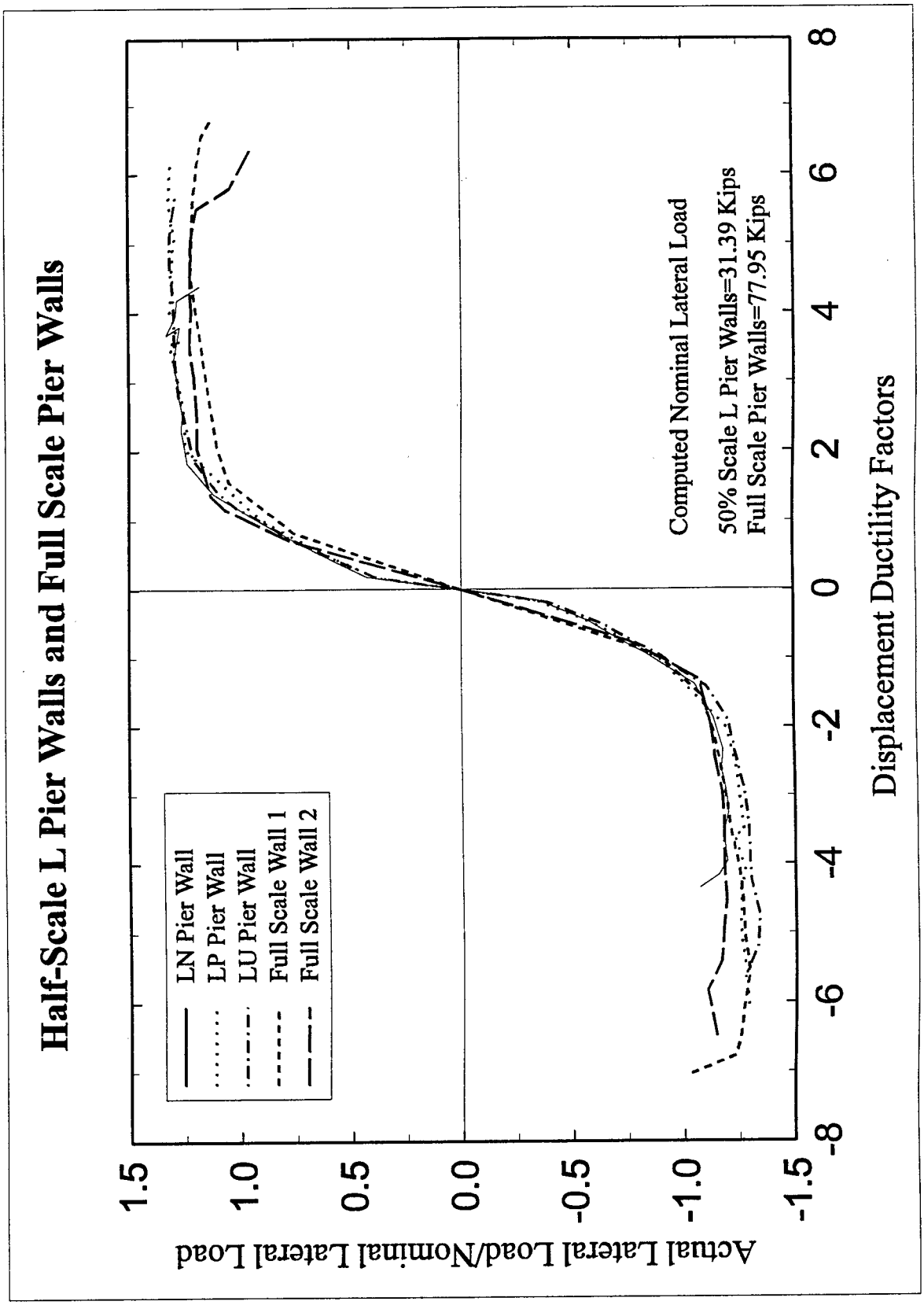

Figure 6.14: Load vs. Ductility of Half-Scale 'L' Pier Walls and Full-Scale Pier Walls

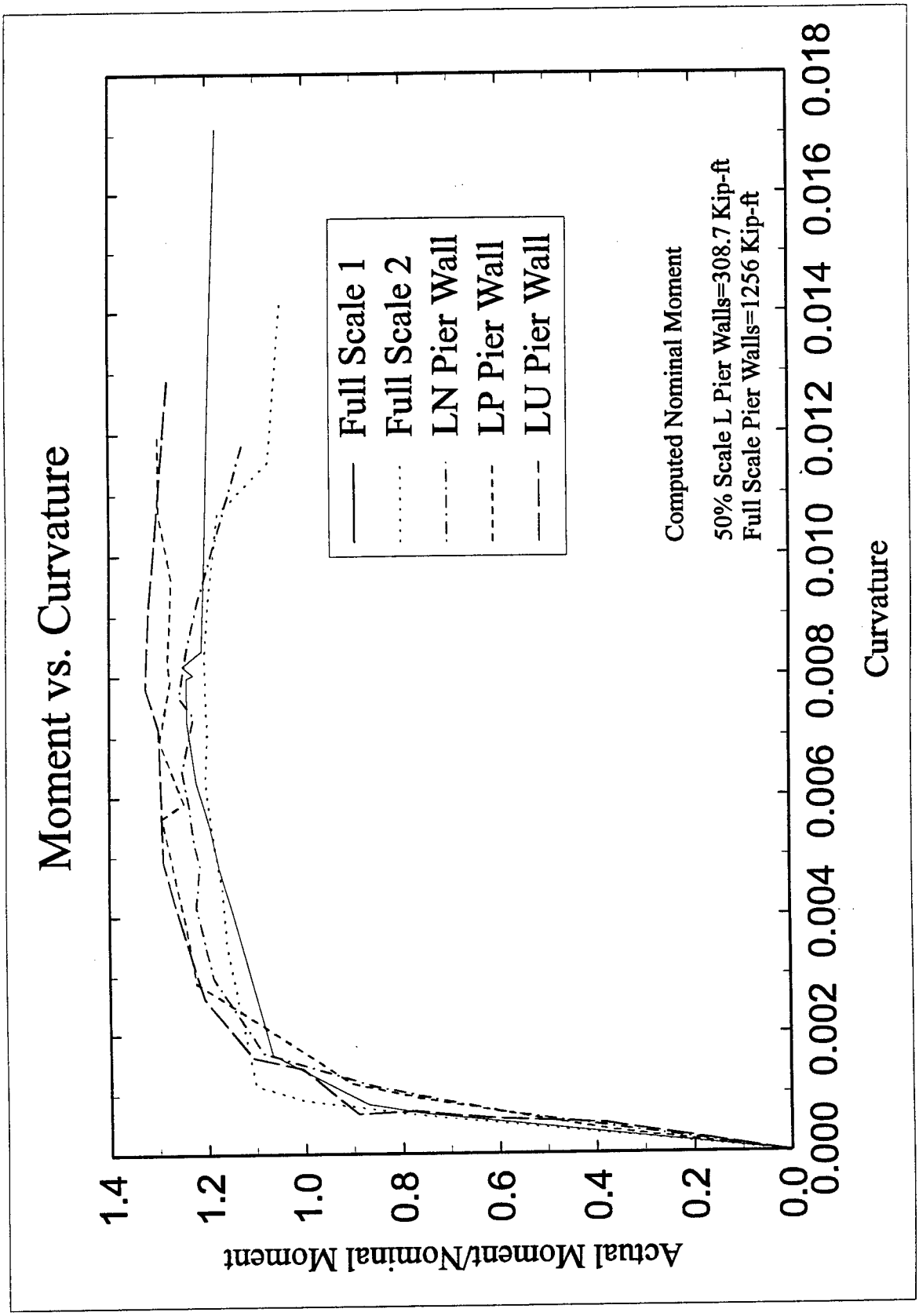

Figure 6.15: Moment vs. Curvature of Half-Scale 'L' Pier Walls and Full-Scale Pier Walls

Pier Wall	ω_1 (Hz)	ω_2 (Hz)	$(\omega_2/\omega_1)^2$	K_1 (kips/in)	K_2 (kips/in)	K_2/K_1	ξ_1 (%)	ξ_2 (%)
Sample 1	8.434	2.911	0.12	32.0	4.9	0.15	1.275	2.532
Sample 2	8.193	2.719	0.11	30.3	4.7	0.16	1.562	2.616

ω_1 = Fundamental mode frequency of repaired pier wall before cyclic tests
ω_2 = Fundamental mode frequency of repaired pier wall after cyclic tests
K_1 = Lateral stiffness of repaired pier wall before cyclic tests
K_2 = Lateral stiffness of repaired pier wall after cyclic tests
ξ_1 = Damping ratio in the fundamental mode of repaired pier wall before cyclic tests
ξ_2 = Damping ratio in the fundamental mode of repaired pier wall after cyclic tests

Table 6.7: Full-Scale Samples: Stiffness Degradation

teresis plots and the modal parameters. Again, the values obtained correlate very well. This stiffness degradation comparison is tabulated in Table 6.7.

6.11 Conclusions

- In the full-scale samples, the lateral stiffness was not affected by the presence of alternating pair of cross-ties.

- While the enhanced cross-ties had worked very well in repairing the damaged pier walls, this performance could not be observed in the full-scale samples. Had the spacing of the horizontal reinforcement bar been increased, the performance difference between an alternating pair of cross-tie and a regular pair of cross-tie could have been better observed.

- Similar ductility values were obtained for both the half-scale and the full-scale samples. Both the full-scale samples achieved a displacement ductility factor greater than six. In the 'L' walls with the same vertical reinforcement ratio, the ductility values ranged from 4.40 to 6.14.

- All half-scale and full-scale samples achieved higher lateral strength than the calculated nominal strength. In the 'L' and 'H' samples, there was an increase of approximately 20% while in full-scale samples, the increase ranged from 20 to 30%.

- There is a good correlation between ductility and strength of half-scale and full-scale samples. There was a difference in lateral stiffness between the half-scale and the full-scale samples. This can be attributed to the difference in size. While the width of the half and the full-scale samples were kept the same, the increase in thickness and height was not kept constant. The thickness was increased by 100% while the height was increased by 63%.

Chapter 7

Conclusions

The cyclic testing of six half-scale, repaired pier walls representing two ratios of vertical reinforcement and two full-scale pier walls led to the following conclusions:

- The strength and ductility of the repaired 'L' walls was similar to the original 'L' walls. The strength of the repaired 'H' walls was higher than the strength of the original 'H' walls; the ductility of the repaired 'H' walls was lower than the ductility of the original 'H' walls.
- The absence of the 5% axial load did not significantly affect the response of the pier wall.
- Pier walls with average to low vertical reinforcement ratios can be repaired with little or no loss of lateral load capacity or displacement ductility.
- Pier walls with the higher reinforcement ratios had more vertical reinforcement bars break than those with the lower reinforcement ratios upon repair and re-tested to the same displacement levels as the original walls. Therefore, some caution must be exercised in the repair of pier walls with high reinforcement ratios.

- Failure of the cross-ties by the opening of their ends was prevented to a large extent by increasing the leg lengths.

- The use of double cross-ties at each vertical reinforcing bar location provided good confinement of the concrete core.

- The T-headed cross-tie reinforcement performed as well or better than the regular cross-tie reinforcement. Further research is need to determine the optimum dimensions of such reinforcement and its economic viability.

- A good correlation between half-scale and full-scale walls was achieved for displacement ductility factors and curvatures. This suggests that half-scale samples can be used to model full-scale pier wall samples.

Reference

[1] Haroun, M.A., Pardoen, G.C., Shepherd, R., Haggag, H.A., and Kazanjy, R.P., "Cyclic Behavior of Bridge Pier Walls for Retrofit," Final Report to the California Department of Transportation, December 1993.

[2] Haroun, M.A., Pardoen, G.C., Shepherd, R., Haggag, H.A., and Kazanjy, R.P., "Assessment of Cross-Tie Performance in Bridge Pier Walls," Final Report to the California Department of Transportation, December 1994.

[3] Department of Transportation, State of California, "Bridge Design Specifications," June 1990.

[4] Priestley, M.J.N., and Park, R.,"Strength and Ductilty of Concrete Bridge Columns under Seismic Loading", ACI Structural Journal, Vol. 84, January-February 1987, pp. 61-76.

[5] Mau, S. T., "Effect of Tie Spacing on Inelastic Buckling of Reinforcing Bars", ACI Structural Journal, Vol. 87, No. 6, November-December 1990, pp. 671-677.

[6] Mau, S. T., and El-Mabsout, M., "Inelastic Buckling of Reinforcing Bars", Journal of Engineering Mechanics, ASCE, Vol. 115, No. 1, January. 1989, pp. 1-17.

[7] Kuchma, D.A., "Compressive Response of Reinforced Concrete Confined by T-headed Reinforcement",Workshop on "Applications of the T-headed Bar in Concrete Design and Construction", St. John's, Newfoundland, August,1994.

[8] Mander, J.B., "Seismic Design of Bridge Piers", Thesis, Civil Engineering Department , University of Canterbury, New Zealand, 1983.

[9] American Concrete Institute,"Building Code Requirements for Reinforced Concrete", ACI 318-89, Detroit, MI, 1989.

[10] Structural Measurement Systems, "SMS MODAL 3.0", Sunnyvale, CA, 1987.

List of Notation

d_b	=	diameter of reinforcement bar
f_c'	=	nominal compressive strength of concrete
f_y	=	nominal yield strength of reinforcement bar
w/c	=	water cement ratio
A_b	=	area of reinforcement bar in T-Headed cross-tie
A_g	=	gross cross-sectional area of the pier wall
A_h	=	area of the plate in T-Headed cross-tie
A_{st}	=	cross-sectional area of reinforcement bar
K_1	=	lateral stiffness of repaired pier wall before cyclic tests
K_2	=	lateral stiffness of repaired pier wall after cyclic tests
L	=	height of the pier wall
L_p	=	plastic hinge length
P	=	nominal axial load capacity of the pier wall
Q_i	=	ideal lateral load corresponding to the pier wall's moment capacity
Q_y	=	lateral load at first yield, assumed to be 75% of Q_i
Δ	=	lateral displacement of pier wall
Δ_u	=	ultimate displacement
Δ_y	=	displacement at first yield
Δ_y'	=	theoretical value of the yield displacement
ϵ_{cu}	=	ultimate strain of concrete, equal to 0.003
ω_1	=	fundamental mode frequency of repaired pier wall before cyclic tests
ω_2	=	fundamental mode frequency of repaired pier wall after cyclic tests
ξ_1	=	fundamental mode damping ratio of repaired pier wall before cyclic tests
ξ_2	=	fundamental mode damping ratio of repaired pier wall after cyclic tests

Reproduced by NTIS

National Technical Information Service
Springfield, VA 22161

This report was printed specifically for your order from nearly 3 million titles available in our collection.

For economy and efficiency, NTIS does not maintain stock of its vast collection of technical reports. Rather, most documents are printed for each order. Documents that are not in electronic format are reproduced from master archival copies and are the best possible reproductions available. If you have any questions concerning this document or any order you have placed with NTIS, please call our Customer Service Department at (703) 605-6050.

About NTIS

NTIS collects scientific, technical, engineering, and business related information — then organizes, maintains, and disseminates that information in a variety of formats — from microfiche to online services. The NTIS collection of nearly 3 million titles includes reports describing research conducted or sponsored by federal agencies and their contractors; statistical and business information; U.S. military publications; multimedia/training products; computer software and electronic databases developed by federal agencies; training tools; and technical reports prepared by research organizations worldwide. Approximately 100,000 *new* titles are added and indexed into the NTIS collection annually.

For more information about NTIS products and services, call NTIS at 1-800-553-NTIS (6847) or (703) 605-6000 and request the free *NTIS Products Catalog,* PR-827LPG, or visit the NTIS Web site **http://www.ntis.gov**.

NTIS
Your indispensable resource for government-sponsored information—U.S. and worldwide

U.S. DEPARTMENT OF COMMERCE
Technology Administration
National Technical Information Service
Springfield, VA 22161 (703) 605-6000